ACTA PROTOZOOLOGICA

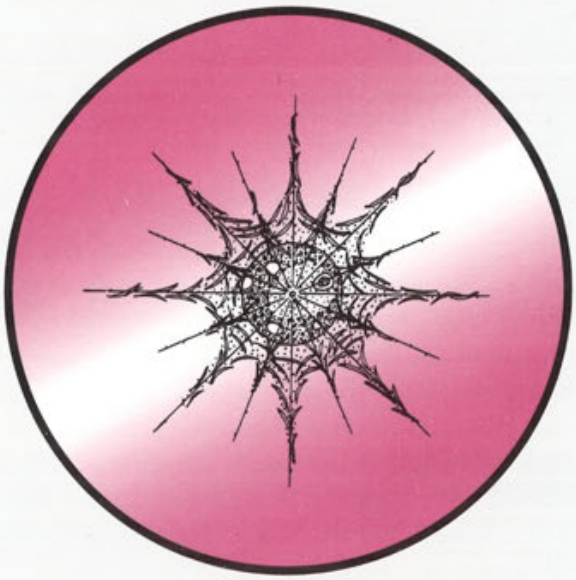

NENCKI INSTITUTE OF EXPERIMENTAL BIOLOGY
WARSAW, POLAND
1997
VOLUME 36 NUMBER 2
ISSN 0065-1583

Polish Academy of Sciences
Nencki Institute of Experimental Biology

ACTA PROTOZOOLOGICA

International Journal on Protistology

ACTA PROTOZOOLOGICA appears quarterly.

The price (including Air Mail postage) of subscription to ACTA PROTOZOOLOGICA at 1997 is: US $ 180.- by institutions and US $ 120.- by individual subscribers. Limited number of back volumes at reduced rate are available. TERMS OF PAYMENT: Cheque, money oder or payment to be made to the Nencki Institute of Experimental Biology. Account Number: 370044-3522-2700-1-73 at Państwowy Bank Kredytowy XIII Oddz. Warszawa, Poland. WITH NOTE: ACTA PROTOZOOLOGICA! For matters regarding ACTA PROTOZOOLOGICA, contact Managing Editor, Nencki Institute of Experimental Biology, ul. Pasteura 3, 02-093 Warszawa, Poland; Fax: 48-22 225342; E-mail: jurek@ameba.nencki.gov.pl

Front cover: *Stephanopogon colpoda.* In: I. B. Raikov - Kariologiya prosteishikh. Izd. Nauka, Leningrad 1967

Printed at the MARBIS, ul. Kombatantów 60, 05-070Sulejówek, Poland

Acta Protozoologica (1997) 36: 83 - 103

ACTA
PROTOZOOLOGICA

Review article

Ultrastructural Features of the Actinosporean Phase of Myxosporea (Phylum Myxozoa): a Comparative Study

Jiří LOM and Iva DYKOVÁ

Institute of Parasitology, Academy of Sciences of the Czech Republic, České Budějovice, Czech Republic

Summary. Ultrastructural features of the actinosporean phase (**A**) of the myxozoan life cycle are presented and compared with corresponding structures of the myxosporean phase (**M**). In both **A** and **M** phases, the same essential cell structures can be found : mitochondria, sometimes with plate- or tubule-like cristae and various inclusions; Golgi in typical or modified form; **rer**; ribosomes, sometimes forming helices of polyribosomes; sporoplasmosomes; phagosomes; various vesicles; reserves such as lipid bodies and beta-glycogen granules; typical microtubular bundles as residues of the mitotic spindle; cell junctions in form of more or less elaborate gap- or septate junctions or desmososmes and pseudopodia-like surface projections. Centrioles are absent. There is no essential difference in the main myxozoan character, polar capsule formation and structure; the identity includes the 11-12 nm fibers on the surface of the nascent polar filament. Very simple stem cells endowed with small amount of cytoplasm and fragments of **rer** (= inner cells of the pre- and extrasporogonic cycles of **M** and infectious cells in the **A** sporoplasm) have the potential to give rise to specialised cells such as sporoblast or plasmodial cells with a wide variety of cell constituents. The greatest diversity is found in **M** sporogonic plasmodia, with a variety of vesicles, fibrillar structures and surface modifications. In both **M** and **A** phases, unique modifications of **er** membranes may be found. Comparison of **A** and **M** fine structure reveals an identical structural pattern and supplies another confirmation of the unity of myxozoan life cycle. Polar capsules of myxozoa and nematocysts of cnidarians are homologous in their structure and way of origin. Septate cell junctions are typical both of cnidaria and of myxozoa. These two features, in addition to a plethora of other characters support the postulated kinship of both groups. The discrepancies in the mode of mitosis, however, warrant further research of their phylogenetical relationships.

Key words: actinospores, Cnidaria, Myxosporea, Myxozoa phylogenesis, ultrastructure.

Abbreviations: A - actinosporean phase, **cc** - capsulogenic cell, **csis** - club-shaped initial stage, **er**-endoplasmic reticulum, **et** - external tube, **g** - gap junction, **h** - host cell or tissue, **L** - lipid inclusion, **m** - mitochondrion, **M** - myxosporean phase, **n** - nucleus, **p** - phagosome; **pc** - polar capsule, **pf** - polar filament, **pl** - plug, **rer** - rough endoplasmic reticulum, **s** - sinuous septate junction, **ser** - smooth endoplasmic reticulum, **sp** - sporoplasm, **ss** - sporoplasmosome, **vc** - valvogenic cell.

INTRODUCTION

As revealed in the pioneering publication of Wolf and Markiw (1984) and later confirmed by a series of experimental papers (e.g., El-Matbouli and Hoffmann 1989; Benajiba and Marques 1993; Yokoyama et al. 1993, 1995b; El-Matbouli et al. 1995; Uspenskaya 1995; Andree and Hedrick 1997), the life cycle of representatives of the phylum Myxozoa Grassé, 1960 consists - at least in some of its members - of two phases. The first is represented by organisms known as myxosporeans (class Myxosporea) developing almost exclusively in fish. The second is represented by organisms - of which relatively few species have been know to date

Address for correspondence: Jiří Lom, Institute of Parasitology, Academy of Sciences of the Czech Republic, Branišovská 31, 370 05 České Budějovice, Czech Republic; FAX: (00420 38) 47743; E-mail: lom@paru.cas.cz

- developing mostly in oligochaetes. Until recently, they have been considered to constitute an independent class Actinosporea, a sister class of Myxosporea within the phylum Myxozoa.

While a large number of papers - about 103 - have dealt with ultrastructure of myxosporeans (**M**), only a few papers were published on the cytological features of the actinosporean phase (**A**), some of the reports going not into much detail (de Puytorac 1963; Ormieres 1970; Marques 1982, 1983, 1984, 1986; Lom and Dyková 1992a; Grossheider 1994; Koller 1994; El-Matbouli et al. 1995; Trouiller et al. 1996; Lom et al. 1997). A thorough comparison of structures and their morphogenesis of the two respective groups is still missing, although much desired to reveal the diversity manifested during the life cycle of myxozoan organisms. In addition, it may result in further confirmation of the common identity of the two phases.

Myxozoan life cycle is quite complicated. The actinosporean spore, end product of the (**A**) phase taking place in the oligochaete host and eventually released from it, floats in the water column. It is supposed - upon contact with the fish surface - to adhere chemotactically to it (Yokoyama et al. 1995a). It discharges sticky polar filaments serving for better attachment to the host tissue, the spore shell opens and the usually large, multinucleate sporoplasm emerges. It contains numerous small uninucleate cells, the infective cells proper, which pervade the host tissue and start first the development in the integument. This process was observed first by Daniels et al. (1976) and followed in detail by Markiw (1989). The released infective germs engage in a presporogonic development, intracellular and intercellular, in which inside a primary (mother) cell, secondary and tertiary cells are formed and then released to continue their growth and proliferation (El-Matbouli et al. 1995). These inner cells - like those inside **M** sporogonic plasmodia or **A** sporoplasm - reside inside a tightly fitting, membrane bound space, as if in a closely adhering vacuole, within the mother cell cytoplasm.

Prior to the appearance of spore-forming, sporogonic stages in the target (final) site of infection, several cycles of presporogonic proliferation may occur. In addition, proliferative cycles which use to be termed extrasporogonic, continue to proceed during sporogenesis. Cells of both pre- and extrasporogonic cycles divide by endogenous budding; inner, secondary cells may produce tertiary, quaternary or even quinquenary cells inside them. These purely proliferative cycles take place in tissues and organs other than the target sites and their cells may be intercellular in tissues (or bloodstream) and/or intracellular, irrespective of whether the sporogonic stage in the target site is histozoic or coelozoic.

M sporogonic stages in form of multinucleate plasmodia may reach large size (up to many millimeters). Very many inner cells are contained in tightly fitting vacuoles in their cytoplasm, i.e., generative cells and in some cases large cells of unknown function [= lobocytes of Grassé and Lavette (1978), who interpreted them as scavenger cells]. Histozoic plasmodia tend to be compact, roundish or ovoid, coelozoic ones may be extremely elongated, even branched and with many lobes or tips.

Generative cells produce **M** spores in two ways: either directly, dividing into a number of cells corresponding to those which after transformation compose the mature spore, or within a pansporoblast. The latter is mostly accepted to be a product of a pair of cells joined together, one (the pericyte) enveloping the other (sporogonic cell) which divides to give generally rise to two spores within a pericyte. Pericyte does not divide, although exceptionally it has been reported to be binucleate (Schubert 1968).

Although the germination of myxosporean spores in the fish digestive tract has been observed as early as 1895 by Thélohan, the only rather trustworthy reports on successful experimental infection of fish by myxosporean spores are by Johnston (1985) in *Parvicapsula* and by Odening et al. (1989) in *Sphaerospora renicola*. According to prevailing evidence, myxosporean spores are only infective for the invertebrate. Within the digestive tract of e.g., a tubificid worm the shell valves separate releasing the sporoplasm. In binucleate sporoplasms the nuclei are known (see Shulman 1966) to fuse accomplishing autogamy. Behaviour of sporoplasms of other types is not known. Earliest stages found in the intestinal epithelium [(intercellularly, exceptionally intracellularly (Lom et al. 1997)] are uni- to binucleate, thus possibly capable of repeated division.

A real presporogonic **A** proliferation in form of radial merogony has only been reported once by Marques (1984) in *Neoactinomyxon eiseniellae*. This problem has to be resolved by more observations; the same applies to the way of origin of pansporocyst. This is a structure in which the spores are produced within the shelter of two or four thinly spread enveloping cells, actively engaged in transport of nutrients from the host to the developing sporoblast cells. Pansporocyst has been supposed to develop either by union of two uninucleate cells and their later differentiation (Ikeda 1912, Marques 1984, Lom and Dyková 1992a) or from a binucleate cell

(Léger 1904) which divides and also produces the enveloping and sporogonic cells.

Once the pansporocyst has been formed, the inner enveloped cells divide producing eventually 8 gametes α and 8 gametes β (both slightly differ morphologically), plus 32 tiny cells, the actual polar bodies of the well proven (Janiszewska 1955) meiotic process. Each of the resulting 8 zygotes produces by an intricate way of cell division and cell differentiation invariably 8 valvogenic and 32 capsulogenic cells, while the sporoplasm develops as a multinucleate*) plasmodium containing inner cells, the actual infective germs.

Mature pansporocysts released from the infected tissues along with the excrements disrupt in water, the generally long projections of their spores instantaneously imbibe water and inflate to real floaters to keep the spore afloat in the water column. The spore's infectivity does not exceed, according to Markiw (1989), two days.

In this paper we try to provide a brief survey of main cytological features in the actinosporean phase, comparing them with corresponding stages of the **M** phase. We juxtapose new experimental data and previous unpublished findings to relevant reports from the existing literature to make the review complete.

MATERIALS AND METHODS

The source of actinosporean stages was the same as in Lom and Dyková (1992) - *Triactinomyxon* sp. from *Tubifex tubifex*, (designation T1), and Lom et al. (1997) - *Aurantiactinomyxon* sp. and raabeia-type actinospore of *Myxobolus cultus* from *Branchiura sowerbyi*). Additional *Triactinomyxon* spp. which could not be identified with any of the hitherto described species were collected in Kyselý potok brook near České Budějovice (T2) and at Bečov near Mariánské Lázně (T3). *Sphaeractinomyxon* sp. actinospores found in an undetermined marine tubificid at the Queensland coast (Australia) were obtained through the courtesy of Dr. F. Roubal.

Myxozoan specimens were in the course of all previous work fixed mainly simply in 1 % or 2 % osmic acid buffered with veronal acetate or 0.1 M sodium cacodylate buffer, sometimes with S-collidine; to a lesser extent, glutaraldehyde fixation followed by osmification was employed.

Ultrathin sections of specimens embedded primarily in Epon-Araldite were routinely double stained with uranyl acetate and lead citrate. They were examined in the JEM 100B and Philips 420 electron microscopes at 80 kV accelerating voltage. For demonstration of polysaccharide reserves, Thiéry method was used.

*) The genus *Tetractinomyxon* with binucleate sporoplasm has been postulated to be a myxosporean by Kent et al. 1994)

CELL STRUCTURES OF THE ACTINOSPOREAN PHASE STAGES

Early cells

The early cells of the **A**-phase found in oligochaete hosts are derived from **M**-phase sporoplasm cells which have a rich variety of cytoplasmic constituents (mitochondria, endoplasmic reticulum, various vesicles, Golgi, sporoplasmosomes, glycogen granules, even lipid inclusions). The solitary occurring early cells (Fig. 1) have surface with a few projections and invaginations (Figs. 2, 3), probably instrumental in endocytosis. Most of them occur intercellularly (Fig. 1), but some are probably intracellullar in all genera (Fig. 3. in Lom et al. 1997). In binucleate cells, the nuclei may be closely apposed (Fig. 4); yet, at variance with a true diplokaryon, such as rarely found also in **M** (*Fabespora vermicola* - Weidner and Overstreet 1979; *Myxidium giardi* - Azevedo et al. 1989) there is a larger gap between the two nuclear envelopes of the neighbouring nuclei. The opposing nuclear membranes may be thickened by apposed dense material (Lom et al. 1997, Marques 1986). In addition to mitochondria, various vesicles, scarce rudimentary Golgi bodies, phagosomes containing particulate material (Figs. 2, 4) and dense bodies, some of which are reminiscent of and actually may be persisting sporoplasmosomes of the **M** sporoplasm.

Pansporocyst envelope cells

As soon as the initial pansporocyst has been formed, its cell differentiate. The two outer cells become the envelope cells (they may divide into four in e.g., *Neoactinomyxon*) and spread flat around the spore-forming inner cells. They are joined to each other by desmosomal junctions. In *Neoactinomyxon* (Marques 1984) the two adjacent cell membranes, reinforced by subtending dense material, are separated by an intercalated substance with a thin axial septum; in raabeia, the central septum seems to be absent (Lom et al. 1997); in *Aurantiactinomyxon* (Fig. 5), there may be an additional mass of fibers subtending and parallel to the membranes. The cell structures including the nucleus preserve their integrity almost to the end of sporogenesis. In addition to scarce small Golgi bodies, these cells contain lipid granules, few cisternae of **er**, phagosomes and dense bodies of various structure and size, sometimes reminding of sporoplasmosomes in the sporoplasm.

Mitochondria have mostly lucent (Fig. 6), sometimes more dense matrix; they often contain a remarkable

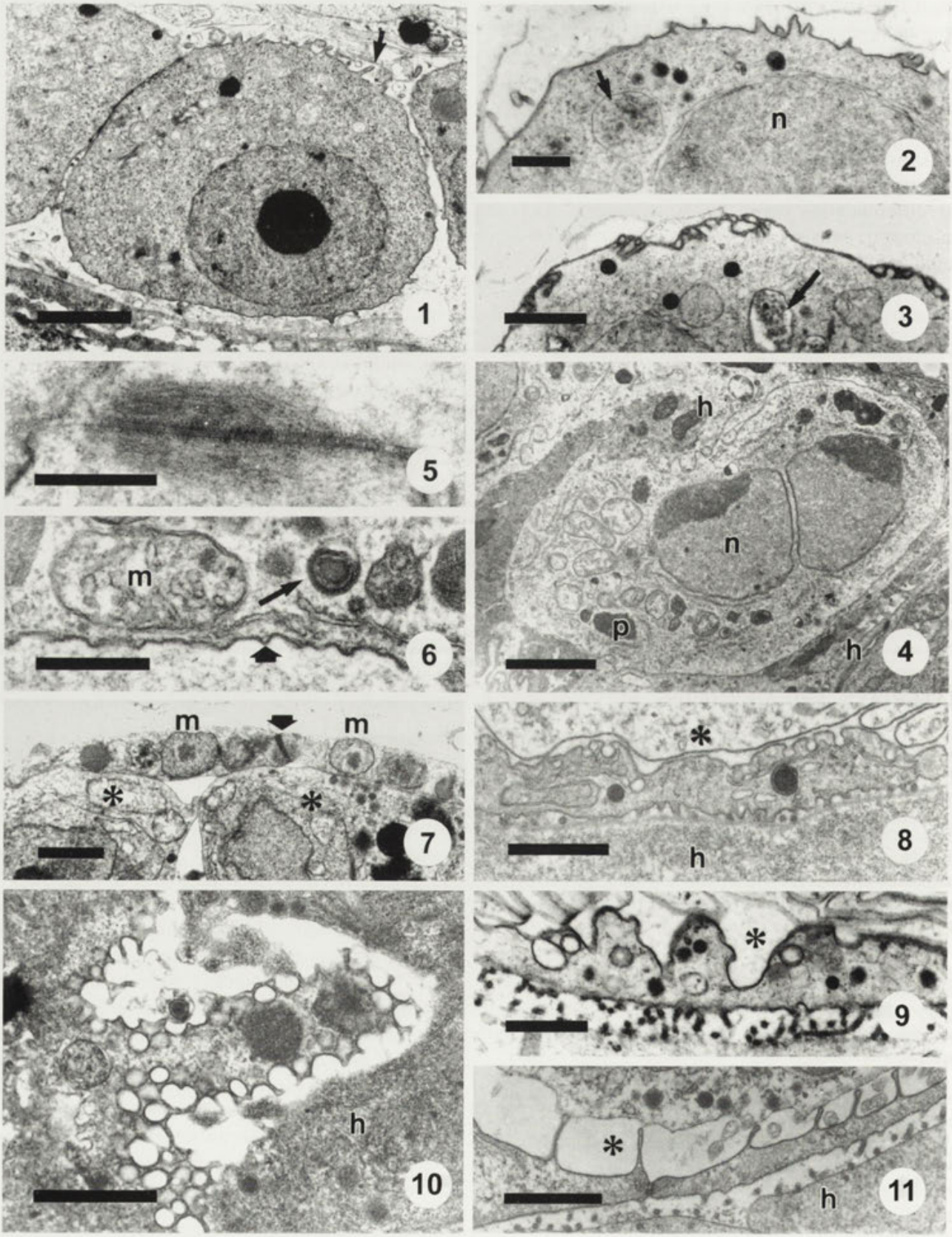

central dense inclusion (Fig. 7). The surface of the envelope cells usually bears villosities - lobose on both internal and outer face (Fig. 8), or lobose internally and tubule-like externally (Fig. 9) or as cup-shaped structures with elevated brims (Fig. 10) or isolated finger-like projections internally (Fig. 11).

Inner pansporocyst cells

The inner cells, as they multiply and differentiate into gametes, display numerous mitochondria and free ribosomes; in other respects they may differ. In *Aurantiactinomyxon* (Fig. 12) there are single **er** cisternae zigzagging through the cytoplasm around the mitochondria while in raabeia they are missing. In *Neoactinomyxon* (Marques 1986) large dense caps adhere to the nuclei, interpreted by that author possibly as an amplified and extruded nucleolar material.

In the course of gamete maturation, polar bodies in form of tiny cells with condensed nuclei and very few cytoplasmic organelles appear (Marques 1986, Lom et al. 1997; Fig. 13) which may persist into the last stage of sporogenesis.

Sporoblast cells during sporogenesis

Capsulogenic cells

They contain a variety of cell constituents; cisternae of **rer** which later swell to vesicles, mitochondria, Golgi, lipid droplets, various vesicles including (auto?)phagosomes (Fig. 15). Microtubules as remnants of the mitotic spindle are often preserved in the cytoplasm. The cytoplasm may contain aggregates of glycogen granules (*Aurantiactinomyxon*, Lom et al. 1997); in *Sphaeractinomyxon amanieui*, bundles of transversely striated 15 nm fibers were recorded (de Puytorac 1963).

Capsulogenic cells adhere to each other as well as to the valvogenic cells by gap junctions (Fig. 14) in which the membranes are set apart at 21 nm, being separated by finely granulated substance.

Capsulogenesis

It starts with a club-shaped initial stage (**csis**) with rigid-looking dense walls and various dense inner inclusions. It is supposed to originate from **er** cisternae (vésicule initiale, Marques 1984). Anteriorly it ends as a tube covered by a membrane overlain mostly by a dense cap (Figs. 16, 17) or by small vesicles like those found in some **M** (*Myxidium gadi*, Feist 1995). Externally, spirally arranged microtubules adhere to the **csis**. Later, **csis** develops into an elongated or bulbous primordium associated with a long narrow tube (external tube, **et**; Fig. 18; homologous with that of myxosporeans, Fig. 19). The **et** grows and becomes coiled inside the capsulogenic cell. Microtubules persist for some time around the tube's distal part and also on the surface of the primordium. Later on, they become rare, less regularly arranged (Fig. 23) and vanish. Both primordium and **et** contain variously structured dense material; in the primordium, it is encircled by dense fibers (Fig. 20 in longitudinal and Fig. 21 in transverse section).

Fibril-like structures subtend longitudinally the wall of **et** (raabeia, Fig. 36 in Lom et al. 1997; Fig. 24). Similar fibrils were also observed in myxosporeans (e.g., in *Henneguya adiposa* - Current 1979; *Thelohanellus nikolskii* - Desser et al. 1983b; *Sphaerospora testicularis* - Sitja-Bobadilla and Alvarez Pellitero 1993c). All existing observations (Ormieres 1970, Marques 1984, Lom and Dyková 1992a, Lom et al. 1997) indicate that the actual polar filament (**pf**) arises by invagination of the **et** into itself. Thus the newly formed **pf** appears first in the **et** and as the **et** shortens, the **pf** appears, coil by coil (Fig. 22), inside the primordium as a longitudinally strongly twisted and compressed hollow structure. The same process exists in myxosporeans (Fig. 25). Once the **et** has been completely inversed, walls of the **pf** are continuous with the primordium wall. At this and the following stages, the primordium contains moderately granular, sometimes fibrillar material (Fig. 27) and often homogeneous or layered, sometimes globular (Fig. 28), dense structures. Similar dense intraprimordial structures can also be observed in **M** - e.g., a large dense globule in *Sphaeromyxa* (Lom 1969), masses of different densities in *Myxobolus funduli* (Current et al. 1979) or an inclusion with concentrically arranged layers in *M. cotti* (Lom et al. 1989).

Beneath the primordium wall, a thick, electron lucent layer differentiates. Marques (1984) claimed that this lucent wall develops first as a dish-shaped structure with

Figs. 1-11. 1-3 - *Triactinomyxon* (T1) early stages. 1 - an intercellularly located cell with surface projections (arrow), bar - 2 μm; 2,3 - details of similar cells with surface projections and invaginations; phagosome marked by arrow, bars - 1 μm; 4 - a binucleate early stage of raabeia with peripheral nucleoli, bar - 2 μm; 5 - a cell junction between two pansporocyst envelope cells of *Aurantiactinomyxon*, bar - 0.5 μm; 6 - a mitochondrium and a dense body reminding of a sporoplasmosome (arrow) of a pansporocyst envelope cell in raabeia (arrowhead: inner face of the cell), bar - 0.5 μm; 7 - part of the pansporocyst envelope cells in *Aurantiactinomyxon*; arrowhead marks the cell junction, asterisks mark the sporoblast cells; 8, 9 - different aspects of surface villosities of pansporocyst envelope cells in *Triactinomyxon* T2 and T1, respectively; asterisks mark the inner face of the cell; 10 - indentations of the inner surface of the pansporocyst envelope cell in raabeia; 11 - finger-like projections on the inner face (asterisk) of the pansporocyst envelope cell in *Sphaeractinomyxon*, bars in 7-11 - 1μm

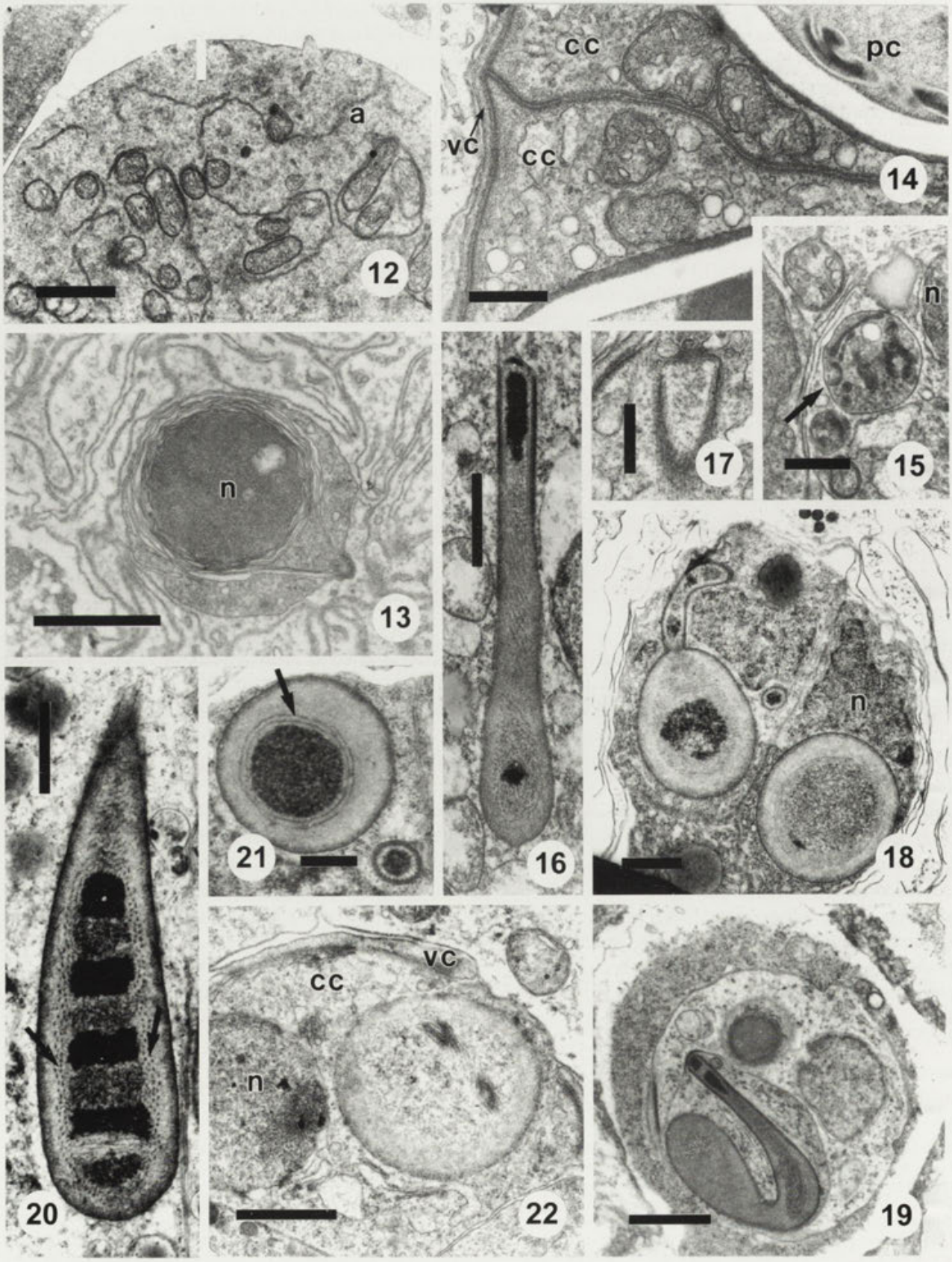

fibrillar stratification already in the "initial vesicle" (the transformed **rer** cisterna from which the capsule develops) and then expands around the primordium. However, this "dish", although frequently recorded, (e.g., Fig. 29) does not occur regularly and is rather an aberrant or abortive development. Abortive capsulogenesis with malformations of **et** could be observed in **A** (Lom et al. 1997) as well as in **M** (e.g., in *Myxobolus* sp. - Desser and Patterson 1978; *Ceratomyxa shasta* - Yamamoto and Sanders 1979; or *Leptotheca*/*Ceratomyxa* - Desportes and Théodorides 1982). A dish-shaped banded structure in the "initial vesicle" [reminiscent of those observed by Marques (1984) in **A**], claimed to start capsulogenesis in *Myxidium giardi* (Benajiba et al. 1993) does not appear to constitute the regular step in capsule morphogenesis.

The lucent layer of the primordium is stratified with several denser thin layers in *Sphaeractinomyxon* (de Puytorac 1963, and Fig. 30); they also appear in *Echinactinomyxon*, *Synactinomyxon*, *Neoactinomyxon* and *Aurantiactinomyxon raabeiiunioris* according to Marques (1984). Such a stratification is rare but not unknown in myxosporeans; one such layer was seen in *Myxidium giardi* (Azevedo et al. 1989) and is more distinct in the genus *Polysporoplasma* (Sitja-Bobadilla and Alvarez-Pellitero 1995). In *Leptotheca*/*Ceratomyxa* (Desportes and Théodorides 1982), the lucent layer is homogeneously pervaded with fibers. In both **A** and **M**, the lucent layer is contiguous with a thinner lucent layer appearing on the developing **pf**, whose lumen is filled with a dense material.

At this stage, the surface of this lucent layer is ridged with thin spiral fibres spaced at 11 nm in raabeia, (Lom et al. 1997) and 11 nm in *Triactinomyxon* (Fig. 31). Similar fibers, spaced at 11 - 12 nm, can also be observed on the nascent **pf** of *Sphaerospora renicola* (Lom et al. 1982), *S. molnari* (Desser et al. 1983a), *Sphaerospora* sp. from *Pangasius sutchi* (Lom and Dyková, in prep.) and *Zschokkella pleomorpha* (Lom et al. 1997). Uspenskaya (1984) published a micrograph of an inverted polar filament of an undetermined myxosporean with surface striation which can be calculated to have an interval of about 16 nm. In a fully mature polar capsule, these fibers disappear; the lucent layer of the **pf**, embedded in the homogeneous dark matrix of the capsule, has a rather fuzzy surface both externally and internally.

The outer dense wall of the primordium is delimited by a thin dense membrane which never detaches from the capsulogenic cell cytoplasm (Fig. 32). Later, the maturing polar capsule may be situated within a space - bound by the above mentioned membrane which, however, can be detached (fixation artefact ?) from the dense layer of the wall - and then it appears as a vacuole (Fig. 33). Similar "vacuoles" occur everywhere among myxosporeans (e.g., *M. cerebralis*, Fig. 34). Even in the primordium, the outer dense membrane around its apex is subtended by dense ridges raising from the primordium wall (Fig. 26) which become more conspicuous ribs ("cotes rayonantes" of Ormieres 1970) radiating from the apex as the capsule matures. Identical ridges are known in myxosporeans (e.g., *Zschokkella* - Lom and de Puytorac 1965b, *Sphaeromyxa* - Lom 1969, *Unicapsula* - Lester 1982).

At the apex of the **A** polar capsule (Figs. 35, 36) the space in the mouth of the inverted **pf** is filled by a "plug" of moderately dense material, which is topped by a cone with an inner core of homogeneous dense substance covered either with a less dense layer (Fig. 35), with a layer of fibers (Fig. 36) or with a layer or even a bundle of short microtubules (Figs. 38, 39). The cone, covered by the cell membrane of the capsulogenic cell, protrudes through the gap between the borders of the shell valves. In myxosporeans, the plug at the apex of the polar capsule is always developed, even in the enigmatic *Tetracapsula* (Canning et al. 1996). However, it usually lacks a covering cone (Fig. 40) or may bear a pad of moderately dense substance (Fig. 41) or filamentous structures (in *Sphaerospora testicularis* - Sitja-Bobadilla and Alvarez-Pellitero 1993c). Only exceptionally there is a dense cone developed similar to that in **A** (in *Myxobolus cotti* - El-Matbouli et al. 1990) or the plug is sheltered by a cone of a few short microtubules (in *Zschokkella nova* - Lom and de Puytorac 1965b).

Valvogenic cells

At the very beginning of their differentiation, they reveal, in addition to usual cytoplasmatic constituents, phagosomes and helices of polyribosomes (Figs. 46, 51).

Figs. 12-22. 12 - part of the pregametic cell in the pansporocyst of *Aurantiactinomyxon*; 13 - small cell of the polar body of *Triactinomyxon* (T2) in late pansporocyst, result of meiotic division; 14 - *Triactinomyxon* (T2) sporoblast: gap junction between capsulogenic cells (**cc**) and valvogenic cell (**vc**). **pc** - an almost mature polar capsule; 15 - a phagosome (arrow) in the capsulogenic cell of *Aurantiactinomyxon*, next to the nucleus (upper right); 16 - an early, club-shaped stage of polar capsule formation in *Sphaeractinomyxon*, bars in 12-16 - 1 μm; 17 - distal end of **et** in *Triactinomyxon* (T2) with vesicles covering the top bar - 0.33 μm; 18 - bulbous capsule primordium and associated **et** in capsulogenic cells of *Triactinomyxon* (T1), bar - 1 μm; 20, 21 - early capsular primordium of *Triactinomyxon* (T1) in longitudinal and transverse section, respectively; circular fibers (arrows) beneath the capsule wall seen in transverse and grazing section, bar - 1 μm and 0.5 μm, respectively; 22 - first turn of the polar filament appearing in the capsule primordium of *Aurantiactinomyxon*, bar - 1 μm

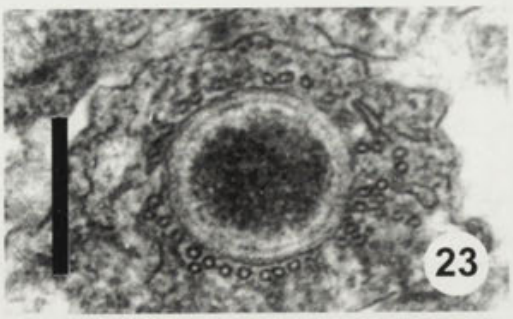

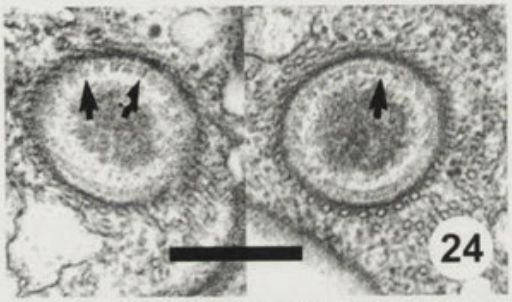

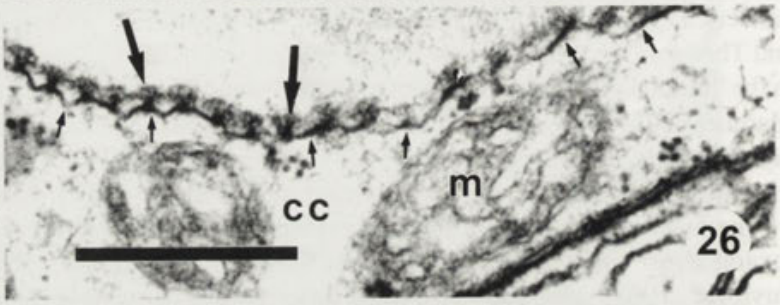

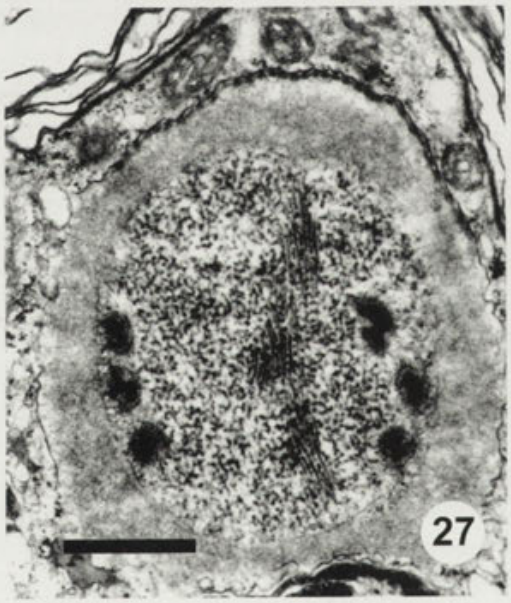

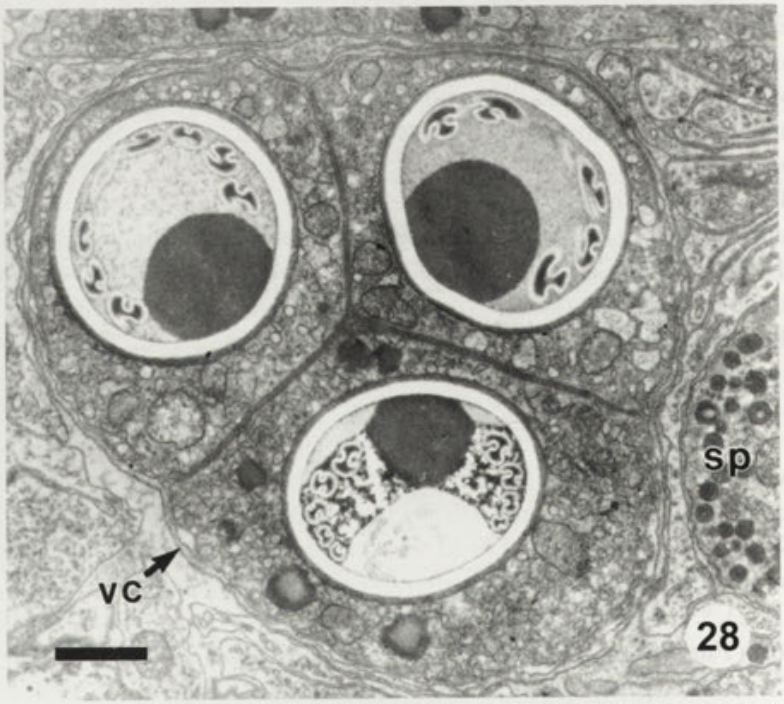

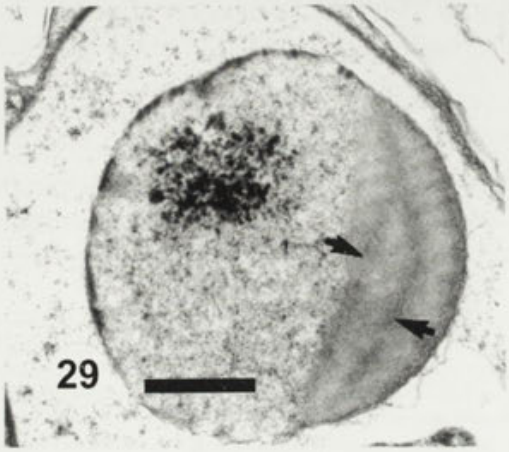

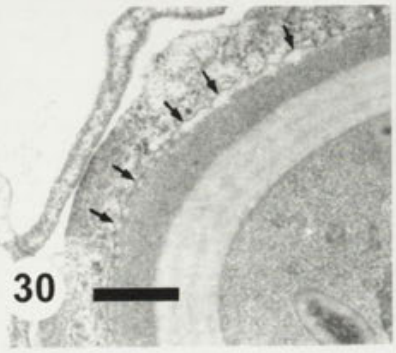

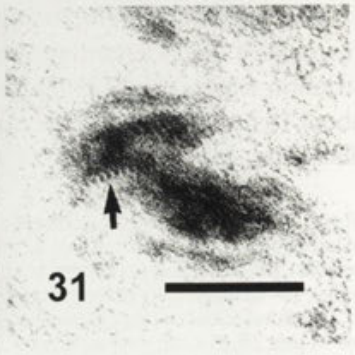

Pinocytosis is also evident. As the cells grow around the capsulogenic cells, they develop junctions between themselves (Fig. 42) and the latter. On their inner face, they may have digitiform projections (Fig. 43). In addition to mitochondria, they include a variety of vesicles, fragments of **er**, ribosomes (polyribosomes in raabeia, Lom et al. 1997) lipid droplets and dense bodies. Eventually, the cells have spread flat around the spore (Fig. 48). In species with caudal processi, these are telescopically folded while resting within the pansporocyst (Fig. 44). The cell membrane becomes subtended by a uniform dense fibrillogranular layer up to 170 nm thick in raabeia (Fig. 45). The cytoplasm gradually vanishes while the nucleus persists in the mature spore as a degraded structure (Fig. 47). Unlike in valvogenic and, later, shell valve cells in **M**, there are no microtubules subtending the valve surface in **A**.

A situation different from other actinospores is found in *Sphaeractinomyxon*. The cell membrane of valvogenic cells is subtended by perpendicularly oriented, sausage-like dense bodies (Figs. 50, 51). The suture between the shell valves is represented by very elaborate cell junctions. It is almost straight (Fig. 50) or extremely sinuous (Fig. 47). The material between the two opposing cell membranes is organised in three interconnected layers (Fig. 49) while granular material adheres to the cytoplasmic face of the cell membranes. Such a structure is unique among myxozoans, although the sinuous course of the suture finds some parallel in valvogenic cells of *Polysporoplasma* (Sitja-Bobadilla and Alvarez-Pellitero 1995).

The shell valves in actinospores differ from those in myxospores by their extreme fineness and thinness (Figs. 32, 48).

Sporoplasmic cells

Early sporoplasms, often still unsheathed by valvogenic cells, may sometimes have thin pseudopodia-like projections (e.g., *Sphaeractinomyxon* (Fig. 52); *Triactinomyxon* or *Aurantiactinomyxon*, Lom et al. 1997). Grown sporoplasm is a multinucleate, simple-membrane bound plasmodium with many inner infectious cells. In addition to numerous nuclei, the plasmodium contains mitochondria, **rer** cisternae sometimes arranged in conspicuous stacks (*Aurantiactinomyxon*, Lom et al. 1997), a variety of small vesicles and Golgi bodies sometimes enveloping the sporoplasmosomes. The latter are spherical, about 160 to 350 nm in diameter. They are unstructured dense bodies (Figs. 52, 53) or have - in what may be developmental stages - a denser core within an outer wall (Figs. 52, 56) or have even an elongated or concave profile (Fig. 53). In *Aurantiactinomyxon*, we have observed fuzzy strands of microfilaments extending through the plasmodium cytoplasm. Glycogen granules may be finely distributed through the sporoplasm or may form dense clusters (in *Aurantiactinomyxon*, Figs. 54, 55).

In **M**, the sporoplasms differ mainly in being at most binucleate or composed of a cell doublet (in Multivalvulida). They have a similar array of cell inclusions. Their sporoplasmosomes have a much greater variety of shapes (overview in Lom et al. 1989) including rod-shaped ones in *Ceratomyxa labracis* (Sitja-Bobadilla and Alvarez-Pellitero 1993a) or *Myxidium gadi*, in which Feist (1995) considered them to originate from the **er**. In **M**, bodies similar to sporoplasmosomes also occur in the PKX cells (e.g., Kent and Hedrick 1985) and in what was believed to be extrasporogonic stages of *Sphaerospora renicola* (Voronin and Chernysheva 1993).

The sporoplasm plasmodium contains infective cells which are isolated or may be as a rule closely associated in pairs with the somatic nuclei of the sporoplasm [e.g., in *Neoactinomyxon* (Marques 1984) or *Aurantiactinomyxon* (Grossheider 1994, Lom et al. 1997)]. The infective cell is the most simple cell of the **A** phase. Shortly after its origin by endogenous budding, it appears as a compact nucleus without any differentiated nucleolus, enclosed within a thin layer of cytoplasm. Later, in its typical form (Fig. 57) it has a nucleus with nucleolus and a small volume of cytoplasm with very few mitochondria, free ribosomes, small fragments - if any - of **er**, few vesicles and no polysaccharide reserves. The nucleus may be rounded, concave, or, in raabeia (Lom et al. 1997), appearing in cross section to subtend most of the cell membrane. The cell is located within a membrane bound space (vacuole) in the sporoplasm (Fig. 58).

In *Neoactinomyxon* (Marques 1984), *Aurantiactinomyxon* (Grossheider 1994, Lom et al. 1997) - the

Figs. 23-31. 23 - distal part of **et** in raabeia with persistent but already irregular corset of microtubule, bar - 0.33 μm; 24 - two transverse sections of raabeia **et** with fine fibers subtending its wall (arrows), bar - 0.25 μm; 25 - *Thelohanellus nikolskyi* capsular primordium with first turns of the early polar filament, bar - 1 μm; 26, 27 - periphery of the early polar capsule stage of *Triactinomyxon* (T1); 26 - dense ribs (large arrows) on the surface of the capsule wall adhering to the membrane (fine arrows) delimiting the capsulogenic cell cytoplasm; 27 - primordium (at the same stage of development) with fibrillar matrix and three turns of immature polar filament, bar - 0.5 and 1 μm, respectively; 28 - section through three immature polar capsules of *Triactinomyxon* (T2) containing globular dense structures, bar - 1 μm; 29 - probably aberrant formation of polar capsule wall in *Triactinomyxon* (T1) with two fibrillar strata (arrows) in what will be the lucent layer of the wall, bar - 1 μm; 30 - part of the primordium of *Sphaeractinomyxon* with two fibrillar strata in the lucent layer of the wall, fine arrows point at the dense membrane around the primordium, bar - 0.5 μm; 31 - fine fibers at the surface of the nascent polar filament of *Triactinomyxon* (T1), bar - 0.2 μm

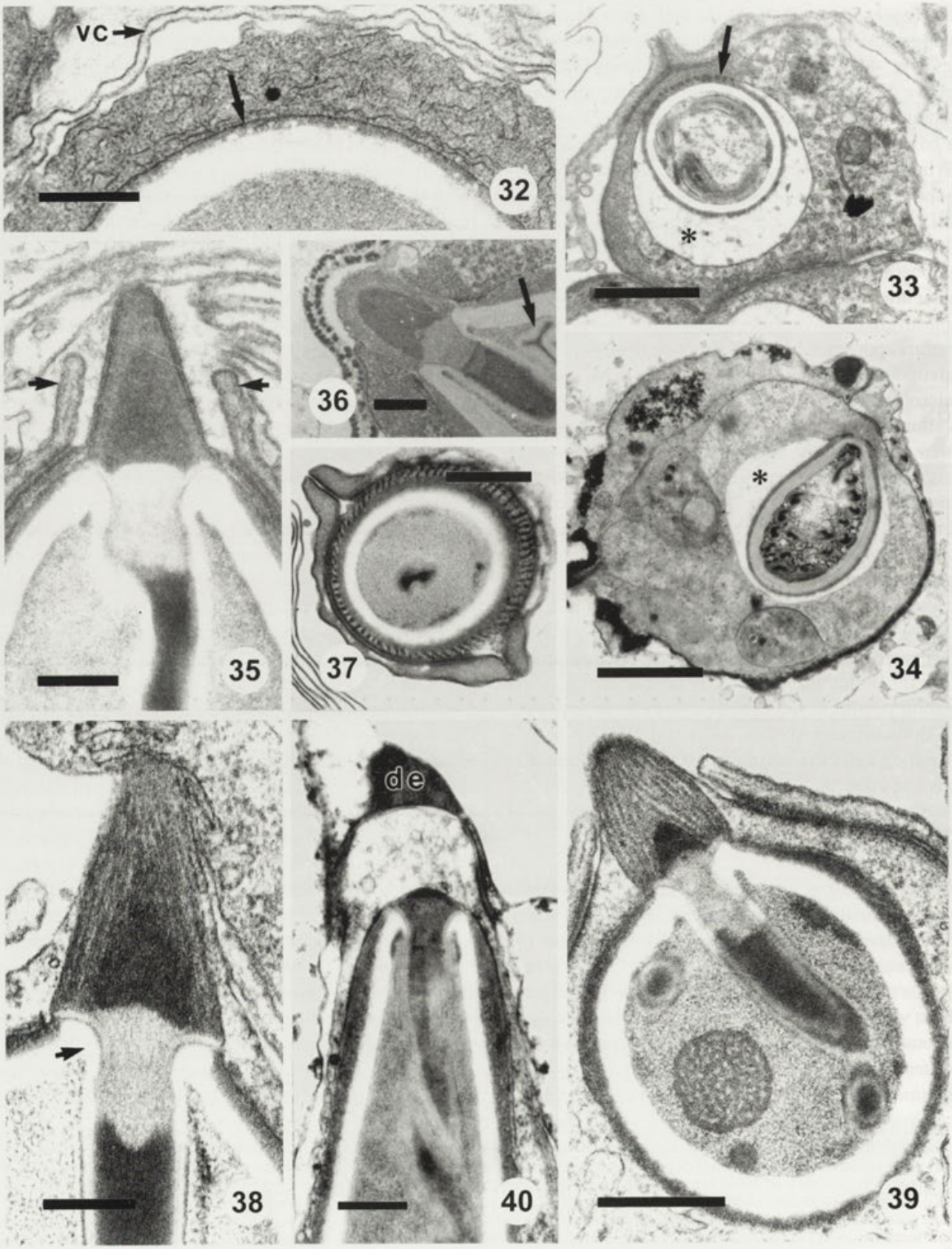

infectious cells are coupled each with one somatic nucleus of the sporoplasm to form closely adhering pairs.

The infectious cell closely reminds of two types of cells of the **M**-phase. First, the inner (secondary or tertiary) cells of extra- or presporogonic stages (Fig. 60) as they are formed within the primary cells (Dyková et al. 1990). Actually, it is these stages that the infective cells develop into as they start the developmental sequence in the fish host (El-Matbouli et al. 1995). Only as the inner cell grows later into the large primary cell, its cytoplasm becomes rich in **er**, Golgi bodies and polysaccharide reserves. Second, it is reminiscent of some sporogonic cells (Fig. 59) within the large **M** plasmodia.

The association somatic nucleus-infectious cell has a certain parallel in **M**. The sporoplasm of *Kudoa* (Lom and Dyková 1988) is a cell doublet consisting of an inner cell closely adhering to the nucleus of the enveloping cell; much like in **A**, the inner cell lack sporoplasmosomes and glycogen reserves. In the sporogonic plasmodium of *Ortholinea fluviatilis*, too, the generative cells closely adhere to the vegetative nuclei of the plasmodium (Lom and Dyková 1996).

Structures in the cytoplasm of A and M

Mitochondria

In actinospores, mitochondria are as a rule equipped with flat cristae (Fig. 61), often having to some extent tubular or disc-shaped appearance; their matrix may be dense in some cases. Sometimes the mitochondria contain a central dense material (Fig. 62) (phospholipid ?) or a small dark inclusion (Fig. 63). In pregametic cells of raabeia, mitochondria contain what appears in side view as paracristalline structures (Fig. 64); transverse section suggests that it may be microtubules with surface ornamentation (Fig. 65).

In myxosporea, there is a comparable diversity of mitochondrial structures. Quite often, the matrix is exceedingly dense ["condensed state"; e.g. in *Myxidium lieberkuehni* (Lom and de Puytorac 1965a)] *M. gadi* (Feist 1995) or *Ortholinea fluviatilis* (Lom and Dyková 1996). There may also be dark inner granules (Fig. 67) or grains of beta-glycogen (*Zschokkella mugilis* - Sitja-Bobadilla and Alvarez-Pellitero 1993b). The inner space of the mitochondrion may be occupied not by a dense body but by a vesicle surrounded by plate-like cristae [in *Kudoa*, Fig. 66, and in capsulogenic cells of *Myxidium gadi* (Feist 1995)]. Paracrystalline bodies, observed in plasmodia of *Henneguya adiposa* (Current 1979), revealed no microtubular structures, unlike raabeia mentioned above; however, simple microtubules were recorded in mitochondria of *Henneguya psorospermica* plasmodium (Lom and de Puytorac 1965a). Various froms of myxozoan mitochondria further expand the structural diversity of eukaryotic mitochondria as demonstrated in e.g., Tandler and Hopper (1972).

Polysaccharides

Polysaccharide reserves in form of beta-glycogen granules are distributed in **A** cells either rather uniformly, or they may form large aggregates, especially in capsulogenic and sporoplasmic cells, a situation commonly found in **M** sporoblast cells (Lom and Dyková 1988, Sitja-Bobadilla and Alvarez-Pellitero 1993b).

Membrane-derived structures

Structures which can be called "pseudoannulate lamellae" have been described by Lom et al. (1997, in Fig. 22) in capsulogenic cells and sporoplasms of *Aurantiactinomyxon*. They consist of flat cisternae comprising between their membranes - unlike in annulate membranes - small vesicles with a tiny central circle as if the nuclear envelope pores were turned by 90°. Their origin from the nuclear envelopes (Fig. 68) is, however, unquestionable and thus these structures are in a way related to the annulate membranes.

In the cytoplasm of *Aurantiactinomyxon* sporoplasmic plasmodium (Lom et al. 1997), vesicles obviously derived from nuclear envelopes (Fig. 69) were observed, containing small flat discs closely apposed to each other as stacks of coins. These are structures quite unique for Myxozoa.

Another kind of special structures was observed in capsulogenic cells of *Aurantiactinomyxon* (Fig. 70). They are obviously associated with or derived from **er** cisternae and assume the form of a grid of interlocked membraneous

Figs. 32-40. 32 - dense membrane (arrow) around the primordium of raabeia, bar - 0.5 µm; 33 - the space (asterisk) between the primordium wall and detached dense membrane in the capsulogenic cell of *Aurantiactinomyxon*, arrow points at the dense ribs, bar - 1 µm; 34 - the same situation as in Fig. 33 in *Myxobolus cerebralis*, bar - 2 µm; 35 - the cone at the apex of polar capsule of *Triactinomyxon* (T2) protrudes between the borders (arrows) of valvogenic cells, bar - 0.33 µm; 36 - a similar cone at the capsule apex in *Sphaeractinomyxon* is covered by a layer of fibers; note the triangular cross section of the first filament turn (arrow); 37 - *Triactinomyxon* (T3): transverse section through a polar capsule with a corset of dense, closely set ribs, bars in 36, 37 - 0.5 µm; 38, 39 - a cone at the apex of capsule in *Aurantiactinomyxon*, covered with microtubules (in 38 leaning against a neighboring sporoblast cell); arrow marks the point where the lucent layer of the capsule wall passes into the filament wall; in 39 the primordium contains a spongy inclusion, bars - 0.25 and 0.5 µm, respectively; 40 - the apex of the capsule in *Henneguya psorospermica*; **de** - dense substance filling the canal for filament discharge, bar - 0.5 µm

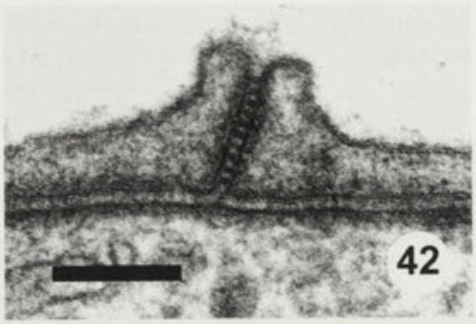

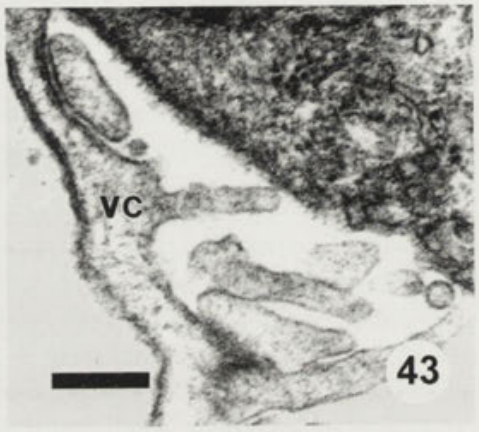

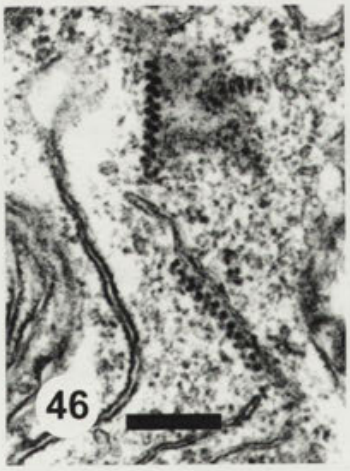

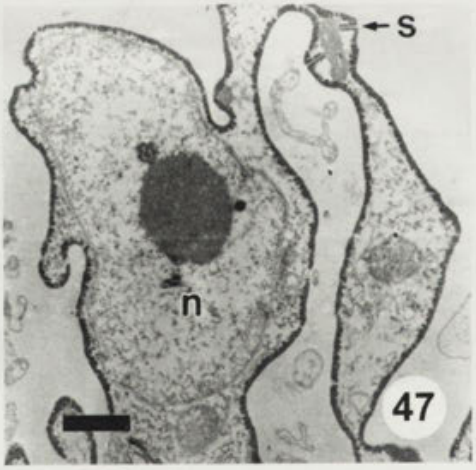

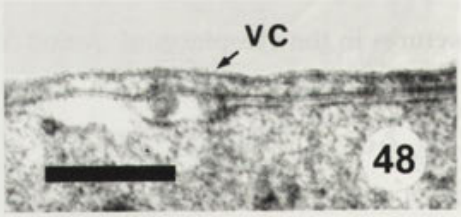

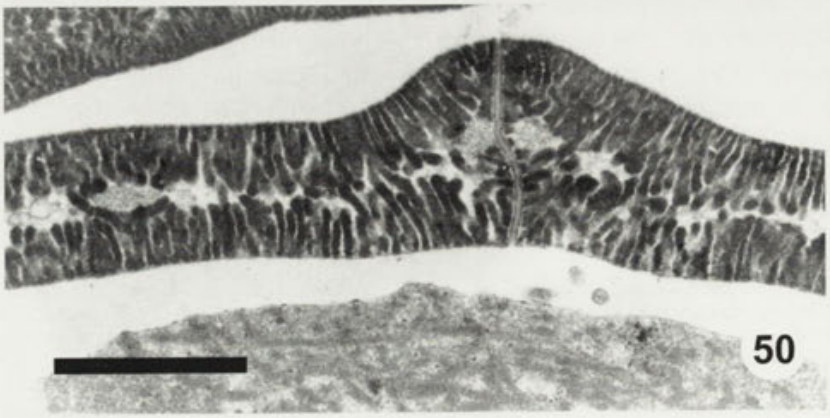

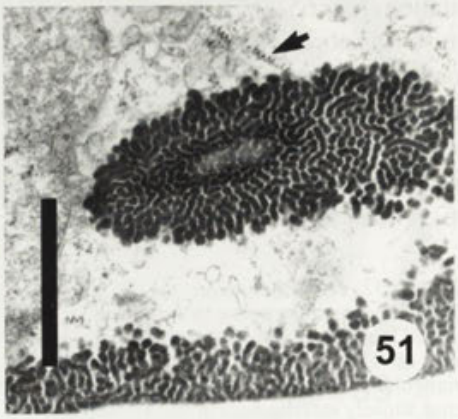

profiles (Fig. 71). No ribosomes seem to be attached and the function is unknown.

Virus particles

Viral infection has only been observed in capsulogenic cells of *Aurantiactinomyxon* (Lom et al. 1997) in which icosohedral bodies were present, measuring 62 nm in diameter with a dense central point. Similar inclusions, though more rarely, were recorded in the cytoplasm of valvogenic cells in *Triactinomyxon* (T2).

Nuclear features

Nuclear division is a cryptomitosis with persisting nuclear envelope and without any centriole or MTOC at poles of the mitotic spindle and with nucleolus shifted aside. There is no distinct equatorial plate. This is what Marques (1986) described in several developmental phases; his claim that in dividing α-cells the nuclear membrane disappears is not clearly supported by his respective micrograph. In myxosporeans, typical cryptomitosis can be found (Pl. 20d in Lom and Dyková 1992b).

Bundles of microtubules, remnants of the mitotic spindle still connecting the two nuclei after the karyokinesis has been completed, can be seen at the isthmus of the two separated cells (Fig. 73) and are common in the cytoplasm of the inner infectious cells in the sporoplasm (Fig. 72). Such bundles are a tale-telling mark of **M** cells.

The nucleoli of actinosporean nuclei are usually centrally located or slightly shifted compact bodies. Sometimes, especially in developing gametes, they appear as concave bodies subtending parts of the nuclear envelope (Lom et al. 1997)

Synaptonemal complexes were signalled for the first time by Marques (1986) in maturing gametes of *Neoactinomyxon eiseniellae* and then were seen in detail in raabeia (Lom et al. 1997). These observations were preceded by Siau (1979) who saw them in **M**, in young stages of *Myxobolus exiguus* and *Ceratomyxa herouardi*.

Cell junctions

Cell junctions are essentially of two types in **A**. In addition to more or less simple gap junctions, with different amount of material intercalated between or subtending the opposing membranes, there are septate junctions between the valvogenic cells. The latter are less elaborate, with the exception of *Sphaeractinomyxon,* than in certain myxosporeans where they are subtended by bundles of microfibrils and by microtubules (*Thelohanellus* - Desser et al. 1983b, *Myxidium* - Azevedo et al. 1989) In some other myxosporeans, junctions between valvogenic cells are more simple, often revealing no septate character at all (e.g., in multivalvulids like *Kudoa lunata* - Lom and Dyková 1988). The other junctions can be designated as gap junctions and similar ones can be found in **M** sporoblasts and between the somatic cells of the "sac" in the strange myxosporean *Tetracapsula* (Canning et al. 1996). Several types of cell junctions serve for attachment of plasmodia of coelozoic myxosporeans to cells of the host tissue (see discussion in Lom and Dyková 1996) and are not found in **A**.

DISCUSSION

Identity and differences in ultrastructural features of the A and M phase

The differences between the **A** and **M** phase of myxozoan life cycle have been emphasized by decades of light microscope observations (origin and structure of spores; different sexual processes; occurrence of large proliferative stages only in **M** and hence the cell-in-cell condition, i.e., occurrence of inner cells in mother cells, prevailing in **M**) while electron microscope findings confirm the identical pattern of essential ultrastructural features throughout the life cycle. It is another corroboration of the unity of the complex myxozoan cycle. The same can be seen in the continuous stem line of pluripotential cells [infective cells of the **A** sporoplasm - inner cells of the **M** proliferative (presporogonic, extrasporogonic and sporogonic) cycle - **M** sporoplasm - gamete forming cells in **A**] giving rise all the time to specialised somatic cells (mother cells or plasmodia of **M** proliferative stages, **M** spore forming

Figs. 41-51. 41 - longitudinal section through the polar capsule of a *Sphaerospora* sp. (courtesy of Dr. R. C. Hamilton). **n** - nucleus of the capsulogenic cell, bar - 1 μm; 42 - septate junction of valvogenic cells of *Aurantiactinomyxon*, bar - 0.2 μm; 43 - projections on the inner face of valvogenic cells of *Aurantiactinomyxon*, bar - 0.25 μm; 44 - transverse section of telescopically folded caudal projection of valvogenic cell in raabeia, bar - 1 μm; 45 - detail of Fig. 44, showing dense substance subtending the cell membrane; arrow points at the space between the cell folds, bar - 0.1 μm; 46 - polyribosomal helices in the cytoplasm of the valvogenic cell in raabeia, bar - 0.25 μm; 47 - part of the valvogenic cell of *Sphaeractinomyxon*; valve suture (s) is in fact a sinuous septate junction, surrounded by the elongate dense bodies; bar - 1 μm; 48 - thin valvogenic cell of *Triactinomyxon* (T2), bar - 0.25 μm; 49 - part of the sinuous septate junction of valvogenic cells of *Sphaeractinomyxon*, bar - 0.1 μm; 50, 51 - perpendicular and grazing section, respectively, of the valvogenic cell of *Sphaeractinomyxon* with different aspect of elongate dense bodies; arrow points at a polyribosomal helix, bars - 1 μm

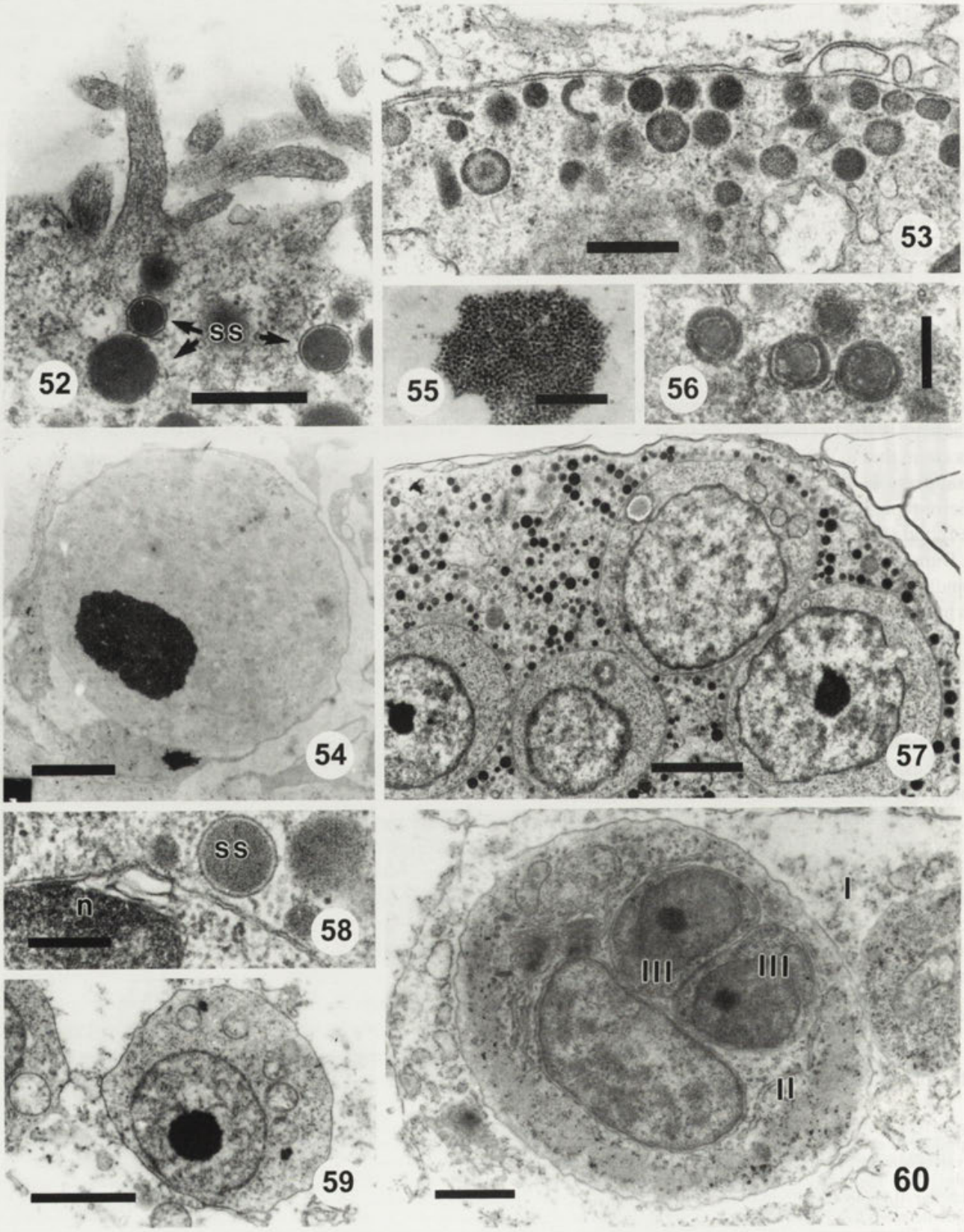

cells; pansporocyst, spore forming and sporoplasmic plasmodium cells in **A**). The stem cells, as exemplified by the infective cells of the **A** sporoplasm or by the inner cells of the **M** proliferative cycles, use to be extremely poor in cytoplasmic organelles yet their progeny displays sometimes far reaching structural diversification.

Ultrastructurally, the differences between **A** and **M** consist in greater variety of elements found in **M**. This applies especially to the proliferative (plasmodial) **M** stages. At their surface, projections much more pronounced than in **A** are well known to occur, often mobile or endocytotically active, sometimes reinforced with microtubular bundles (in *Leptotheca*/ *Ceratomyxa* - Desportes and Théodorides 1982); there may be a conspicuous surface coat (e.g., elaborately structured in *Myxobolus disparoides* - Uspenskaya 1982, or with more layers in *Henneguya* - Current 1979, Current and Janovy 1978). At the plasmodium surface, phagocytosis of whole host cells may also take place (e.g., *Myxobolus cerebralis* - Uspenskaya 1984).

Inside the plasmodial cytoplasm, the gamut of cell structures is also much wider; to quote some, extensive system of various vacuoles (e.g., in *Sphaeromyxa* - Grassé and Lavette 1978); dense crystalline inclusions (*Myxidium giardi* - Paperna et al. 1987); multilamellate bodies allegedly linked with lysosomal system (*Myxidium gadi* - Feist 1995) or striated fibers (*Kudoa lunata* - Lom and Dyková 1988).

The valvogenic cells of **M** spores, too, display structures missing in **A** spores, in which their absence is probably due to the thinness of **A** spore valves. First of all, there are microtubules supporting the surface of the valve cells and instrumental in formation of surface ridges: a unique feature is the occurrence of two types of microtubules in *Myxidium giardi*, 14 nm and 23 nm in diameter (Azevedo et al. 1989, Benajiba et al. 1993). Microtubules also reinforce the caudal processi of valve cells (e.g., in *Henneguya adiposa* - Current 1979). There are other features, too, such as special masses ("valve forming material", e.g., in *Henneguya* - Current 1979, Azevedo and Matos 1989) of dense substance to be deposited eventually beneath the cell membrane, or granular glycocalyx produced on the surface of the valves (in *Thelohanellus nikolskyi* - Desser et al. 1983b).

The richer variety of cell structures as well as of developmental stages seems to indicate that fish hosts offer more convenient conditions for expression of myxozoan evolutionary potential while there is some constraint in invertebrates, alternate hosts serving (always ?) just for completion of the sexual phase and transmission.

Phylogenetic relationships as reflected in cell structures.

Recently, molecular analyses of a few myxozoan species have indicated that the place of myxozoa is with metazoans rather than in the protistan realm. The results of Smothers et al. (1994) and of Schlegel et al. (1996) suggested their grouping with Bilateria, specifically nematodes while Siddall et al. (1995) postulate the inclusion of myxozoans as a branch of greatly derived parasitic cnidarians, as a sister group of the fish infecting narcomedusan *Polypodium hydriforme*. This is thus far the final step of considerations of metazoan affinities for Myxozoa starting with Štolc (1899) a century ago and focusing later on cnidarian relationships (especially Weill 1938, see also discussion in Siddall et al. 1995). This relationship seemed confirmed, in addition to similarities between nematocysts and polar capsules, by radial symmetry of some myxozoans and comparisons of nurse cell or trophamnion of developing narcomedusan embryo and pansporoblast or pansporocyts envelopes of myxozoan spores. The astonishing similarities in polar capsule and nematocyst structure and morphogenesis were brought to attention by electron microscopists (since Lom and de Puytorac 1965b and Westfall 1966).

Metazoan kinship of myxosporeans is supported by features such as structural and functional differentiation of cells, separation of soma and germen (although no tissues, sperms or oocytes occur), cellular junctions, and as listed by Siddall et al. (1995), collagen production and acetylcholine/cholinesterase activity. While the latter activity is the only character which has not yet been found or even examined in myxozoa, the single evidence of collagen postulated by Siddall et al. (1995) to be produced by pansporoblasts of *Thelohanellus nikolskyi* is not con-

Figs. 52-60. 52 - surface projections of sporoplasmic cell in *Sphaeractinomyxon*, bar - 0.5 µm; 53 - sporoplasmosomes of various appearance at the periphery of sporoplasm in *Aurantiactinomyxon*, bar - 0.5 µm; 54, 55 - aggregations of beta-glycogen granules in the sporoplasm of an *Aurantiactinomyxon* spore under low and higher magnification; bar - 3 µm and 0.5 µm, respectively; 56 - sporoplasmosomes of raabeia; bar - 0.25 µm; 57 - simple structure of infectious cells in *Triactinomyxon* (T1) sporoplasm, bar - 2 µm; 58 - the interface between infectious cell and sporoplasm consists of two membranes (*Sphaeractinomyxon*), bar - 0.25 µm; 59 - generative cell in the plasmodium of *Myxobolus cerebralis*, bar - 2 µm; 60 - the complex of two simple tertiary cells (III) within a secondary cell (II) of extrasporogonic cycle of *Sphaerospora renicola*; I - primary cell, bar - 1 µm

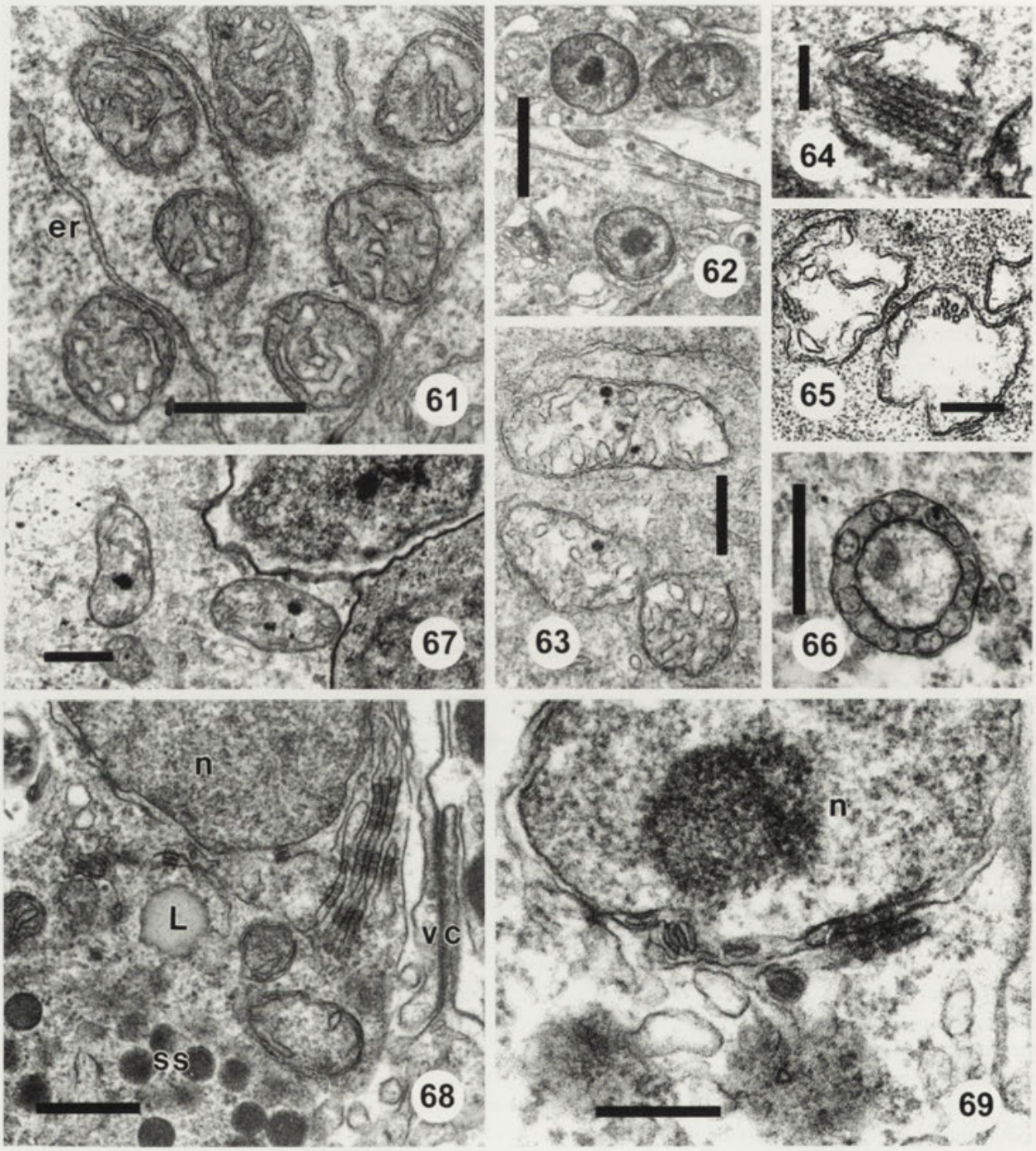

Figs. 61-69. 61 - mitochondria in the pregametic cell of *Aurantiactinomyxon*, bar - 0.5 μm; 62 - mitochondria in the pansporocyst envelope cells of *Aurantiactinomyxon*, bar - 1 μm; 63 - mitochondria in the early cell of raabeia, bar - 0.5 μm; 64, 65 - mitochondria in the pregametic cells of raabeia with microtubules sectioned longitudinally and transversally, bars - 0.2 μm and 0.4 μm, respectively; 66 - mitochondrium in the sporogonic plasmodium of *Kudoa lunata*; bar - 0.5 μm; 67 - mitochondria in the sporogonic plasmodium of *Myxobolus* sp. from the gills of *Lota lota*, bar - 0.5 μm; 68 - sporoplasmic cells of *Aurantiactinomyxon*: origin of annulate lamellae-like structure from nuclear envelopes, bar - 0.5 μm; 69 - origin of vesicles with stacks of discs from nuclear envelope in the sporoplasm of *Aurantiactinomyxon*, bar - 0.33 μm

vincing. The picture in their paper was reproduced from Desser et al. (1983b) where the caption said that the tropocollagen fibers were situated not at the pansporoblast but between the plasmodium and host tissue, being evidently secreted by the host cells.

Ultrastructural comparisons refer to several points:

Nematocysts vs. polar capsules.

Electron microscopy has not only confirmed the long known similarity of cnidarian nematocysts formed within

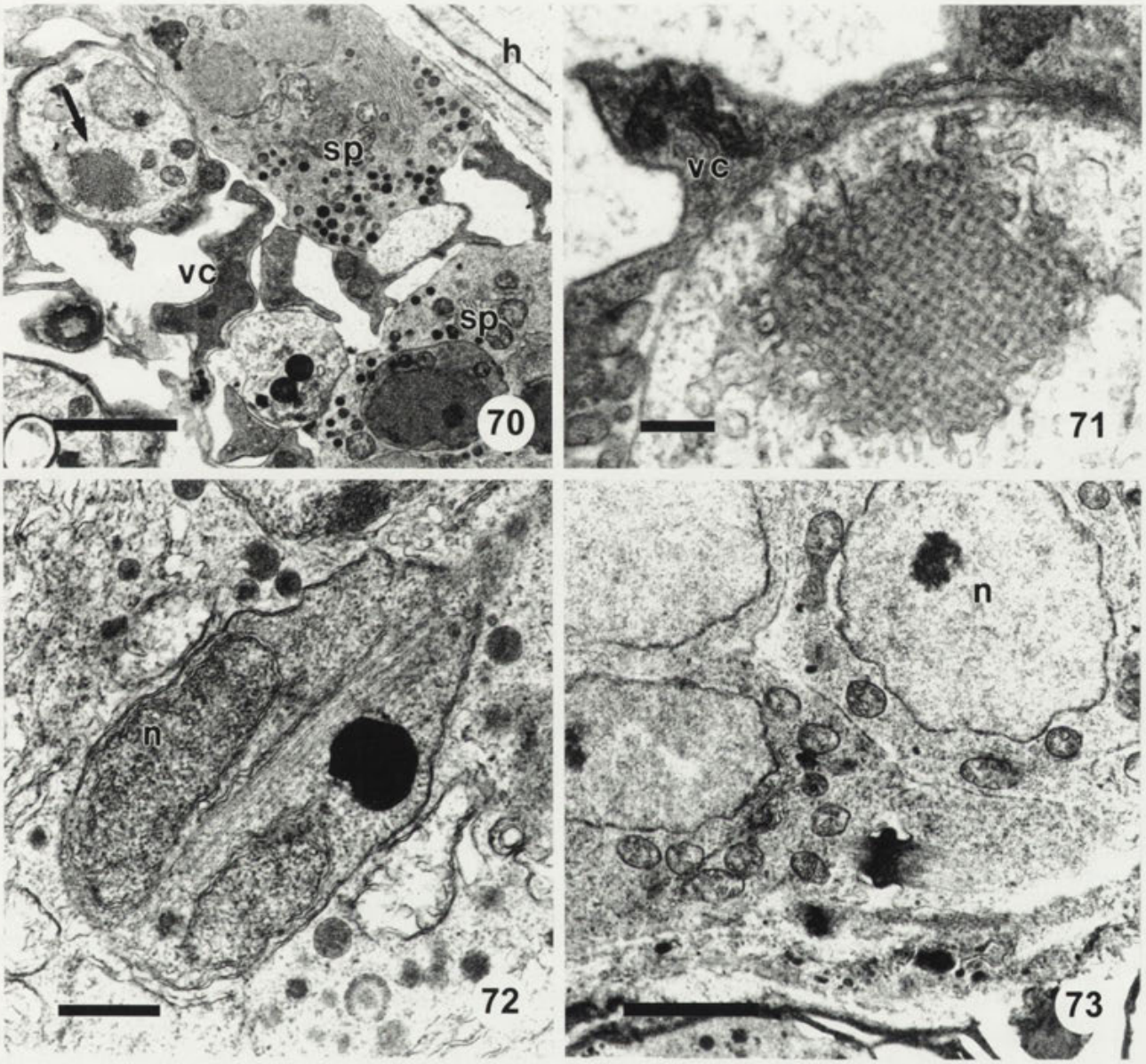

Figs. 70-73. 70 - sporoblast of *Aurantiactinomyxon* with the grid-like structure in the capsulogenic cell (arrow), bar - 5 μm; 71 - grid-like structure at higher magnification; 72 - microtubular bundle in the newly formed infectious cell in *Aurantiactinomyxon* sporoplasm, bars in 71, 72 - 0.5 μm; 73 - isthmus after a completed cell division of pregametic cells of *Aurantiactinomyxon* with persisting microtubules, bar - 2 μm

their nematocytes and polar capsules originating in the capsulogenic cells; it has shown that they must be homologous. Papers dealing with ultrastructure of nematocysts (Slautterback 1961, Westfall 1966, Watson 1988, Tardent 1995 - see these two last papers for other citations) and polar capsules (Lom and de Puytorac 1965b, Schubert 1968, Lom 1969, Ormieres 1970, Desser and Patterson 1978, Grassé and Lavette 1978, Current 1979, Current et al. 1979, Desportes and Théodorides 1982, Desser et al. 1983b, Marques 1984, Lom and Dyková 1988, Sitja-Bobadilla and Alvarez-Pellitero 1993c) have shown their essentially identical structure and morphogenesis involving formation of a voluminous primordium and a long, thin external tube. The only two cases in which capsulogenesis was observed to proceed without external tube formation were two rather atypical myxosporeans, *Fabespora vermicola* (Weidner and Overstreet 1979) and *Tetracapsula* (Canning et al. 1996).

Homology of the two organelles can be examined first of all in their morphogenesis. Existing data allow for a thorough comparison. The origin of the early capsule primordium in myxozoans was seen in cisternae

of the **rer** (Schubert 1968, Desser and Patterson 1978, Grassé and Lavette 1978,) or either in vesicles of **ser** or Golgi (Lom 1969); however, no decisive evidence was supplied and thus the origin from Golgi cannot be excluded. It is the vesicles of the latter which give rise to the first stage of the nematocyst primordium (Westfall 1966, Carré and Carré 1973, Holstein 1981,) in form of a saccule with a central granular product and a peripheral lucent layer; Watson (1988) specified the first stage as a result of fusion of vesicles of the trans part of Golgi. There is a close juxtaposition of **rer** cisternae to the Golgi vesicles in nematocyte cytoplasm perhaps in homology with capsulogenic cells. The very primordium then elongates at the apex to protrude as the external tube (**et**).

Similar to polar capsule primordium, nematocyst primordium is caged in a corset of microtubules (at variance with myxozoans, they extend from a pair of centrioles near the Golgi; centrioles are absent in **M**); the corset later shifts distally to the end of the **et**. The actual extrudible filament of nematocysts is formed by invagination of the **et**; the ultrastructural observations on this process (e.g., Slautterback and Fawcett 1959; Reisinger 1964; Holstein 1981) were corroborated by *in vivo* observations in the siphonoporan *Apolemia* (Carré and Carré 1973) and recorded by film by Holstein (1980). Similarly, all available evidence shows that the same process is involved in formation of the myxozoan polar filament (Lom and Dyková 1992b).

There are other identical features: pleated configuration of the resting polar filament; double layered capsule and also filament wall, the inner, lucent layer being composed of chitin in myxozoans and in many cnidarians, too; dense intracapsular matrix with various compact or granular inclusions; the dense supporting rods encircling the upper part of cnidosysts of various cnidarians (Westfall 1966; Carré and Carré 1973; Holstein 1981, 1988; Hausmann and Holstein 1985) are obviously identical with the dense ridges of myxozoans discussed above. The fine, 14 nm fibers slanted at 75° at the surface of the evaginated cnidocyst filament (Hausmann and Holstein 1985) seem comparable with the fine fibers set 16 or 11-12 nm apart on the not yet fully mature polar filament.

Cell junctions

Septate junctions (the term being first defined in *Hydra* by Wood 1959) are known to be the most characteristic cell junctions in invertebrates. The essential features of their organisation are identical from cnidarians (one can add from myxozoans) to arthropodes (Wood 1985), although there are variations in structural details. Similarly, the complexity of septate junctions varies in myxozoans, from junctions where the intermembraneous striation is hardly discernible to highly elaborate junctions of *Sphaeractinomyxon* shell valves. Septate and gap junctions of different complexity, desmosomal junctions (and hemidesmosomes in myxosporeans) as well as layers of transmembrane particles in the junctions (Desportes-Livage and Nicolas 1990) well known in e.g., septate junctions of *Hydra* (Wood 1977), clearly reveal metazoan affinities of myxozoans.

Other cell structures

Cnidaria are known to have mitochondria generally equipped with conventional flat cristae. Myxozoan mitochondria are sometimes related to those found in some protistans in that their cristae have tubular structure [in the genus *Henneguya*: in *H. psorospermica* plasmodium (Lom and de Pytorac 1965a); in *H. exilis* plasmodium and sporoplasm (Current and Janovy 1977) and *H. adiposa* sporoblast cells (Current 1979)] and in the presence of strikingly distinct DNA fibers . The lattice- or grid-like structures from *Ortholinea fluviatilis* cells (Lom and Dyková 1996) and from *Aurantiactinomyxon* bear, curiously enough, some resemblance to prolamellar bodies in higher plants (as described by Gunning and Steer 1975). This does not imply that they may be in any way related, their role is unknown.

A metazoan feature can also be seen to some extent in the intercellular spaces in myxosporean spores. Finding of actin-like microfilaments in such space in *Fabespora vermicola* spores (Weidner and Overstreet 1979) is in favour of such a conception.

If we accept myxozoans as a group of cnidarians (Siddall et al. 1995), they must had undergone incredibly drastic reduction of their organization in the course of adaptation to their present way of life, no matter how primitive branch of cnidarians was their source. Loss of organization in tissues of various types is understandable as a result of this reduction, and so is perhaps also the disappearance of oocytes and of spermatozoides which are flagellated (Carré and Carré 1992). Less understandable is, however, the disappearance of centrioles and notably the occurrence of a primitive protistan-type cryptomitosis. This proceeds without centrioles and with intranuclear spindle within persisting nuclear envelope. The early light microscope records of nuclear divisions in cnidarians report regular metazoan orthomitosis (e.g., McConell 1936). Centrioles were seen at the nucleus (e.g., Raikova 1980 in *Polypodium hydriforme*) and at

the sperm nucleus in *Cordylophora caspia* (Franzen 1996). Electron microscope observations confirm these findings (e.g., Szollosi 1964; Lentz 1966; and personal communications by R. L. Wood and U. Ehlers). Further, if we accept that gamete production was reduced to the simple type encountered in gamogenesis of actinospores, why is there another simple, autogamous sexual process in the myxosporeans as a part of the life cycle ?

Is it feasible to assume that regression due to parasitism involves such profound cytological changes as the type of mitosis, not to mention the appearance of tubular mitochondrial cristae in some cases ? If not, an elegant solution of the problem would be to accept Shostak's (1993) theory on symbiogenetic origin of cnidocysts in Cnidaria were it not for the contradictory sequence data indicating that cnidarians are phylogenetically older than myxozoans (Schlegel et al. 1996). Also, polar capsules do not seem to play an indispensable role in the life cycle of myxozoans and hence it is difficult to assume that they were an apomorphy proper to these organisms. The elucidation of the problem warrants further studies on cytology and sequence data of both groups as well as sequence analysis of cnidocyst and polar capsule proteins.

Ackonowledgements: This paper was supported by the Grant Agency of the Czech Republic, Grant No. 204/94/0286

REFERENCES

Andree K. B., Hedrick, R. P. (1997) Molecular phylogenetics unites actinosporean and myxosporean stages of *Myxobolus cerebralis*, the causative agent of whirling disease in salmonid fish. *J. Eukaryot. Microbiol.* **44:** (in press)

Azevedo C., Matos E. (1989) Some ultrastructural data on the spore development in a *Henneguya* sp. parasite of the gill of a Brazilian fish. *Parasitol. Res.* **76:** 131-134

Azevedo C., Lom J., Corral L. (1989) Ultrastructural aspects of *Myxidium giardi* (Myxozoa, Myxosporea), parasite of the European eel *Anguilla anguilla*. *Dis. aquat. Org.* **6:** 55-61

Benajiba M. H., Marques A. (1993) The alternation of actinomyxidian and myxosporidian sporal forms in the development of *Myxidium giardi* (parasite of *Anguilla anguilla*) through oligochaetes. *Bull. Eur. Ass. Fish. Pathol.* **13:** 100-103

Benajiba M. H., Marques A., Bouix G. (1993) Ultrastructural data on the sporogenesis of *Myxidium giardi* Cépede, 1906 (Myxozoa, Myxosporidia), parasite of *Anguilla anguilla* (Teleostea). *Europ. J. Protistol.* **29:** 254-261

Canning E. U., Okamura B., Curry A. (1996) Development of a myxozoan parasite *Tetracapsula bryozoides* gen. n. et sp.n. in *Cristatella mucedo* (Bryozoa: Phylactolaemata). *Folia Parasitol.* **43:** 249-261

Carré C., Carré D. (1973) Etude du cnidome et de la cnidogénèse chez *Apolemia uvaria* (Lesueur, 1811) (Siphonophore physonecte). *Exp. Cell Res.* **81:** 237-249

Carré D., Carré C. (1992) Biologie et étude ultrastructurale des spermatozoides du cnidaire *Clytia hemispherica* (Leptomedusae): mise en évidence d'un processus acrosomal. *Can. J. Zool.* **70:** 866-873

Current W. L. (1979) *Henneguya adiposa* Minchew (Myxosporida) in the channel catfish: ultrastructure of the plasmodium wall and sporogenesis. *J. Protozool.* **26:** 209-217

Current W. L., Janovy J. Jr. (1977) Sporogenesis in *Henneguya exilis* infecting the channel catfish: an ultrastructural study. *Protistologica* **13:** 157-167

Current W.L., Janovy J Jr. (1978) Comparative study of ultrastructure of interlamellar and intralamelar types of *Henneguya exilis* Kudo from channel catfish. *J. Protozool.* **25:** 56-65

Current W. L., Janovy J. Jr., Knight S. A. (1979) *Myxosoma funduli* Kudo (Myxosporida) in *Fundulus kansae*: ultrastructure of the plasmodium wall and of sporogenesis. *J. Protozool.* **26:** 574-583

Daniels S. B., Hermann R. L., Burke C. N. (1976) Fine structure of an unidentified protozoan in the epithelium of rainbow trout exposed to water with *Myxosoma cerebralis*. *J. Protozool.* **23:** 402-410

Desportes I., Théodorides J. (1982) Données ultrastructurales sur la sporogénese de deux myxosporidies rapportées aux genres *Leptotheca* et *Ceratomyxa* parasites de *Merluccius merluccius* (L.) Téleostéen Merluciidae). *Protistologica* **18:** 533-557

Desportes-Livage I., Nicolas G. (1990) The plasma membrane of myxosporidian valve cells: Freeze fracture data. *J. Protozool.* **37:**243-249

Desser S. S., Patterson W. B. (1978) Ultrastructural and cytochemical observations on sporogenesis of *Myxobolus* sp. (Myxosporidia: Myxobolidae) from the common shiner *Notropis cornutus*. *J. Protozool.* **25:** 314-326

Desser S. S., Molnar K., Horvath I. (1983a) An ultrastructural study of the myxosporeans, *Sphaerospora angulata* and *Sphaerospora carassii* in the common carp, *Cyprinus carpio* L. *J. Protozool.* **30:** 415-422

Desser S. S., Molnar K., Weller I. (1983b) Ultrastructure of sporogenesis of *Thelohanellus nikolskii* Akhmerov, 1955 (Myxozoa, Myxosporea) from the common carp *Cyprinus carpio*. *J. Parasitol.* **69:** 504-518

Dyková I., Lom J. , Korting W. (1990) Light and electron microscopic observations on the swimbladder stages of *Sphaerospora renicola*, the parasite of carp (*Cyprinus carpio*). *Parasitol. Res.* **76:** 228-237

El-Matbouli M., Hoffmann R. W. (1989) Experimental transmission of two *Myxobolus* spp. developing bisporogony via tubificid worms. *Parasitology Research* **76:** 461-464

El-Matbouli M., Fischer-Scherl T., Hoffmann R. W. (1990) Light and electron microscopic studies on *Myxobolus cotti* El-Matbouli and Hoffmann, 1987 infecting the central nervous system of the bullhead (*Cottus gobio*). *Parasitol Res.* **76:** 219-227

El-Matbouli M., Hoffmann R. W., Mandok C. (1995) Light and electron microscopic observations on the route of the triactinomyxon-sporoplasm of *Myxobolus cerebralis* from epidermis into rainbow trout cartilage. *J. Fish Biol.* **46:** 919-935

Feist S. W. (1995) Ultrastructural aspects of *Myxidium gadi* (Géorgevitch, 1916) (Myxozoa: Myxosporea). *Europ. J. Protistol.* **31:** 309-317

Franzen A. (1996) Ultrastructure of spermatozoa and spermiogenesis in the hydrozoan *Cordylophora lacustris* with comments on structure and evolution of the sperm in the Cnidaria and the Porifera. Invertebr. *Reprod. Develop.* **29:** 19-26

Grassé P.-P., Lavette A. (1978) La myxosporidie *Sphaeromyxa sabrazesi* et le nouvel embranchement des Myxozoaires (Myxozoa). Recherches sur l'état pluricellulaire primitif et considérations phylogénetiques. *Ann. Sci. Natur.*, Zoologie (Paris) **20:** 193-285

Grossheider G. (1994) Untersuchungen zum Lebenszyklus von *Sphaerospora renicola* Dyková et Lom, 1982 und *Hoferellus cyprini* Berg, 1898 (Myxozoa: Myxosporea) aus der Niere des Karpfens *Cyprinus carpio* L. Thesis, University of Hannover, 1-143

Gunning B. E. S., Steer M. W. (1975) Ultrastructure and the biology of plant cells. Edward Arnold Ltd., London

Hausmann K., Holstein T. (1985) Bilateral symmetry in the cnidocil-nematocyst complex of the freshwater medusa *Craspedacusta sowerbii* Lankester (Hydrozoa, Limnomedusae). *J. Ultrastruct. Res.* **90:** 89-104

Holstein T. (1980) Morphogenese der Nematocysten bei *Hydra attenuata* (Cnidaria). *Wiss. Film* Nr. **25:** 14-22

Holstein T. (1981) The morphogenesis of nematocytes in *Hydra* and *Forskalia*: an ultrastructural study. *J. Ultrastruct. Res.* **75:** 276-290

Holstein T. (1988) The cnidocil apparatus of hydrozoans: a progenitor of higher metazoan mechanoreceptors ? In: The Biology of Nematocysts, (Eds. D. H. Hessinger and H. M. Lenhoff), Academic Press Inc., San Diego, 53-73

Ikeda J. (1912) Studies on some sporozoan parasites of sipunculoids. I. The life history of a new Actinomyxidian, *Tetractinomyxon intermedium* gen. et sp. nov. *Arch. Protistenkd.* **25:** 240-272

Janiszewska J. (1955) Actinomyxidia. Morphology, ecology, history of investigations, systematics, development. *Acta Parasit. Polon.* **2:** 405-443

Johnston A. K. (1985): Pathogenesis and life cycle of the myxozoan *Parvicapsula* sp. infecting marine cultured coho salmon. PhD Dissertation, University of Washington, Seattle

Kent M. L., Hedrick R. P. (1985) PKX, the causative agent of proliferative kidney disease (PKD) in Pacific salmonid fishes and its affinities with the Myxozoa. *J. Protozool.* **32:** 254-260

Kent M. L., Margolis L., Corliss J. O. (1994) The demise of a class of protists: Taxonomic and nomenclatural revisions proposed for the protist phylum Myxozoa Grassé, 1970. *Can. J. Zool.* **72:** 932-937

Koller E. (1994) Verbreitung von Actinosporea in zwei Salmoniden-Teichwirtschaften. Diploma thesis, University of Munich, 1-99

Léger L. (1904) Considérations sur le genre *Triactinomyxon* et les Actinomyxidies. *C. R. Soc. Biol. Paris* **56:** 846-848

Lentz T. L. (1966) The cell biology of *Hydra*. North Holland Publ. Co. Amsterdam, 1-199

Lester R. J. G. (1982) *Unicapsula seriolae* n.sp. (Myxosporea, Multivalvulida) from Australian yellowtail kingfish *Seriola lalandi*. *J. Protozool.* **29:** 584-587

Lom J. (1969) Notes on the ultrastructure and sporoblast development in fish parasitizing myxosporidia of the genus *Sphaeromyxa*. *Z. Zellforsch.* **97:** 416-437

Lom J., Dyková I. (1988) Sporogenesis and spore structure in *Kudoa lunata* (Myxosporea, Multivalvulida). *Parasitol. Res.* **74:** 521-530

Lom J., Dyková I. (1992a) Fine structure of *Triactinomyxon* early stages and sporogony: Myxosporean and actinosporean features compared. *J. Protozool.* **39:** 16-27

Lom J., Dyková I. (1992b) Protozoan parasites of fishes. Development in Aquaculture and Fisheries Sciences, Elsevier, Amsterdam

Lom J., Dyková I. (1996) Notes on the ultrastructure of two myxosporean (Myxozoa) species, *Zschokkella pleomorpha* and *Ortholinea fluviatilis*. *Folia Parasitol.* **43:** 189-202

Lom J., Puytorac P. de (1965a) Observations sur l'ultrastructure des trophozoites de Myxosporidies. *C. R. Acad. Sci. Paris* **260:** 2588-2590

Lom J., Puytorac P. de (1965b) Studies on the myxosporidian ultrastructure and polar capsule development. *Protistologica* **1:** 53-65

Lom J., Dyková I., Lhotáková Š. (1982) Fine structure of *Sphaerospora renicola* Dyková and Lom, 1983, a myxosporean from carp kidney and comments on the origin of pansporoblasts. *Protistologica* **18:** 489-502

Lom J., Feist S. W., Dyková I., Kepr T. (1989) Brain myxoboliasis of bullhead, *Cottus gobio* L., due to *Myxobolus jiroveci* sp.nov.: light and electron microscope observations. *J. Fish Dis.* **12:** 15-27

Lom J., Yokoyama H., Dyková I. (1997) Comparative ultrastructure of *Aurantiactinomyxon* and *Raabeia*, actinosporean stages of myxozoan life cycles. *Arch. Protistenkd.* **148:** 173-189

Markiw A. (1989) Portals of entry for salmonid disease in rainbow trout. *Dis. aquat. Org.* **6:** 7-10

Marques A. (1982) Complexes synaptonémaux et stades initiaux chez les Actinomyxidies. *C.R. Acad. Sci. Paris* **295:** 501-504

Marques A. (1983) La fécondation et les premieres stades de la sporogénese d'une Actinomyxidie. *C.R. Acad. Sci. Paris* **296:** 717-720

Marques A. (1984) Contribution à la connaissance des Actinomyxidies. Ultrastructure, cycle biologique, systématique. Thesis. Université S.T.L. Montpellier

Marques A. (1986) La sexualité chez les Actinomyxidies: Etude chez *Neoactinomyxon eiseniellae* (Ormieres et Frézil, 1969), Actinosporea, Noble, 1980; Myxozoa, Grassé, 1970. *Ann. Sci. Nat., Zool., Paris* 13e sér., **8:** 81-101

McConnel C. (1936) Mitosis in *Hydra*. Mitosis on the indifferent interstitial cells of *Hydra*. Wilh. *Roux Arch f. Entwicklungsmech.* **135:** 202-210

Odening K., Walter G., Bockhardt I. (1989) Zum Infektionsgeschehen bei *Sphaerospora renicola* (Myxosporidia). *Angew. Parasitol.* **30:** 131-140

Ormieres R. (1970) Formation des capsules polaires dans la spore de l'Actinomyxidie *Aurantiactinomyxon eiseniellae* Orm.Fré. (Etude ultrastructurale). *C.R. Acad. Sc. Paris* **271:** 2326-2328

Paperna I., Hartley A. H., Gross R. H. (1987) Ultrastructural studies on the plasmodium of *Myxidium giardi* (Myxosporea) and its attachment to the epithelium of urinary bladder. *Int. J. Parasitol.* **17:** 813-819

Puytorac P. de (1963) L'ultrastructure des cnidocystes de l'Actinomyxidie: *Sphaeractinomyxon amanieui* sp.nov. *C. R. Acad. Sc. Paris* **256:** 1594-1596

Raikova E. V. (1980) Morphology, ultrastructure and development of the parasitic larva and its surrounding trophamnion of *Polypodium hydriforme* Ussov (Coelenterata). *Cell Tissue Res.* **206:** 487-500

Reisinger E. (1964) Das Integument der Coelenteraten, acoelomaten und coelomaten Würmer. *Studium gen.* **17:** 125-142

Schlegel M., Lom J., Stechmann A., Bernhard D., Leipe D., Dyková I., Sogin M. L. (1996) Phylogenetic analysis of complete small subunit ribosomal RNA coding region of *Myxidium lieberkuehni*: Evidence that Myxozoa are Metazoa and related to Bilateria. *Arch. Protistenkd.* **147:** 1-9

Schubert G. (1968) Elektronenmikroskopische Untersuchungen zur Sporenentwicklung von *Henneguya pinnae* Schubert (Sporozoa, Myxosporidea, Myxobolidae). *Z. Parasitenkd.* **30:** 557-77

Shulman S. S. (1966) Myxosporidia of the fauna of USSR. Nauka, Leningrad. (in Russian)

Shostak S. (1993) A symbiogenetic theory for the origins of cnidocysts in Cnidaria. *BioSystems* **29:** 49-58

Siau Y. (1979) Observations en microscopie electronique de complexes synaptonématiques chez des Myxosporidies. *C. R. Acad. Sc. Paris* **288:** 403-404

Siddall M. E., Martin D. S., Bridge D., Desser S. S., Cone D. K. (1995) The demise of a phylum of protists: phylogeny of Myxozoa and other parasitic Cnidaria. *J. Parasitol.* **81:** 961-967

Sitja-Bobadilla A., Alvarez-Pellitero P. (1993a) Light and electron microscopical description of *Ceratomyxa labracis* n. sp. and a redescription of *C. diplodae* (Myxosporea: Bivalvulida) from wild and cultured Mediterranean sea bass *Dicentrarchus labrax* (L.) (Teleostei: Serranidae). *Systematic Parasitol.* **26:** 215-223

Sitja-Bobadilla A., Alvarez-Pellitero P. (1993b) *Zschokkella mugilis* n.sp. (Myxosporea: Bivalvulida) from mullets (Teleostei: Mugilidae) of Mediterranean waters: light and electron microscopic description. *J. Euk. Microbiol.* **40:** 755-764

Sitja-Bobadilla A., Alvarez-Pellitero P. (1993c): Ultrastructural and cytochemical observations on the sporogenesis of *Sphaerospora testicularis* (Protozoa: Myxosporea) from Mediterranean sea bass, *Dicentrarchus labrax* (L.). *Europ. J. Protistol.* **29:** 219-229

Sitja-Bobadilla A., Alvarez-Pellitero P. (1995) Light and electron microscopic description of *Polysporoplasma* n.g. (Myxosporea: Bivalvulida), *Polysporoplasma sparis* n.sp. from *Sparus aurata* (L.) and *Polysporoplasma mugilis* n.sp. from *Liza aurata* L. *Europ. J. Protistol.* **31:** 77-89

Slautterback D. B. (1961) Nematocyst development. In: The Biology of *Hydra*, (Eds. H. M. Lenhoff and W. F. Loomis). Univ. of Miami Press, Coral Gables, Florida, 79-129

Slautterback D. B., Fawcett D. W. (1964) The development of the cnidoblasts in Hydra. An electron microscope study of cell differentialion *J. Biophys. Biochem. Cytol.* **5:** 441-452

Smothers J. F., Dohlen C. D. von, Smith L. H. Jr., Spall R. D. (1994) Molecular evidence that the myxozoan protists are metazoans. *Science* **265:** 1719-1721

Štolc A. (1899) Actinomyxidies, nouveau groupe de Mesozoaires parent des Myxosporidies. *Bull. Internat. Acad. Sci. Boheme* **22:** 1-12

Szollosi D. (1964) The structure and function of centrioles and their satellites in the jellyfish *Phiallidium gregarium*. *J. Cell Biol.* **21:** 165-179

Tandler B., Hoppel C. L. (1972) Mitochondria. Academic Press Inc., New York

Tardent P. (1995) The cnidarian cnidocyte, a high-tech cellular weaponry. *BioEssays* **17:** 351-362

Thélohan P. (1895) Recherches sur les myxosporidies. *Bull.Sci. Fr. Belg.* **26:** 100-394

Trouiller A., El-Matbouli M., Hoffmann R. W. (1996) A new look at the life cycle of *Hoferellus carassii* in the goldfish (*Carassius auratus auratus*) and its relation to "kidney enlargement disease". *Folia Parasitol.* **43:** 173-187

Uspenskaya A. V. (1982) The ultrastructure of the so-called "cysts" of several myxosporean species. *Parazitologiya* **16:** 13-17 (in Russian)

Uspenskaya A. V. (1984) Cytology of myxosporidians. Nauka, Leningrad. (in Russian)

Uspenskaya A. V. (1995) Alternation of actinosporean and myxosporean phases in the life cycle of *Zschokkella nova* (Myxozoa). *J. Euk. Microbiol.* **42:** 665-668

Voronin V. N., Chernysheva N. B. (1993) An intracellular gill parasite as the possible causative agent of mortality during swim-bladder inflammation in common carp, *Cyprinus carpio* L. *J. Fish Dis.* **16:** 609-611

Watson G. M. (1988) Ultrastructure and cytochemistry of developing nematocysts. In: The Biology of Nematocysts. (Eds. D. A. Hessinger and H. M. Lenhoff) Academic Press Inc., San Diego, 143-164

Weidner E., Overstreet R. M. (1979) Sporogenesis of a myxosporidan with motile spores. *Cell Tissue Res.* **201:** 331-342

Weill R. (1938) L'interpretation des Cnidosporidies et la valeur taxonomique de leur cnidome. Leur cycle comparée à la phase larvaire des Narcomeduses Cuninides. *Trav. Stat. Zool. Wimmereaux* **13:** 727-744

Westfall J. (1966) The differentiation of nematocysts and associated structures in the cnidaria. *Z. Zellforsch.* **75:** 381-403

Wood R. L. (1959) Intercellular attachment in the epithelium of *Hydra* as revealed by electron microscopy. *J. Biophysic. Biochem. Cytol.* **6:** 343-352

Wood R. L. (1977) The cell junctions of hydra as viewed by freeze-fracture replication. *J. Ultrastruct. Res.* **58:** 299-315

Wood R. L. (1985) The use of hydra for studies of cellular ultrastructure and cell junctions. *Arch. Sc. Geneve* **38:** 371-383

Wolf K., Markiw M. E. (1984) Biology contravenes taxonomy in the Myxozoa: new discoveries show alternation of invertebrate and vertebrate hosts. *Science* **225:** 1449-1452

Yamamoto T., Sanders J. E. (1979) Light and electron microscopic observations of sporogenesis in the myxosporida, *Ceratomyxa shasta* (Noble, 1959). *J. Fish Dis.* **2:** 411-428

Yokoyama H., Ogawa K., Wakabayashi H. (1993) Involvement of *Branchiura sowerbyi* (Oligochaeta: Annelida) in the transmission of *Hoferellus carassii* (Myxosporea: Myxozoa), the causative agent of kidney enlargement disease (KED) of goldfish *Carassius auratus*. *Fish Pathol.* (formerly *Gyobyo Kenkyu*) **23:** 135-139

Yokoyama H., Ogawa K. Wakabayashi H. (1995a) Chemoresponse of actinosporean spores of *Myxobolus cultus* to skin mucus of goldfish *Carassius auratus*. *Dis. aquat. Org.* **21:** 7-11

Yokoyama H., Ogawa K., Wakabayashi H. (1995b) *Myxobolus cultus* n.sp. (Myxosporea: Myxobolidae) in the goldfish *Carassius auratus* transformed from the actinosporean stage in the oligochaete *Branchiura sowerbyi*. *J. Parasitol.* **81:** 446-451

Received on 18th March, 1997

Acta Protozoologica (1997) 36: 105 - 110

ACTA
PROTOZOOLOGICA

Observations on the Morphology of *Caenomorpha uniserialis* Levander, 1894 (Ciliophora, Heterotrichida) Isolated from a Wastewater Treatment Plant

Olivier DECAMP and Alan WARREN

Department of Zoology, The Natural History Museum, London, UK

Summary. The morphology and infraciliature of *Caenomorpha uniserialis* Levander, 1894, isolated from a wastewater treatment plant, were studied. A comparison of these results with previous descriptions of *C. uniserialis* in the literature reveals a wider range of cell size and important differences in the infraciliature. The relationships between environmental conditions and variations in the characters used for the identification of *C. uniserialis* are discussed.

Key words: Caenomorphidae, *Caenomorpha uniserialis*, infraciliature, morphology, sapropel.

INTRODUCTION

The family Caenomorphidae Poche, 1913 (suborder Armophorina), comprises the genera *Cirranter* Jankowski, 1964, *Ludio* Penard, 1922, and *Caenomorpha* Perty, 1852. Members of this family have been described as "small, with a round or conical body which is twisted to the left. The body cilia consist of small kineties or cirrus-like tufts" (Small and Lynn 1985).

The genus *Caenomorpha* is medusoid-shaped with an armour-like shield. The somatic ciliation is reduced, consisting of a perizonal stripe of five ciliary rows winding around the body above the adoral zone of membranelles (AZM), a caudal set of kineties, and one or two anterior rows of cirri (Jankowski 1964). In the case of *C. medusula* Perty, 1852, and *C. uniserialis* Levander, 1894, the anterior rows of cirri consist of 1-2 kineties arranged in a zig-zag pattern (Fernandez-Galiano and Fernandez-Leborans 1980, Martin-Gonzalez et al. 1987, Sola et al. 1990).

The numbers of macronuclei, posterior spines, and the bell ciliation are used for species identification. Species range from simple cells, such as *C. simplex* Jankowski, 1964, to complex cells, such as *C. sapropelica* Kahl, 1927 or *C. lauterborni* Kahl, 1927. The number of species assigned to the genus *Caenomorpha* ranges from 8 (Jankowski 1964), to 10 (Sola et al. 1990), although Kahl (1935) also recognised 6 variants of *C. medusula*. All species are sapropelic, mostly found in fresh water, but some are present in marine habitats (Kahl 1935, Curds et al. 1983, Sola et al. 1990, Carey 1992).

Most morphological studies of *Caenomorpha* have been carried out on *C. medusula* (Villeneuve-Brachon 1940, Rosa 1976, Fernandez-Galiano and Fernandez-Leborans 1980, Dragesco and Dragesco-Kernéis 1986, Martin-Gonzalez et al. 1987). *Caenomorpha uniserialis*

Address for correspondence: Olivier Decamp, Faculty of Applied Biological Science, Hiroshima University, 4-4 Kagamiyama 1-Chome, Higashi-Hiroshima 739, Japan; Fax: +81-824-247059; E-mail: ode@ue.hiroshima-u.ac.jp

has been investigated by Kahl (1935), Jankowski (1964) and Sola et al. (1990). Sola et al. (1990) described the morphology of *C. uniserialis* in detail, including the somatic and buccal infraciliature of specimens isolated from river lagoon sediments.

Specimens for the present study were isolated from artificially-constructed reed beds used for the treatment of wastewaters by a process known as the Root Zone Method. Observations of cells were carried out both *in vivo* and following impregnation with silver. The aim of this paper is to provide new data on the morphology of *C. uniserialis*. The relationship between environmental conditions and the characters used for the identification of *C. uniserialis* are discussed.

MATERIALS AND METHODS

Samples were collected between September and November 1993, from the wastewater treatment plant at Audlem (Cheshire, United Kingdom), operated by North West Water Ltd. There were ten artificially-constructed reed beds at Audlem, each 6.0 m long x 2.3 m wide x 0.6 m deep. A variety of planting media were used including soil, gravel, and compressed fly-ash. Eight beds were planted with the common reed *Phragmites australis* whilst two were left unplanted. Each bed was dosed with 1.5 m^3 of settled sewage per day, which is a loading equivalent of 4.5-4.7 pe/m^2. The population equivalent (pe) is the volume of wastewater produced per capita per day and is around 300 dm^3 in the UK (Gray 1989).

The interstitial fluid within an unplanted soil bed was sampled by pipette. The upper layers of soil were removed until the liquid level was reached. The interstitial liquid and soil were gently homogenised before being extracted with a pipette. Redox potential and conductivity were measured using a portable Oakton Water Test meter (model no. WD-00677-00, Oakton Inc., USA). The samples were brought back to the laboratory for identification of the ciliated protozoa, measurement of biochemical oxygen demand (BOD), and enumeration of total bacteria and *Escherichia coli*.

The ciliates were identified on a morphological basis by observing cells *in vivo* using differential interference contrast (DIC) light microscopy, and by silver carbonate staining (Fernandez-Galiano 1976). All measurements were made after fixation in osmium (OsO_4) vapour.

Escherichia coli were enumerated by a plate count method following growth on MacConkey agar for 24 hours at 37°C. Total bacteria were enumerated by a plate count method following growth on nutrient agar for 3 days at 20°C.

RESULTS AND DISCUSSION

Description of the environment

The samples were taken near the input pipe where the bed was rich in organic matter and bacteria (Table 1). The wastewater was characterised by a BOD ranging from 44 mg/l to 312 mg/l. The concentration of total bacteria and *E. coli* in the influent ranged from 6.5 x 10^6/ml to 1.68 x 10^9/ml for total bacteria, and from 1.76 x 10^5/ml to 5.3 x 10^6/ml for *E. coli*. These ranges of BOD and bacterial concentrations are typical of primary settled sewage (Painter 1971, Batchelor et al. 1990, Butler et al. 1990).

Table 1. Physicochemical and bacterial characteristics of the interstitial fluid from the soil reed bed at Audlem, Cheshire, UK

temperature (°C)	7.1 - 8.6
pH	6.8 - 7.1
conductivity (mS)	655 - 973
redox-potential (mV)	-20 - -23
BOD_5 (mg/l)	270 - 410
total number of bacteria (cfu/ml)*	1.0 x 10^5 - 2.5 x 10^6
number of *E. coli* (cfu/ml)	2.66 x 10^4 - 3.21 x 10^5

*cfu - colony forming units

Gambrell and Patrick (1978) characterised anoxic environments has having a redox potential between +400 mV and -400 mV. The redox potential within the reed bed was between -20 mV and -23 mV thus indicating an absence of free dissolved oxygen. The relatively low redox potential recorded here is consistent with those recorded previously in similar environments, e.g. between +60 mV and -60 mV for unplanted soil beds (Hofmann 1990); between 0 and -100 mV for reed beds with dying roots (Armstrong et al. 1990).

The ciliate community of the interstitial fluid was dominated by *Metopus es, M. striatus*, *Tetrahymena* sp., *Caenomorpha medusula*, *C. uniserialis* and *Plagiopyla* sp. (Decamp 1996a,b). These ciliates, with the possible exception of *Tetrahymena* which is encountered in a wide range of environments, are typical of anaerobic-anoxic environments (Madoni 1990, Foissner et al. 1992, Patterson and Hedley 1992).

Description of *Caenomorpha uniserialis*:

General morphology (Figs. 1,2,4; Table 2)

The specimens observed in our samples showed a great variety of size, with a mean total length of 66.1µm (36-90µm) after fixation in osmium vapour. The figures given by Sola et al. (1990), with the same fixation process, are within the range of measurements reported here (Table 2). The nuclear apparatus consisted of a large spherical macronucleus (around 15µm diameter) and a single micronucleus (Figs. 1, 2, 4). This is consistent with previous descriptions of *C. uniserialis* (Jankowski 1964, Sola et al. 1990). The lower part of the cell was characterised by a long spine and a second highly complicated spine,

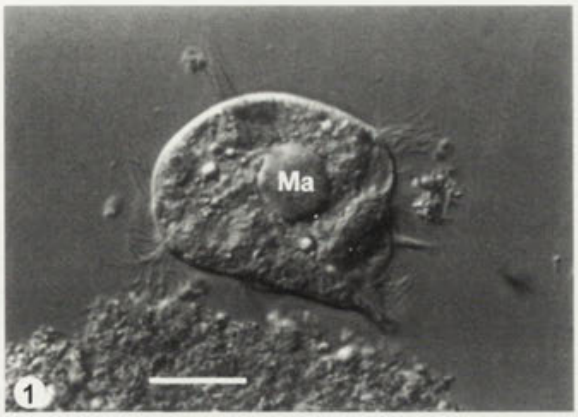

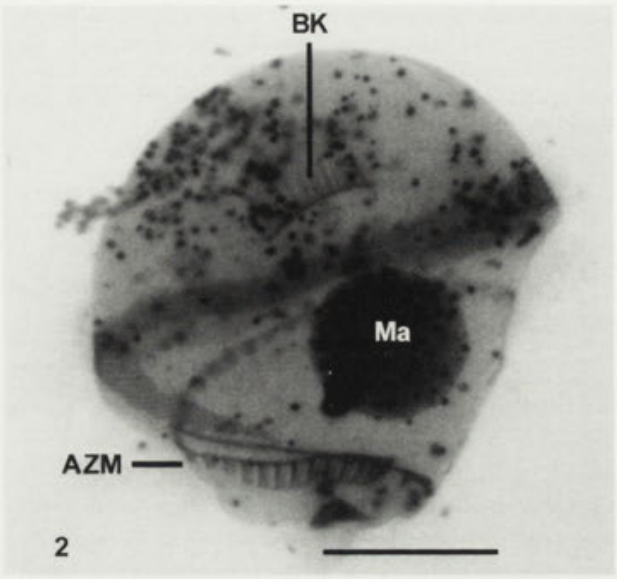

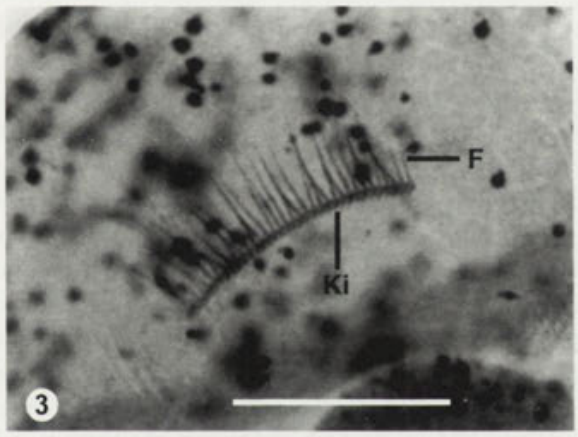

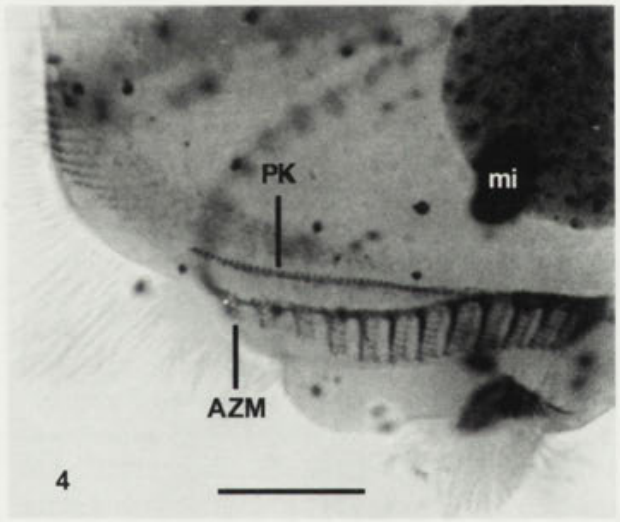

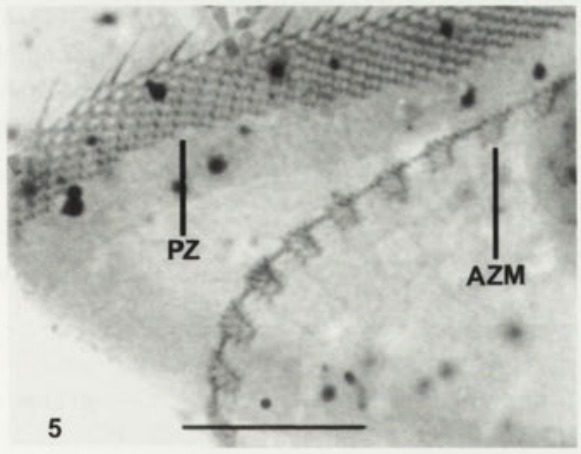

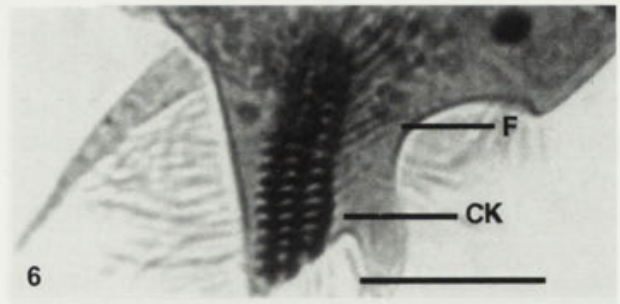

Figs. 1-6. *Caenomorpha uniserialis in vivo* (Fig. 1) and after silver carbonate impregnation (Figs. 2-6). 1 - using differential interference contrast microscopy, bar - 20µm; 2 - infraciliature and nuclear apparatus, bar - 20µm; 3 - bell kinety, bar - 10µm; 4 - posterior region of cell, showing the paroral kinety and AZM, bar - 10µm; 5 - perizonal zone and AZM in the median part of the cell, bar - 10µm; 6 - infraciliature associated with the spine complex, bar - 10 µm. Abbreviations: AZM - adoral zone of membranelles; BK - bell kinety; CK - caudal kinety; F - fibrillar system; Ki - kinetosomes; Ma - macronucleus; mi - micronucleus; PK - paroral kinety; PZ - perizonal zone

similar to those described by Kahl (1935), Jankowski (1964), Sola et al. (1990), and Foissner et al. (1992).

Both the average size and the range of sizes exhibited by *C. uniserialis* isolated during the present study were much greater than those reported by Sola et al. (1990) (Table 2). These differences may be explained by physicochemical and biological conditions in the environment from which they were isolated. Cell size of ciliates is

Table 2. Biometric measurements of *C. uniserialis*: total length (in μm) of specimens isolated from the wastewater treatment plant at Audlem (present study) compared with those isolated from a river lagoon in Spain (Sola et al. 1990). All measurements following fixation in OsO_4 vapour

	present study (n = 27)	Sola et. al (1990) (n = 15)
minimum	36.0	52.0
maximum	90.0	64.9
mean	66.1	56.9
standard of deviation	13.0	4.3
standard error	2.5	1.1
coefficient of variation	19.7	1.9

known to be influenced by environmental parameters such as temperature (Laybourn-Parry 1984), salinity (Jones and Gates 1994), presence of predators (Kuhlmann and Heckmann 1985), and the amount, size and type of food available (Hewett 1980, Laybourn-Parry 1984, Fenchel 1987, Perez-Uz 1993). The presence of food has a direct impact on the growth rate of the population and on the cell volume. For example, after the onset of starvation, cell division continues for 1-2 generations, thus producing smaller-sized cells (Fenchel 1987). Conversely ciliates in exponential growth phase are larger than cells in stationary phase (Perez-Uz 1993). The richer environment of the wastewater treatment plant with its high concentration of bacteria could explain the larger average size of the *C. uniserialis* observed here compared to that reported by Sola et al. (1990) for specimens isolated from a river lagoon. The wider range of size could be explained by the variety of microniches found in the soil beds; ciliates occupying microniches with high concentrations of bacteria are likely to be in exponential growth, whereas those in areas with lower concentrations of bacteria are likely to be in lag or stationary phase and therefore be smaller in size. The variation in concentration of bacteria may be explained by the irregular flow of wastewater through the soil bed or the relative distance from the input pipe. A possible alternative explanation for the differences between the present population and that studied by Sola et al. (1990) is that *C. uniserialis* includes two (or more) genotypically differentiated strains or sibbling species. Culture experiments in controlled laboratory conditions are necessary to test these hypotheses.

Infraciliature (Figs. 2-6; Table 3)

The infraciliature was located in four areas of the cell (Fig. 2): (i) the bell kinety, located in the anterior part of the body, (ii) the perizonal zone, which wound around the body on the edge of the pellicular armour following the upper margin of the peristome, (iii) the oral ciliature comprising the AZM and the paroral kinety, and (iv) the short rows of kineties on the base of the spine complex. The main characteristics of the infraciliature, and those reported by Sola et al. (1990), are given in Table 3.

(i) Bell kinety (Fig. 3). The kinety in the anterior part of the body comprised 60-80 kinetosomes arranged in a zig-zag pattern. This arrangement of the kinetosomes confirms the description of Sola et al. (1990), i.e. that the anterior ciliature is a kinety and not a row of cirri as suggested by Jankowski (1964). The kinety observed in our specimens, however, was significantly smaller than that described by Sola et al. (1990), which consisted of 90-100 kinetosomes (Table 3).

(ii) Perizonal zone (Fig. 5). The perizonal zone comprised 100-120 kineties with each kinety made of 10-15 pairs of kinetosomes and terminating near the oral region. This is consistent with the description given by Sola et al. (1990).

(iii) Oral infraciliature (Figs. 4, 5). The AZM comprised 32-40 membranelles. Each membranelle consisted of 3 rows of 4-5 kinetosomes in the median part of the cell (Fig. 5), and up to 8-10 kinetosomes near the mouth (Fig. 4). By contrast, Sola et al. (1990) described an AZM made of 40-50 membranelles with 3 rows of 5-10 kinetosomes each. The paroral kinety consisted of 2 parallel rows of kinetosomes, very close to each other (Fig. 4).

(iv) Kineties on the base of the spine complex (Fig. 6). The spine complex supported 3 or 4 short kineties with between 8 and 16 kinetosomes each

Table 3. Infraciliature of *C. uniserialis*: comparison of data reported during the present study with that of Sola et al. (1990)

	present study (n = 10)	Sola et. al (1990)
Bell kinety		
number of kinetosomes	60 - 80	90 - 100
Perizonal zone		
number of kineties	100 - 120	100 - 120
number of dikenetids per kinety	10 - 15	10 - 15
AZM		
number of membranelles	32 - 40	40 - 50
number of rows of kinetosomes per membranelle and	3	3
number of kinetosomes per row	4 - 10	5 - 10
Posterior spines		
number of kineties	3 - 4	3 - 4
number of kinetosomes per kinety	8 - 16	15 - 20

(Fig. 6). Sola et al. (1990) described the same number of kineties made of 15-20 kinetosomes each. Fibrillar systems similar to those described by Sola et al. (1990) were visible linking the kinetosomes to each other, and to the anterior part of the cell (Fig. 6).

The variation in cell size is easier to explain than the variation in the number of kinetosomes in the bell kinety and spine kineties (Table 3). It has been suggested that larger cell size would lead to larger numbers of kinetosomes per kinety (Perez-Uz 1993). The present study failed to confirm this for *C. uniserialis* since large cells generally had fewer kinetosomes in the bell and spine kineties. It is possible, however, that the numbers of kinetososmes on the bell and spine kineties are not stable characters. Morphological studies on clonal cultures under controlled laboratory conditions should be carried out in order to determine the variability of these and other characters currently used to describe species of *Caenomorpha* (Rosa 1976, Fernandez-Galiano and Fernandez-Leborans 1980, Martin-Gonzalez et al. 1987, Sola et al. 1990).

In conclusion, it can be seen that *C. uniserialis* exhibits greater morphological variation in terms of its cell size and infraciliature than previously reported (Sola et al., 1990). Possible explanations for this variability include (i) that there are two (or more) genetically differentiated strains or sibbling species of *C. uniserialis*, or (ii) that the morphology of *C. uniserialis* changes under different environmental conditions. Further studies are required in order to determine which (if either) of these explanations is correct.

Acknowledgements. This work was supported by a grant (CI1*-CT90-0675) from the European Commission. We thank B. Perez-Uz for comments on the original manuscript.

REFERENCES

Armstrong W., Armstrong J., Beckett P. M. (1990) Measurement and modelling of oxygen release from roots of *Phragmites australis*. In: Constructed Wetlands in Water Pollution Control, (Eds. P. F. Cooper and B. C. Findlater). Pergamon Press, Oxford, 41-51

Batchelor A., Scott W. E., Wood A. (1990) Constructed wetland research programme in South Africa. In: Constructed Wetlands in Water Pollution Control, (Eds. P. F. Cooper and B. C. Findlater). Pergamon Press, Oxford, 373-382

Butler J. E., Ford M. G., Loveridge R. F., May E. (1990) Design, construction, establishment and operation of gravel-bed hydroponic (GBH) systems for secondary and tertiary sewage treatment. In: Constructed Wetlands in Water Pollution Control, (Eds. P. F. Cooper and B. C. Findlater). Pergamon Press, Oxford, 539-542

Carey P. (1992) Marine Interstitial Ciliates. An Illustrated Key. Natural History Museum Publications. Chapman and Hall, London

Curds C. R., Gates M. A., Roberts D. M. (1983) British and Other Freshwater Ciliated Protozoa. Part II. Ciliophora: Oligohymenophora and Polyhymenophora. Synopses of the British Fauna. New Series; 22. Cambridge University Press, Cambridge

Decamp O. (1996a) Silver carbonate impregnation of specimens of *Metopus es* Kahl, 1932 (Ciliophora, Heterotrichida). *Quek. J. Microsc.* **37:** 536-540

Decamp O. (1996b) The microbial ecology of the root zone method of wastewater treatment. Doctoral thesis. University of Leicester, UK

Dragesco J., Dragesco-Kernéis A. (1986) Ciliés Libres de l'Afrique Intertropicale. Introduction à la Connaissance et à l'Etude des Ciliés. Editions de l'ORSTOM, Institut Français de Recherche Scientifique pour le Développement en Coopération, Paris

Fenchel T. (1987) Ecology of Protozoa. Science Tech Publishers, Madison/Springer Verlag, Berlin

Fernandez-Galiano D. (1976) Silver impregnation of ciliated protozoa: procedure yielding good results with the pyridinated silver carbonate method. *Trans. Am. Micros. Soc.* **95:** 557-560

Fernandez-Galiano D., Fernandez-Leborans G. (1980) *Caenomorpha medusula* Perty, 1852 (Heterotrichida, Armophorina): Nouvelles données sur la ciliature et l'infraciliature. *Protistologica* **16:** 5-10

Foissner W., Berger H., Kohmann F. (1992) Taxonomische und Ökologische Revision der Ciliaten des Saprobiensystems. Band II: Peritrichia, Heterotrichida, Odontostomatida Informationsberichte des Bayer. Lamdesamtes für Wasserwirtschaft, Heft 5/92, Munich

Gambrell R. P., Patrick W. H. J. (1978) Chemical and microbiological properties of anaerobic soils and sediments. In: Plant Life in Anaerobic Environments, (Eds. D. D. Hook and R. M. M. Crawford). Ann Harbor Sci. Pub. Inc., Ann Harbor, 375-423

Gray N. F. (1989) Biology of Wastewater Treatment. Oxford University Press, Oxford

Hewett S. W. (1980) Prey-dependent cell size in a protozoan predator. *J. Protozool.* **27:** 311-313

Hofmann K. (1990) Use of *Phragmites* in sewage sludge treatment. In: Constructed Wetlands in Water Pollution Control, (Eds. P. F. Cooper and B. C. Findlater). Pergamon Press, Oxford, 269-277

Jankowski A. W. (1964) Morphology and evolution of Ciliophora. III. Diagnoses and phylogenesis of 53 sapropelbionts, mainly of the order Heterotrichida. *Arch. Protistenk.* **107:** 185-294

Jones T.C., Gates M.A. (1994) A morphometric study of euryhalinity in marine populations of the ciliate genus *Euplotes*. *J. Euk. Microbiol.* **41:** 303-316

Kahl A. (1935) Urtiere oder Protozoa. Wimpertiere oder Ciliata (Infusoria) Jena

Kuhlmann H.-W, Heckmann K. (1985) Interspecific morphogens regulating prey-predator relationships in protozoa. *Science* **227:** 1347-1349

Laybourn-Parry J. (1984) A Functional Biology of Free-living Protozoa. Croom Helm, London

Levander K. M. (1894) Beiträge zur Kenntniss einiger Ciliaten. *Acta pro Soc. Fauna et Flora Fenn.* **9:** 1-87

Madoni P. (1990) The ciliated protozoa of the monomictic Lake Kinneret: species composition and distribution during stratification. *Hydrobiol.* **160:** 111-120

Martin-Gonzalez A., Serrano S., Fernández-Galiano D. (1987) Cortical morphogenesis and conjugation process in *Caenomorpha medusula* (Ciliophora, Heterotrichida). *Europ. J. Protistol.* **23:** 111-121

Painter H. A. (1971) Chemical, physical, and biological characteristics of wastes and waste effluents. In: Water and Water Pollution Handbook, (Ed. L. L. Ciaccio). Marcel Dekker, New York, 329-364

Patterson D. J., Hedley S. (1992) Free-living Freshwater Protozoa. A Colour Guide. Wolfe Publishing Ltd, London

Perez-Uz B. (1993) Estudios morfologico comparativo de algunos clones del genero *Uronema* en condiciones de cultivo. Tesis Doctoral, Universidad Complutense de Madrid, Spain

Rosa M. R. D. S. (1976) Observations sur l'infrastructure du cilié hétérotriche Armophorina: *Caenomorpha medusula* Perty, 1852. *J. Protozool.* **23:** 56, 19A

Small E. B., Lynn D. H. (1985) Phylum Ciliophora Doflein, 1901. In: An Illustrated Guide to the Protozoa, (Eds. J. J. Lee, S. H. Hutner and E. C. Bovee). Society of Protozoologist, Lawrence, Kansas, 393-575

Sola A., Guinea A., Longás J. F., Fernandez-Galiano D. (1990)

Nouvelles données sur l'infraciliature somatique et buccale de *Caenomorpha uniserialis* Levander, 1894. *Arch. Protistenk.* **138:** 233-238

Villeneuve-Brachon S. (1940) Recherches sur les Ciliés Hétérotriches. *Arch. Zool. Exp. et Gén.* **82:** 1-180

Received on 1st October, 1996; accepted on 2nd January, 1997

Acta Protozoologica (1997) 36: 111 - 119

ACTA
PROTOZOOLOGICA

Tetrahymena Recovering from a Heavy Accumulation of a Gold Salt

Jytte R. NILSSON

Department of Cell Biology and Anatomy, Zoological Institute, University of Copenhagen, Copenhagen, Denmark

Summary. After 24 h in 15 mM aurothiomalate (GSTM), *Tetrahymena* has accumulated visible amounts of gold (LM: yellow; EM: electron dense) in refractive granules and the culture has half the cell concentration of control cultures (Nilsson 1993). The purpose was to study whether the cells were capable of full recovery with elimination of accumulated gold after removal of GSTM from the medium. When left at the original high cell concentration, the ciliates did not proliferate and gold remained detectable for at least 24 h, i.e. a slow turnover of gold. After dilution to a low cell concentration, however, the ciliates resumed proliferation after a slightly prolonged lag period during which measurable amounts of gold were defecated. During the lag period, the fine structure altered with the change in metabolism of high density cells to that of low density cells; moreover, gold-containing, dense granules enlarged by fusion with one another. After the first cell doubling, dense granules were seen only occasionally and gold (electron-dense material) could no longer be detected in *Tetrahymena*. Turnover of gold was high only in fast proliferating cells.

Key words: aurothiomalate, cell recovery, *Tetrahymena*.

INTRODUCTION

Exposure to heavy metals is a hazard not only of a polluted environment but also of therapy with heavy metal-containing drugs. Heavy metals common in drugs are gold, bismuth, and platinum and during therapy they may accumulate in various tissues, causing malfunctioning or intoxication (e.g., ref. Nilsson 1988, 1993, 1996). In therapy of rheumatoid arthritis, about 70% of the administered gold is retained in the body (Brown and Smith 1980, Basco et al. 1988, Carter 1988) and gold may be detectable in patients for up to 20 years after the end of treatment (Sadler 1976, Vernon-Roberts et al. 1976, Carter 1988). The fact that heavy metals, such as gold, are deposited in tissues, indicates a capture by proteins (Sadler 1976, Biggs et al. 1979, Brown and Smith 1980, Schmitz et al. 1980, Brady 1982, Butt et al. 1986) before storage in intracellular compartments from which turnover may be slow.

Sodium aurothiomalate (GSTM) has long been used in therapy of rheumatoid arthritis and is, together with other gold salts, still considered a most efficacious treatment of the disease (Sadler 1976, Cheatum 1996). The disease is rarely cured but the symptoms are suppressed so gold therapy may extend for years (Sadler 1976, Klinkhoff and Teufel 1995, Cheatum 1996). A problem is that the individual tolerance to standard doses of gold drugs varies considerably, whereas conditions are improved in 60% of the patients, another 40% develop gold-induced intoxication (Sadler 1976) traditionally leading to termination of the gold cure. However, changing the dose, and not the

Address for correspondence: Jytte R. Nilsson, Department of Cell Biology and Anatomy, Zoological Institute, University of Copenhagen, Universitetsparken 15, DK-2100 Copenhagen Ø, Denmark; Fax: (+45)35321200

drug, to suit such patients, has revealed effective, tolerated doses about 40-fold lower than the standard ones (Klinkhoff and Teufel 1995, Cheatum 1996). This large difference in tolerance to gold drugs may reflect a low and high capacity, respectively, of individuals to render the drug innocuous. The ciliate, *Tetrahymena*, has a high capacity for rendering GSTM innocuous because the cells are affected almost identically by the drug in concentrations over a 30-fold range (Nilsson 1993).

The mode of action of GSTM is not fully understood but gold is the active moiety (Lipsky et al. 1979, Brown and Smith 1980). The drug affects the release or activity of lysosomal enzymes (Vernon-Roberts 1979, Brown and Smith 1980, Mehta and Webb 1982, Graabæk and Pedersen 1988, Mallya and Van Wart 1989) and gold accumulates in lysosomes (Strunk and Ziff 1970, Lawson et al. 1977, Nakamura and Igarashi 1977, Ghadially 1979, Pääkkö et al. 1984, Nilsson 1993). Considering the inflammatory conditions of rheumatoid arthritis, the findings indicate that the lysosomal system is the target site of the drug. Usually, components of the lysosomal system turn over rapidly and also patients excrete 30% of the administered gold (Sadler 1976), - so why is the turnover of accumulated gold so slow, and variable?

The question may be studied conveniently in axenic cultures of *Tetrahymena pyriformis*. The ciliate was used recently in a study on dose-dependent effects, and intracellular distribution, of 0.5-15 mM GSTM (Nilsson 1993). An unaffected endocytic rate and continued cell proliferation at a slightly decreased rate without a lag period, contradict marked effects of GSTM on lysosomal enzyme activity; however, small refractive granules appeared in all treated cells (Nilsson 1993). With time, the lysosome-like granules (Nilsson 1989) accumulated dose-dependent amounts of gold (yellow colour/electron-dense material). The granules remained constant in number in proliferating cells but increased in non-proliferating cells (Nilsson 1993) indicating a low and high rate, respectively, of turnover of GSTM.

The present study was undertaken to reveal whether, or not, *Tetrahymena* has the capacity of full recovery after a heavy accumulation of gold, and to determine whether recovery is dependent on cell proliferation as indicated by preliminary light microscopical observations (Nilsson 1993). *Tetrahymena* was exposed to the high concentration of 15 mM GSTM for 24 h, i.e. 8 normal cell generations. The question asked was: are the cells capable of removing all accumulated gold?

MATERIALS AND METHODS

Tetrahymena pyriformis GL was grown axenically at 28°C in 2% proteose peptone, enriched with 0.1% yeast extract and inorganic salts (Plesner et al. 1964). Methods used in determination of cell growth, i.e. counting of cell concentration, rate of endocytosis, and fixation of cells for electron microscopy, were as described previously (Nilsson 1993).

Hundred-ml cell cultures in 500-ml Fernbach flasks were aerated and agitated; they were used at a density of 3-4 x 10^4 cells/ml. Sodium aurothiomalate (GSTM) monohydrate (Aldrich Co. Ltd., F.W. 401; 48.27 w% Au) was added at a final concentration of 15 mM from 200 mM stock solutions to one half of the culture and the other half served as the control after addition of water in a volume corresponding to that containing the drug. Addition of GSTM to the organic growth (PP) medium did not alter pH or cause visible precipitation (Nilsson 1993). After 24 h, the drug was removed by spinning down the cells in a hand centrifuge, removal of the supernatant, and restoration to the original volume with fresh PP medium, or the washing was repeated twice; control cells were treated similarly. The washed cells were left at the original, high density from which a low density culture (3-4 x 10^4 cells/ml) was formed after dilution with fresh PP medium. For spectrophotometry, low density cultures were formed by dilution (1:11) of the 24 h GSTM-treated cultures with fresh PP medium and corresponding control cells were diluted 1:20.

The gold content of the culture medium was measured spectrophotometrically (UV-1201 Spectrophotometer, Shimadzu Corp., Japan) within the range of 200-400 nm. Cell samples (1 ml) withdrawn from GSTM-treated and control cultures were passed through 5 µm Millipore filters and the cell free samples were kept frozen at -22°C until measured. Before spectrophotometry at room temperature all samples were diluted 1:10 with water to ensure comparable amounts of PP medium; the baseline was determined with PP medium and the standard was 15 mM GSTM in PP medium, both were diluted 1:10. The ultraviolet absorption of GSTM-containing samples rose steeply around 230 nm, reaching maxima at 244 and 278 nm, and trailing out towards 400 nm with a minor broad peak at 337 nm in agreement with the spectra of gold (Weast 1973, Grootveld and Sadler 1983, Kassam et al. 1987). The ratio of 278 nm/244 nm peaks was 0.7 during cell exposure to GSTM and 0.3 in the medium of recovering cells. In order to include all three maxima, the data were expressed as the total area of absorption below 350 nm; the area of the spectra (2-fold enlarged) were measured using a Kontron Mini-Mop semiautomatic image analysis system (Kontron GMBH, Munich, Germany).

The frequency of organelles (mitochondria, peroxisomes, granules, lipid droplets, and autophagic vacuoles) was determined by counting on low power electron micrographs. In each sample, organellar profiles (incomplete profiles were estimated for their fractional value) were counted in about 10 cells.

RESULTS

Light microscopy

After 24 h in 15 mM aurothiomalate (GSTM), the *Tetrahymena* cultures had a density of about 5 x 10^5 cells ml, whereas control cultures had the maximal density

of 10^6 cells/ml. Due to the high density of both cultures, all cells had small, refractive granules which were more abundant and often of larger size in GSTM-treated cells (Fig. 1) where they also had a distinct yellow colour (gold) as described previously (Nilsson 1993).

To study recovery, the GSTM-containing medium was replaced with fresh growth (PP) medium leaving the cells at the original, high density from which a portion was diluted to form a low density culture. The cell concentration of high density cultures remained constant, or in-

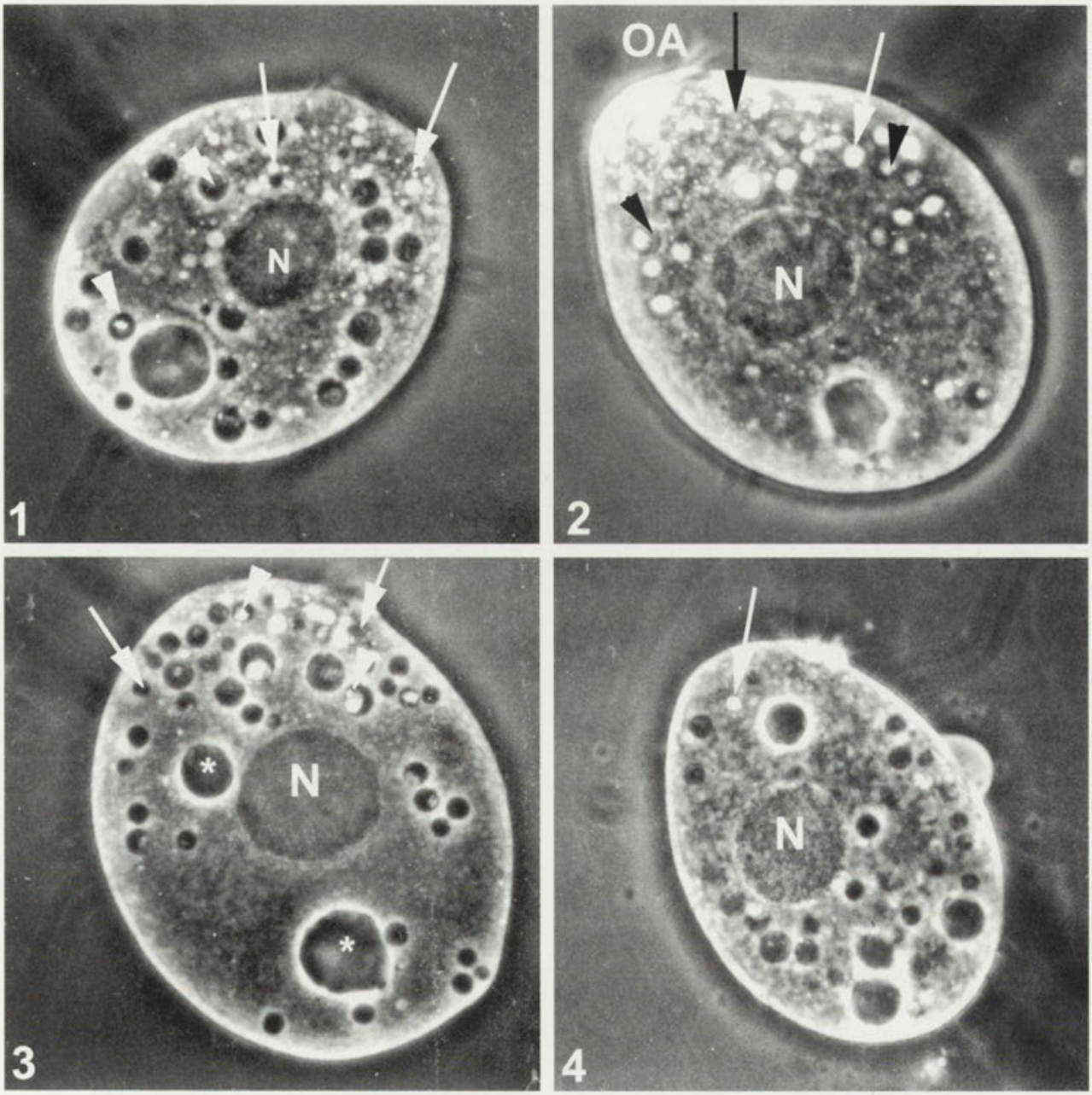

Figs. 1-4. Phase contrast microscopy of *Tetrahymena in vivo* (x 970). 1 - *Tetrahymena* after a 24-h exposure to 15 mM GSTM. Many small, and larger, refractive granules (arrows) are scattered throughout the cell; refractive material is also seen in food vacuoles (arrowheads), partly derived from fusion with the granules. Nucleoli, along the rim of the nucleus (N), are large (fused). 2 - recovering (predivision) cell by the end of the lag period (about 3 h). Refractive material is concentrated mainly in anterior end (OA) in small and enlarged granules (arrows) but also in food vacuoles (arrowheads). In the nucleus (N), nucleoli are still fused. 3 - recovering cell in early division (4.5 h) with 2 contractile vacuoles (*). The refractive granules (arrows) have decreased in number. The refractive solid balls, or conglomerates of small entities, in food vacuoles (arrowheads) resemble extruded defecation balls. Unfused nucleoli in the nucleus (N). 4 - young, newly divided cell (5.5 h) resembles active proliferating control cells. Apart from an occasional dense granule (arrow), it is devoid of refractive material and gold (yellow material) could no longer be detected

creased in number maximally by a factor of 0.5. In both instances, the number of refractive granules remained high in the cells and although some yellow colouring (gold) was lost after 24 h, some remained detectable after 48 h. Turnover of gold was clearly low in these high density cultures.

The cells recovering at low density (3-4 x 10^4 cells/ml) exhibited a lag period, identical to that of corresponding control cells, before initiating proliferation. The lag period was about 3 h but it varied slightly from one experiment to another, possibly due to the stress of handling during washing and centrifugation, but it remained identical for GSTM-treated cells and their similarly handled control cells. In fact, the lag period of recovering GSTM-treated cells was 0.5 h longer than that of their control cells because the lag period of control cells diluted from 5 x 10^5 cells/ml cultures (i.e. the density after 24 h in 15 mM GSTM), was 0.5 h shorter than that of control cells diluted from 10^6 cells/ml cultures. Hence, the identical lag periods of recovering GSTM-treated and their control cells disguise this density dependency of the lag period. Irrespective of the length of the lag period, the first cell doubling was achieved within 2.5 h in recovering GSTM-treated and control cultures, i.e. 10% shorter than the normal doubling time of *Tetrahymena* but further proliferation occurred at normal rate. The rate of endocytosis in recovering GSTM-treated cells was not different from that of the control cells.

During the lag period, the GSTM-recovering cells increased gradually in size and contained many refractive granules, mainly concentrated in the anterior region. By the end of the lag period (Fig. 2), cells had many large granules with visible yellow material (gold), also seen in digestive vacuoles, and the rate of defecation was high; the yellow defecation balls accumulated at the bottom of the culture flask. After initiated proliferation, dividing cells had few granules and refractive material was confined mainly to digestive vacuoles (Fig. 3). After the population had doubled, the cells were almost devoid of refractive material (Fig. 4) and yellow material (gold) was no longer detectable. Cells recovering at low density were studied further in the electron microscope (see below).

Since recovering cells excreted yellow defecation balls, the amount of gold should increase in the medium; the problem was investigated by spectrophotometry. The data for cells diluted (1:11) from a 24-h GSTM culture of 4.9 x 10^5 cells/ml are shown in Fig. 5. The cells multiplied after a 3.3-h lag period and had doubled in number by 5.8 h, and the amount of gold in the medium increased sharply around 2 h of recovery, i.e. high rate of defecation,

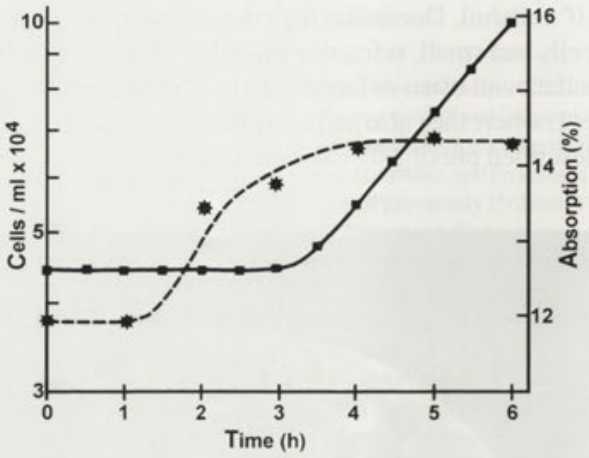

Fig. 5. Growth characteristics (■) and content of gold (*) in the medium of *Tetrahymena* recovering after 24 h in 15 mM GSTM. The original culture was diluted 1:11. Note, the 3.3-h lag period and the relatively short cell doubling time. The data of spectrophotometry (200-400 nm) are measured areas of absorption below 350 nm, expressed as percent of that of 15 mM GSTM in cell-free growth medium. See text for further explanation

and levelled out by 4-5 h of recovery, i.e. with proliferation and little refractive material in the cells. The amount of gold excreted from the 44.5 x 10^3 cells/ml equalled 0.33 mM GSTM (2.2% of 15 mM GSTM). The original cells (4.9 x 10^5 cells/ml) after 24 h in GSTM, should then have contained 3.6 mM GSTM which, together with the amount measured in their medium, namely 11.2 mM GSTM (74.5% of the 15 mM GSTM/PP value), corresponds to 98% (14.8 mM) of the added 15 mM GSTM.

Electron microscopy

In the original 15 mM GSTM culture, the 24-h treated cells had detectable gold as electron-dense material in dense granules, small vacuoles, and vesicles (Figs. 6-8); moreover, they had dilated rough endoplasmic reticulum as reported previously (Nilsson 1993). The high cell density conditions were reflected in dark type mitochondria and peroxisomes, presence of glycogen particles and lipid droplets (Figs. 6, 7), as well as condensed chromatin granules and fused nucleoli, features common to those of the high density control cells.

The fine structure of recovering cells was studied only for low density cells which proliferated after a 2.5-h lag period and had doubled by 5 h of recovery.

After 3 h of recovery, i.e. by the end of the lag period, the structure of the cells had changed from that of the original, high density cells in 15 mM GSTM, to a more active state as the nucleoli were no longer fused and chromatin granules were dispersed (not shown). The mitochondria and peroxisomes were still of the dark type

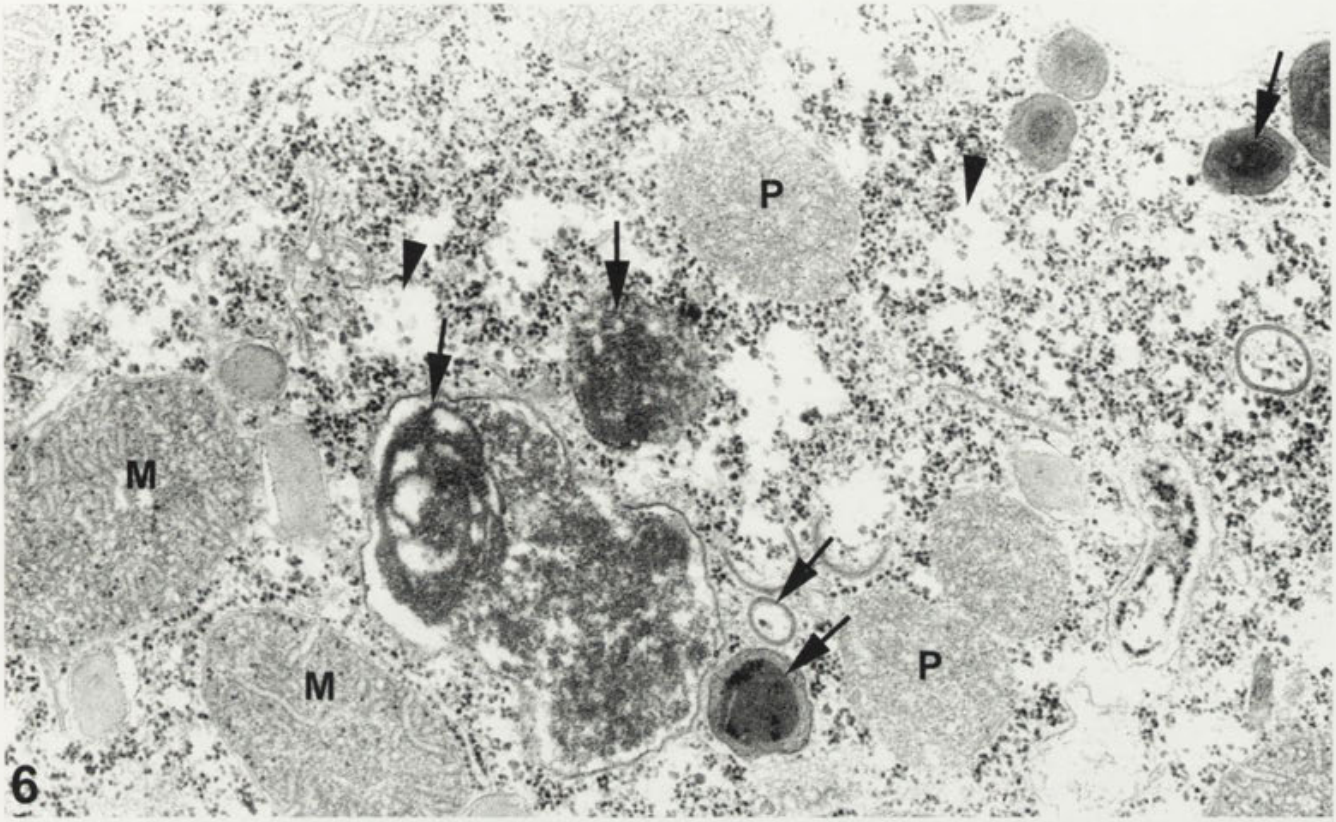

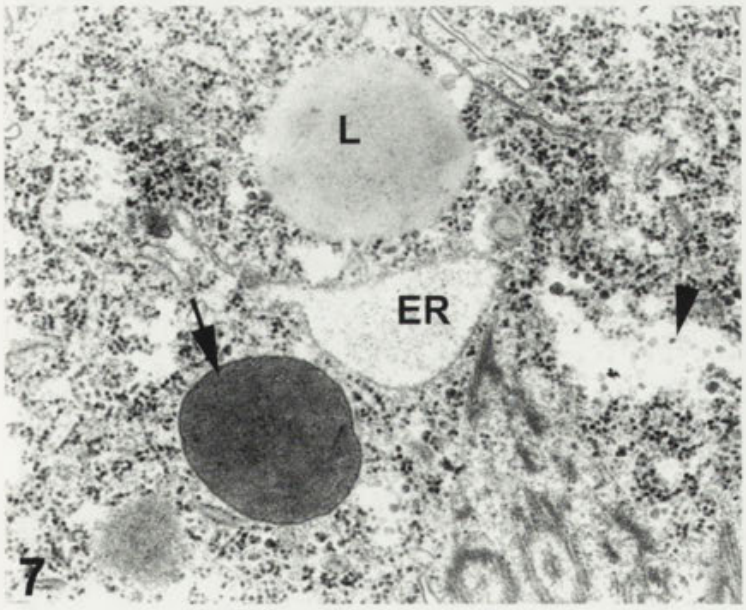

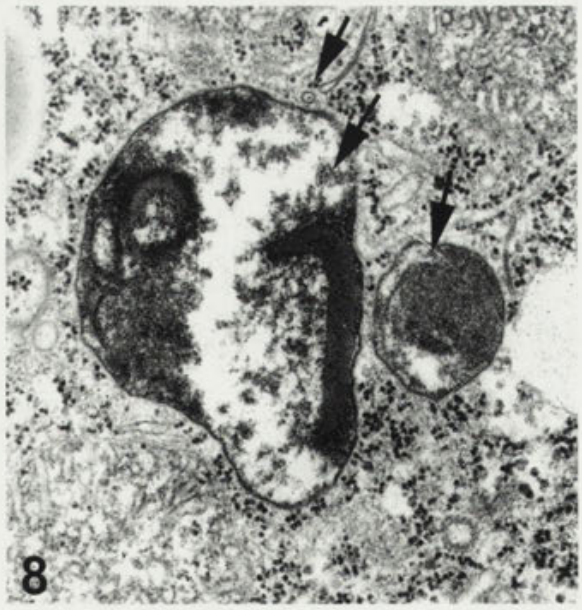

Figs. 6-8. Fine structure of *Tetrahymena* after 24 h in 15 mM GSTM (x 39600). Typical of GSTM-treated cells are the various small, and large, dense granules (arrows) containing gold (electron-dense material), and dilated endoplasmic reticulum (ER, Fig. 7). High density conditions are indicated by dense mitochondria (M) and peroxisomes (P), and the presence of glycogen islands (arrowheads) and lipid droplets (L)

but less dense, some glycogen was still present, and lipid droplets were abundant (Figs. 9-11) and they appeared often with an uneven outline as though being dissolved (Figs. 9-10). Several dense granules with electron-dense contents (gold), were enlarged and showed clear evidence of having been formed by fusion of small granules (Fig. 9), they probably correspond to the enlarged granules seen by light microscopy (Fig. 2). Electron-dense con-

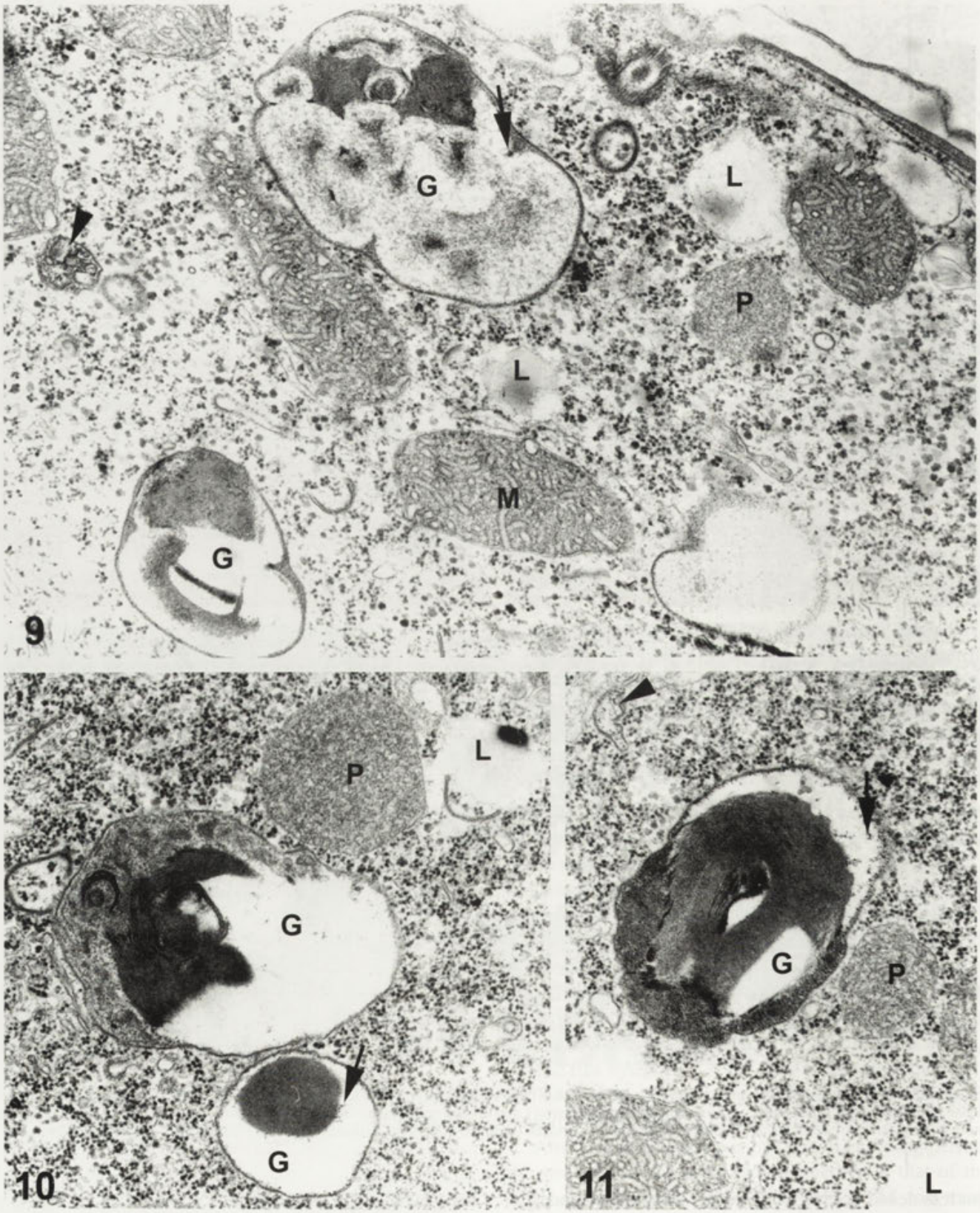

Figs. 9-11. 3-h recovering *Tetrahymena* (x 39600). The large granular structures (G) show sign of recent fusion of smaller granules. Gold, as electron -dense dots (arrows), is seen in the granules (G) and small vesicles (arrowheads). Mitochondria (M) and peroxisomes (P) are still rather dense. Lipid droplets (L) frequently occur with an irregular outline as if being dissolved

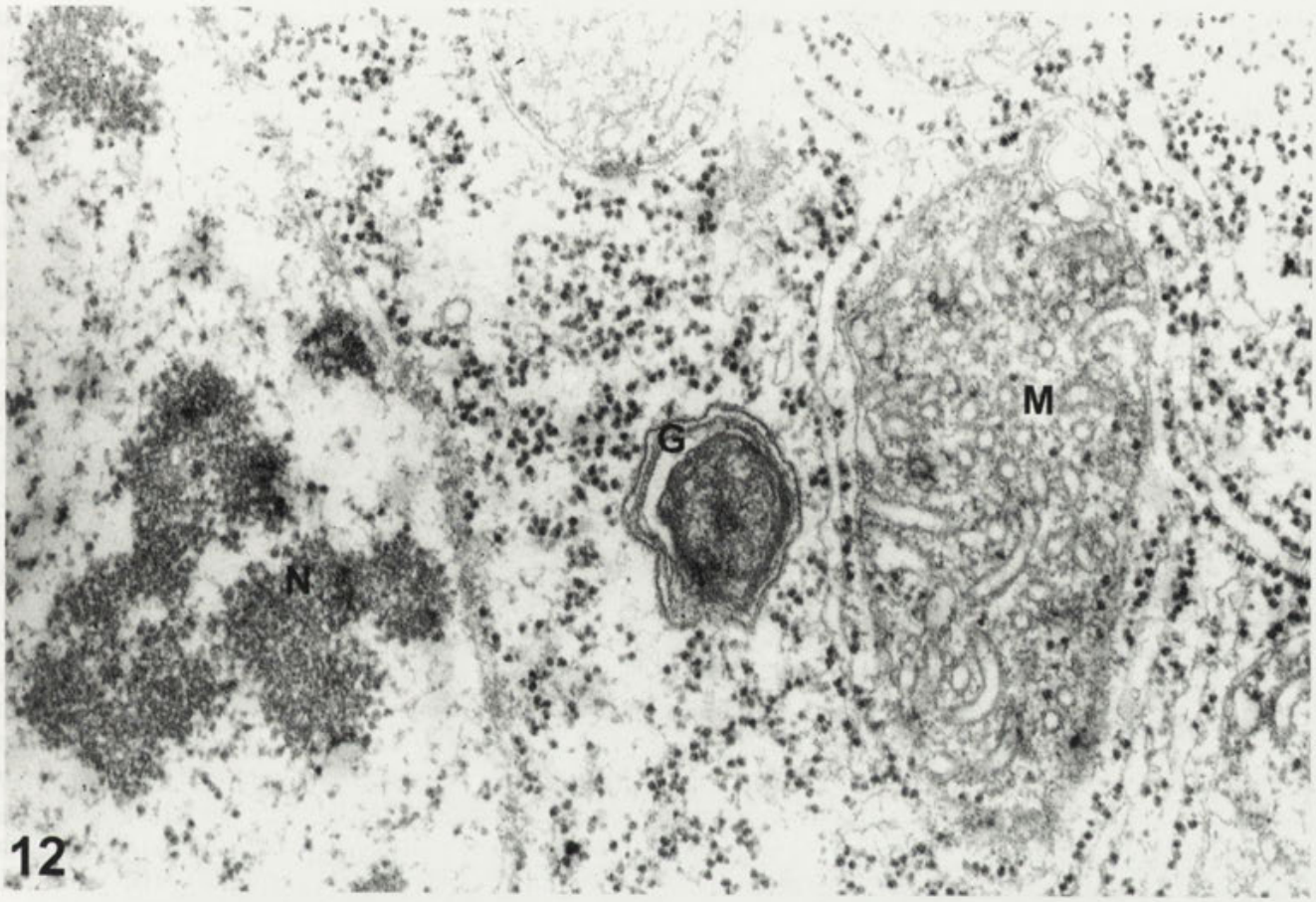

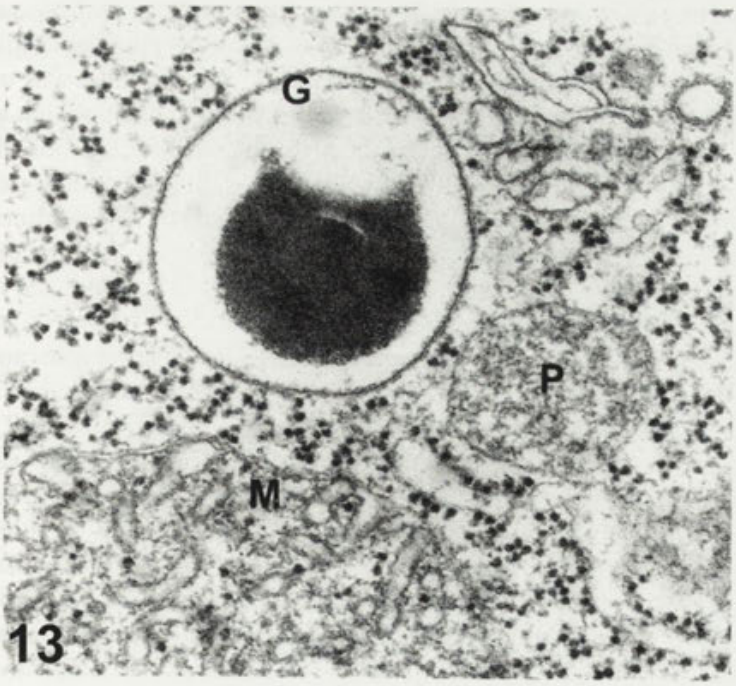

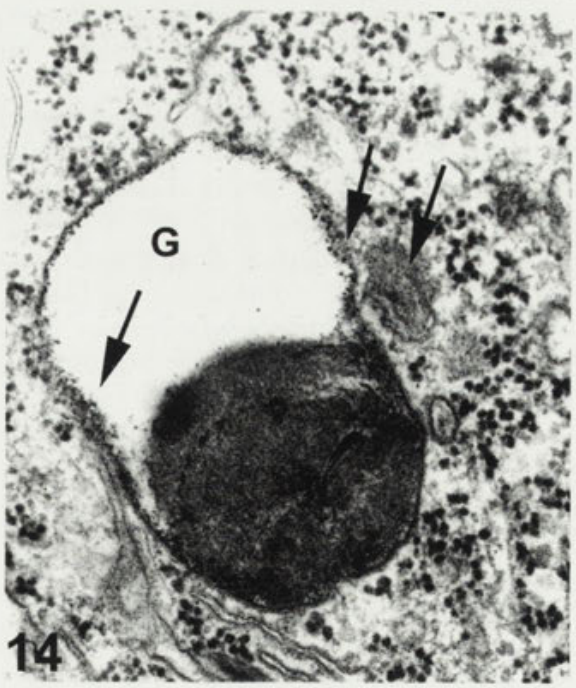

Figs. 12-14. Recovering *Tetrahymena* (x 68000). 12 - from a 5-h recovering cell. Active proliferation is indicated by small nucleoli (N), light type mitochondria (M), and absence of glycogen. 13 - from a 5-h recovering cell. Occasional dense granule (G), typical in structure but devoid of gold (compare to Fig. 14). 14 - from a 3-h recovering cell. Note, gold (arrows) as electron-dense dots in dense granule (G) and adjacent small vesicle

Table 1. Frequency of cell organelles in *Tetrahymena* recovering from 24 h in 15 mM GSTM

Condition	Mitochondria	Peroxisomes	Granules	Lipid Droplets
24 h in GSTM	1*	0.40*	0.41	0.03
3 h Recovery	1	0.45	0.33	0.12
5 h Recovery	1**	0.30**	0.02	0.02

* dark type organelle
** light type organelle

glomerates seen in some food vacuoles, as during exposure to GSTM (Nilsson 1993), could originate from uptake of GSTM before it was removed from the medium or from the contents of dense granules after their fusion with digestive vacuoles. Gold (electron-dense dots) appeared in scant amounts in various small vesicles (Figs. 9, 11). Conspicuous, however, was the disappearance of the dilated rough endoplasmic reticulum seen during exposure to GSTM.

After 5 h of recovery and doubling of the population, all cells should have divided. Active proliferation (Nilsson 1981) was reflected in light type of mitochondria and peroxisomes (Figs. 12, 13) and absence of glycogen, but occasionally, a lipid droplet or dense granule was seen. Gold (electron-dense dots) was no longer detected in the cells, not even in an occasional dense granule (Fig. 13, compare with Fig. 14 of dense granule in 3-h recovering cell).

During the recovery, some change in the frequency of the cell organelles was noted and their profiles were counted in the original GSTM-treated and recovering cells. The data, expressed per mitochondrion, showed (Table 1) that the number of dense granules decreased from 0.41 to 0.02 during the recovery, a finding which eliminates the possibility that the decreased number of granules occurred merely by simple dilution through cell division. The data on lipid droplets were interesting, during the lag period they increased 4-fold in number but decreased again after completion of the first cell doubling.

DISCUSSION

During the 24-h exposure to 15 mM GSTM (aurothiomalate), *Tetrahymena* accumulated visible amounts of gold (Nilsson 1993, present study) but with GSTM removed from the medium, gold should no longer enter the cells. For full recovery, the cells should resume proliferation at the normal rate of control cells and gold (yellow colour/electron-dense material) should no longer be detectable in the cells. Recovering GSTM-treated cells initiated proliferation in low density cultures and only after a lag period, somewhat longer than that of control cultures diluted from a similar cell density. The prolonged lag period of recovering GSTM-treated cells, may relate to the time required to generate the extra energy involved in handling of the drug remaining inside the cells.

The intracellular handling of GSTM during cell recovery is likely to follow the same path as that operating during exposure to the drug (Nilsson 1993), apart from lack of extracellular entry. In general, cells have binding proteins, e.g., the low molecular weight proteins, metallothioneins (MT), which bind heavy metals (Brady 1982), including gold (Schmitz et al. 1980, Butt et al. 1986, Mallya and Van Wart 1989). The capacity of MT to bind gold was studied in rats by Saito and Kojima (1996) who found that increased doses of gold salt induced increasing amounts of cytosolic MT but only 14% of the increased amount of gold was bound by MT, the majority (79%) bound to high molecular weight proteins (HP). Hence, even though MT may sufficiently regulate low amounts of intracellular gold, HP proteins may be essential for coping with large amounts. In fact, intoxication induced by gold therapy, may be related directly to the individual capacity for activating HP genes. In *Tetrahymena*, GSTM also induces protein synthesis, as visualized by the appearance of dilated rough endoplasmic reticulum (Nilsson 1993, present study) which was no longer seen in recovering cells, hence indicating that as gold no longer enters the cells, the need for the GSTM-induced protein(s) ceases. The intracellular distribution of gold in recovering *Tetrahymena* should then be confined primarily to cell compartments, as was found to be the case. Elimination from the cells of gold accumulated in dense granules was indicated previously (Nilsson 1993) to involve fusion of the granules with digestive vacuoles and subsequent defecation, according to a common detoxification mechanism in *Tetrahymena* (Nilsson 1989, 1993, 1996). In the present study, however, early recovery was associated primarily with fusion of gold-containing granules with one another to form larger granules. Whether these granules empty their contents into digestive vacuoles by fusion or by direct defecation, remains unanswered; in theory, both possibilities are likely as the membrane structure of dense granules is the same as that of digestive vacuoles (Nilsson 1989).

Although gold (electron-dense material) remained detectable in recovering cells, it was confined to the lysosomal system. By the end of the lag period (i.e. just as cell

divisions started), the number of electron-dense granules had decreased moderately; but after the first cell doubling, granules were seen only occasionally and, interestingly, gold (electron-dense dots) was no longer detectable in these. This finding indicates a complete removal of gold from the cells. Moreover, the spectrophotometric measurements of gold in the culture medium revealed a substantial increase of gold concomitantly with a high rate of defecation in recovering cells.

The question raised in the Introduction can then be answered in the affirmative: *Tetrahymena* is capable of full recovery after a heavy accumulation of the gold drug, GSTM, but only under conditions permitting cell proliferation, i.e. in low density cultures. Proliferation resumed at normal rate and gold was no longer detectable after completion of the first cell cycle. However, removal of accumulated gold seemed to require additional energy as reflected in the extended lag period before initiation of proliferation. Proliferating *Tetrahymena* has a high metabolic rate, associated with a high activity of the lysosomal system, factors which may be the prerequisite for a rapid turnover of accumulated gold. With a low activity of the lysosomal system, as in non-proliferating *Tetrahymena* and cells in most tissues, accumulated gold turns over slowly.

Acknowledgements. Alice Rong Kristiansen is thanked for excellent technical assistance, and the financial support of the Carlsberg Foundation is gratefully acknowledged.

REFERENCES

Basco J., Uzonyi I., Dezcö B. (1988) Determination of gold accumulation in human tissue caused by gold therapy using X-ray fluorescence analysis. *Appl. Radiat. Isot.* **39:** 323-326

Biggs D.F., Boland D.M., Davis P, Wakaruk J. (1979) *In vitro* binding and pharmacokinetics of gold salts in plasma proteins and chelating agents. *J. Rheumatol.* (suppl. 5) **6:** 68-73

Brady F.O. (1982) The physiological function of metallothionein. *Trends. Biochem. Sci.* **7:** 143-145

Brown D.H., Smith W.E. (1980) The chemistry of the gold salts used in the treatment of rheumatoid arthritis. *Chem. Soc. Rev.* **9:** 217-240

Butt T.R., Sternberg E.J., Mirabelli C.K., Crooke S.T. (1986) Regulation of metallothionein gene expression in mammalian cells by gold compounds. *Mol. Pharmacol.* **29:** 204-210

Carter T.R. (1988) Intramammary lymph node gold deposits simulating microcalcifications on mammograms. *Hum. Pathol.* **19:** 992-994

Cheatum D.E. (1996) How far can you go? Use of very low dosage of gold in patients with mucocutaneous reactions. *J. Rheumatol.* **23:** 944

Ghadially F.N. (1979) The aurosome. *J. Rheumatol.* (suppl. 5) **6:** 45-50

Graabæk P.M., Pedersen S.M. (1988) Effect of two gold compounds on lysosomes. *Ann. Rheum. Dis.* **47:** 509-514

Grootveld M.C., Sadler P. (1983) Differences between the structure of the anti-arthritic gold drug "Myocrisin" in the solid state and in solution: a kinetic study of dissolution. *J. Inorg. Biochem.* **19:** 51-64

Kassam Y.B., Kean W.F., Lock C.J.L., Buchanan W.W., Simons G.T., Harvey D.A. (1987) Variation in physical and biological properties of solid gold sodium thiomalate on dissolution: An electron microscopic and energy dispersive spectroscopic study. *J. Reumatol.* **14:** 209-215

Klinkhoff A.V., Teufel A. (1995) How low can you go? Use of very low dosage of gold in patients with mucocutaneous reactions. *J. Rheumatol.* **22:** 1657-1659

Lawson K.J., Danpure C.J., Fyfe D.A. (1977) The uptake and subcellular distribution of gold in liver cells after *in vivo* administration of sodium aurothiomalate. *Biochem. Pharmacol.* **26:** 2417-2426

Lipsky P.E., Ugai K., Ziff M. (1979) Alterations in human monocyte structure and function induced by incubation with gold sodium thiomalate. *J. Rheumatol.* (suppl. 5) **6:** 130-136

Mallya S.K., Van Wart H.E. (1989) Mechanism of inhibition of neutrophil collagenase by gold(I) chryso-therapeutic compounds. Interaction of a heavy metal binding site. *J. Biol. Chem.* **264:** 1594-1601

Mehta S., Webb H.E. (1982) Lysosomal enzyme changes in macrophages from mice given myocrisin and infected with avirulent semliki forest virus. *Br. J. exp. Path.* **63:** 443-446

Nakamura H., Igarashi M. (1977) Localization of gold in synovial membrane of rheumatoid arthritis treated with sodium aurothiomalate. *Ann. Rheum. Dis.* **36:** 209-215

Nilsson J.R. (1981) On cell organelles in *Tetrahymena*. With special reference to mitochondria and peroxisomes. *Carlsberg Res. Commun.* **46:** 279-304

Nilsson J.R. (1988) Cytotoxic effects of cisplatin, cisdichlorodiammineplatinum(II), on *Tetrahymena*. *J. Cell Sci.* **90:** 707-716

Nilsson J.R. (1989) *Tetrahymena* in cytotoxicology: with special reference to effects of heavy metals and selected drugs. *Eur. J. Protistol.* **25:** 2-25

Nilsson J.R. (1993) Effects of a gold salt and its intracellular distribution in *Tetrahymena*. *Acta Protozool.* **32:** 141-150

Nilsson J.R. (1996) Effects of a bismuth salt on cell proliferation, endocytosis, and fine structure of *Tetrahymena*. *Eur. J. Protistol.* **32:** 283-292

Pääkkö P., Antilla S., Sutinen S. (1984) Lysosomal gold accumulation in pulmonary macrophages. *Ultrastruct. Pathol.* **7:** 289-294

Plesner P., Rasmussen L., Zeuthen E. (1964) Techniques used in the study of synchronous *Tetrahymena*. In: Synchrony in Cell Division and Growth (Ed. E. Zeuthen). Interscience, New York, 543-563

Sadler P.J. (1976) The biological chemistry of gold: a metal-drug and heavy-atom label with variable valency. *Struct. Bonding* (Berlin) **29:** 171-215

Saito S., Kojima Y. (1996) Relative gold-binding capacity of metallothionein: studies in renal cytosols of gold-injected rats. *Res. Commun. Mol. Pathol. Pharmcol.* **92:** 119-126

Schmitz G., Minkel D.T., Gingrich D., Shaw III C.F. (1980) The binding of gold(I) to metallothionein. *J. Inorg. Biochem.* **12:** 293-306

Strunk S.W, Ziff M. (1970) Ultrastructural studies of the passage of gold thiomalate across the renal glomerular capillary wall. *Arthritis and Rheumatism* **13:** 39-52

Vernon-Roberts B. (1979) Action of gold salts on the inflammatory response and inflammatory cell function. *J. Rheumatol.* (suppl. 5) **6:** 120-129

Vernon-Roberts B., Doré J.L., Jessop J.D., Henderson W.J. (1976) Selective concentration and localization of gold in macrophages of synovial and other tissues during and after chrysotherapy in rheumatoid patients. *Ann. Rheum. Dis.* **35:** 377-486

Weast R.C., ed. (1973) Handbook of Chemistry and Physics (53rd ed.). The Chemical Rubber Co.

Received on 13th November, 1996; accepted on 15th February, 1997

Acta Protozoologica (1997) 36: 121 - 124

ACTA
PROTOZOOLOGICA

Modified Patch-Clamp Method for Studying Ion Channels in *Stentor coeruleus*

Piotr KOPROWSKI, Mirosława WALERCZYK, Bożena GROSZYŃSKA, Hanna FABCZAK and Andrzej KUBALSKI

Department of Cell Biology, M. Nencki Institute of Experimental Biology, Polish Academy of Sciences, Warszawa, Poland

Summary. We have modified the procedure of Saimi and Martinac (1989) to study ion channels in plasma membrane of *Paramecium*. The modifications include a change in isolation of plasma membrane and changes in the process of GΩ-seal formation and electrophysiological recording. We have applied the procedure to investigate ion channels in *Stentor coeruleus*. Activities of two types of ion channels we encountered are presented in this report.

Key words: ciliates, ion channels, patch-clamp, *Stentor coeruleus*.

INTRODUCTION

As it has been shown (Saimi and Martinac 1989) the patch-clamp technique (Hamill et al. 1981) can be applied to isolated membrane vesicles of the ciliate *Paramecium*. Direct patch-clamp experiments on intact or deciliated ciliates were not successful (Saimi and Martinac 1989, Koprowski and Kubalski unpublished).

The step-up photophobic response (backward swimming induced by a sudden increase in light intensity) of the ciliate *Stentor coeruleus* is associated with the generation of a graded membrane receptor potential followed by an all-or-none action potential (Wood 1976, S. Fabczak et al. 1993). The light induced motile response of *S. coeruleus* is modified by cGMP (H. Fabczak et al. 1993) and inhibited by *l-cis*-diltiazem (S. Fabczak et al. 1994) - a potent blocker of cGMP-dependent ion channels (Haynes 1992). In order to detect presence of such channels in the plasma membrane of *Stentor* we have applied the patch-clamp method to isolated membrane blisters induced by a high concentration of monovalent ions (in the absence of divalent cations) in the medium. To our knowledge this is the first patch-clamp study on *S. coeruleus*.

Address for correspondence: Andrzej Kubalski, Department of Cell Biology, Nencki Institute of Experimental Biology, ul. Pasteura 3, 02-093 Warszawa, Poland; E-mail: kubalski@nencki.gov.pl

MATERIALS AND METHODS

Cell culture

Stentor coeruleus cells were grown in a medium containing 0.5 mM $CaCl_2$, 1 mM $MgSO_4$, 1 mM $NaNO_3$, 0.1 mM KH_2PO_4, 1 mM Tris-HCl, pH 7.0 at room temperature. The cells were fed with *Tetrahymena*

pyriformis cells, which were cultured axenically at room temperature in 1% proteose peptone (Difco Laboratories, Detroit, MI) supplemented with 0.1% yeast extract (Difco). One day before an experiment fed *Stentor* cells were transferred to casaminoacid media (Forte et al. 1986) consisted of 0.1 g/l glucose, 0.1 g/l casein hydrolysate peptone #20 (Gibco, Scotland) 0.5 mM K_2HPO_4, 0.2 mM $MgSO_4$, 0.5 mM $CaCl_2$, 10 mg/l stigmasterol, 7.5 mg/l phenol red, 5 mM HEPES, adjusted to pH 7.0 - 7.4 with NaOH.

All chemicals used in this study were of analytical-reagent grade and, if not otherwise stated, were purchased from Sigma (St. Louis, MO).

Electrical recording and data processing

Single channel recordings were performed according to standard patch-clamp technique (Hamill et al. 1981). The recordings were carried out at room temperature with an Axopatch 200B amplifier (Axon Instruments, Foster City, CA.). Pipettes (K-series borosilicate glass, WPI, Sarasota, FL.) were pulled (P-97, Sutter Instrument, Novato, CA) to a resistance of 7-10 MΩ in 250 mM NH_4Cl. They were coated with transparent nail enamel.

The data were acquired and stored on a computer running the Digidata 1200A/Axoscope 1.0 acquisition system and analyzed with pCLAMP6 software. The recordings were filtered at 1 kHz with a Bessel filter. The sampling rate was 5 kHz. In the case of the cGMP -dependent single channel currents they were further filtered in pCLAMP6 Fetchan at 0.5 kHz.

RESULTS AND DISCUSSION

Paramecium cells when transferred to a solution containing a high concentration of Na-glutamate without divalent cations (blistering solution) formed small membrane vesicles along their body surface. The blisters could be stripped from the cells and transferred to another solution (GΩ-seal forming solution) for electrophysiological recording (Saimi and Martinac 1989). This procedure could not be directly applied to isolate membrane vesicles and record from *Stentor coeruleus* plasma membrane. In the case of *Stentor* the effective Na ions concentration was 25 mM and was much lower than in *Paramecium* (150 mM). Beside 25 mM NaCl the blistering solution contained: 10^{-5} M Ca^{2+} (buffered with ethylene glycol *bis*-(*b*-aminoethyl ether) *N,N,N',N'*- tetraacetic acid (EGTA)), 0.01 mM ethylenediamide-tetraacetic acid (EDTA), 5 mM HEPES, pH 7.0. Within 1 min after *Stentor* cells were transferred into the blistering solution large blisters of 50-100 µm in diameter appeared mostly around the frontal parts of the cells (Fig. 1). These blisters were too large and too fragile to be stripped from the bodies of the ciliates and transferred to another chamber containing GΩ-seal forming solution. Instead, we cut the blisters off with a glass capillary from the cells that were

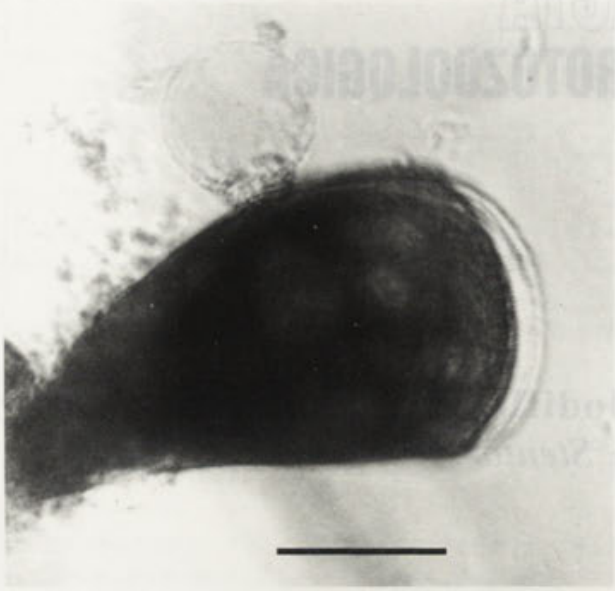

Fig.1. Blistering cell of *Stentor coeruleus* as seen under the light microscope; bar - 100 µm

attached to the bottom of the chamber. The removed blisters adhered to the glass bottom and they remained there during the experiment. We performed the surgery shortly after the blisters were formed since the cells tended to lyse when kept in blistering solution too long. To avoid contamination of the isolated blister by the content of other disintegrating cells in the experimental chamber, the chamber was then perfused with a fresh blistering solution. GΩ seal (2-5 GΩ) could be formed between the membrane of the isolated blister and the tip of the pipette filled with 250 mM NH_4Cl, 2 mM $MgCl_2$, 10^{-7} M Ca^{2+}, 0.1 mM EDTA, 5 mM HEPES, pH 7.2. After GΩ seal was formed, the membrane patch was excised from the blister by withdrawing the tip of the pipette from the chamber. During this brief air exposure the tip of the pipette with the patch of excised membrane was transferred to another chamber. These two chambers were connected together with an agar bridge so the reference grounding level was the same in each of them. The second chamber contained bath solution similar to the solution in the pipette. The isolated blister could remain in the chamber containing blistering solution for hours. The blister could be sampled with fresh pipettes many times which made this method very efficient.

We have encountered several different channel activities in this preparation. Two of them were easy to distinguish because these channels needed Ca^{2+} or cGMP to be activated. Results presented here summarize our

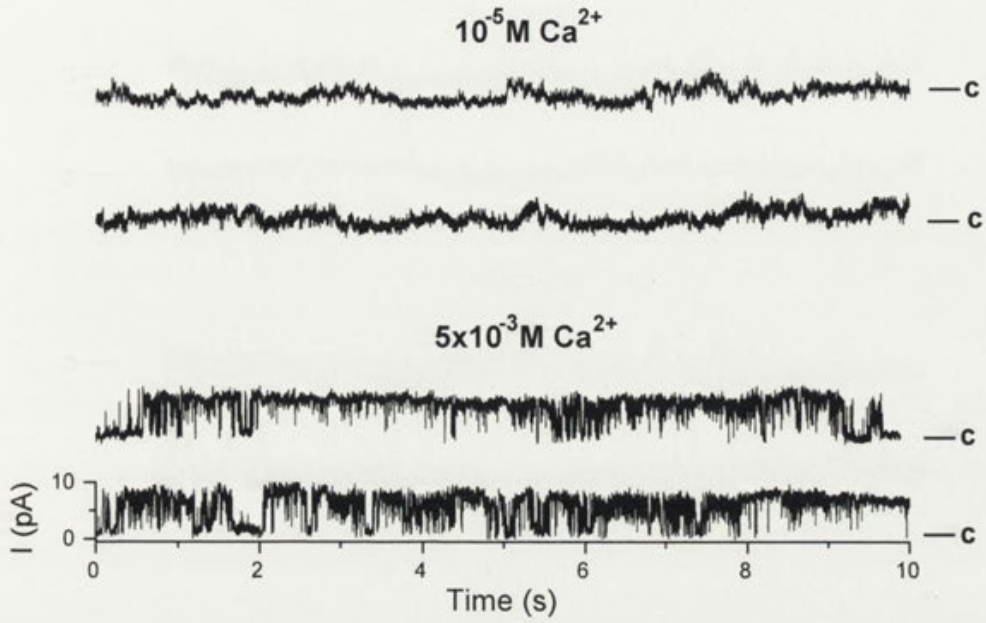

Fig.2. Activities of the Ca^{2+}-activated channel in control solution (10^{-5} M Ca^{2+}) and in the presence of 5 x 10^{-3} M Ca^{2+} recorded at pipette voltage +60 mV from one membrane patch. The two upper and two lower traces represent continuous recordings. Axes displayed at the bottom apply to all traces; „c" represents the closed level of the channel and the upward current deflections represent inward current across the membrane

experience from more than 20 excised inside-out membrane patches.

Typical activities of Ca^{2+}-activated ion channel are represented in Fig. 2. All traces were recorded from the same membrane patch containing at least one channel only. The two upper traces were recorded in the experimental solution containing 10^{-5}M of calcium ions and the two lower traces in the presence of 5 x 10^{-3} M $CaCl_2$. The pipette voltage was +60 mV and the channel conductance in symmetric NH_4Cl was about 90 pS. The open probability P_o was calculated by integrating the total current passing through the channel during the recording time (60 s) and dividing this integral by the recording time and the single channel current. For the channel in Fig. 2, P_o was 0 in control (10^{-5} M Ca^{2+}) and 0.01 in the presence of 10^{-4} M Ca^{2+}. At concentrations of 5 x 10^{-3} M and 10^{-2} M Ca^{2+}, P_o of this channel was 0.29 and 0.83 respectively. Taking into account that the conductance of this channel was measured in symmetric NH_4Cl and that its conductance in symmetric KCl would be larger, it is very likely that this channel belongs to the family of large conductance (unitary conductance of ≅ 200 pS in symmetric 100 mM KCl) calcium-activated potassium channels (maxi K_{Ca}) (Latorre 1994). Ca^{2+}-activated potassium channels were described in the plasma membrane of *Paramecium* (Saimi and Martinac 1989, Kubalski et al. 1989). In another patch containing many Ca^{2+}-activated channels we observed channel activities even in the absence of calcium ions. Their open probability decreased significantly, however, after Mg^{2+} ions were chelated by addition of EDTA (not shown). Therefore, we assumed that the Ca^{2+}-activated ion channel in *Stentor* might be also regulated by magnesium.

Another channel activity that we readily encountered was that of cGMP-regulated ion channel. The cGMP-activated channels are small conductance channels (30 pS and less (Torre and Menini 1994)). To study these channels we usually pulled pipettes with much finer tips to get rid of the large number of background channels (probably chloride or anion channels). We applied cGMP only in the case when the background channel noise was very low. It was sometimes very helpful to wait a few minutes until some of the active channels became silent. The two upper traces in Fig. 3 show activities of cGMP -activated currents in the presence 100 µM cGMP in the bath. Two lower traces come from the same membrane patch and were recorded in the presence of 400 µM cGMP. All four traces were recorded at pipette voltage +60 mV. The single channel conductance of the cGMP- activated channel was 21 pS. The cGMP concentration necessary for the activation of this type of channel has usually been lower in other preparations (Torre and

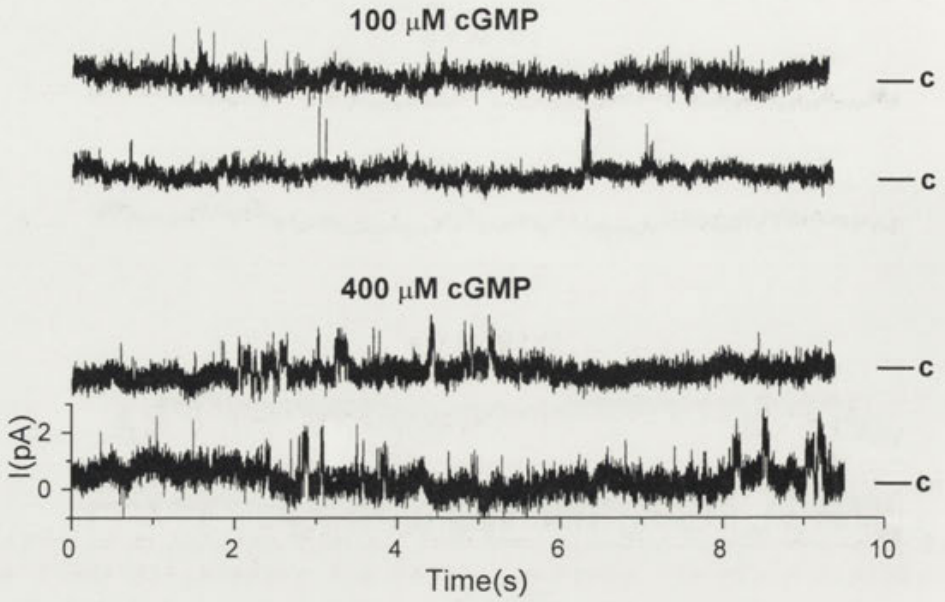

Fig.3. Activities of the cGMP-activated channel in the presence of 100 and 400 μM cGMP. The pipette voltage was +60 mV. The two upper and two lower traces represent continuous recordings. Axes displayed at the bottom apply to all traces; „c" represents the closed level of the channels and the channel openings represent inward current across the cell membrane

Menini 1994). A detailed description of this channel will be presented elsewhere.

The method presented in this report modifies the former procedure for isolating the plasma membrane of ciliates for patch-clamp studies. We believe that the blisters contain plasma and/or alveolar or ciliary membrane only and that they are not contaminated by membranes of intracellular organelles. This belief is supported by the presence of Ca^{2+}-activated and cGMP-activated channels that are likely to exist in the plasma membrane. We developed this method mostly to study cGMP-dependent current in *Stentor* and we hope that this technique in combination with behavioral and biochemical studies will be a powerful tool for the study of phototransduction in ciliates.

Acknowledgments. We thank Dr. Ching Kung from the University of Wisconsin for lending us his equipment. This work was supported in part by grant No. 6PO4C-086-12 from the Committee for Scientific Research and by Statutory grant to the Nencki Institute of Experimental Biology.

REFERENCES

Fabczak H., Park P.-B., Fabczak S., Song P.-S. (1993) Photosensory transduction in ciliates. II Possible role of G-protein and cGMP in *Stentor coeruleus*. *Photochem. Photobiol.* **57:** 702-706

Fabczak S., Fabczak H., Tao N., Song P.-S. (1993) Photosensory transduction in ciliates. I An analysis light-induced electrical and motile responses in *Stentor coeruleus*. *Photochem. Photobiol.* **57:** 696-701

Fabczak S., Fabczak H., Song P.-S. (1994) Ca^{2+} ions mediate the photophobic response in *Blepharisma* and *Stentor*. *Acta Protozool.* **33:** 93-100

Forte M., Hennessey T., Kung C. (1986) Mutation resulting in resistance to polyene antibiotics decrease voltage-sensitive calcium channel activity in *Paramecium*. *J. Neurogenet.* **3:** 75-85

Hamill O. P., Marty A., Neher E., Sakmann B., Sigworth F. J. (1981) Improved patch-clamp techniques for high-resolution current recording from cells and cell-free membrane patches. *Pfluegers Arch.* **391:** 85-100

Haynes L. W. (1992) Block of the cyclic GMP-gated channel of vertebrate rod and cone photoreceptor by l-cis-diltiazem. *J.Gen. Physiol.* **100:** 783-801

Kubalski A., Martinac B., Saimi Y. (1989) Proteolytic activation of a hyperpolarization- and calcium-dependent potassium channel in *Paramecium*. *J. Membrane Biol.* **112:** 91-96

Latorre R. (1994) Molecular workings of large conductance (maxi) Ca^{2+}-activated K^+ channels. In: Handbook of Membrane Channels. (Ed. C. Peracchia) Academic Press, 79-102

Saimi Y., Martinac B. (1989) Calcium-dependent potassium channel in *Paramecium* studied under patch clamp. *J. Membrane Biol.* **112:** 79-89

Torre V., Menini A. (1994) Selectivity and single-channel properties of the cGMP-activated channel in Amphibian retinal rods. In: Handbook of Membrane Channels. (Ed. C. Peracchia) Academic Press, 345-358

Wood D. (1976) Action spectrum and electrophysiological responses correlated with the photophobic response of *Stentor coeruleus*. *Photochem. Photobiol* **24:** 261-266

Received on 10th December, 1996; accepted on 10th April, 1997

Acta Protozoologica (1997) 36: 125 - 130

ACTA
PROTOZOOLOGICA

Sedimentation Velocity of *Loxodes striatus* Immobilized by $MnCl_2$

Dorothea-Ch. NEUGEBAUER, Sigrun MACHEMER-RÖHNISCH, Hans MACHEMER and Richard BRÄUCKER

Arbeitsgruppe Zelluläre Erregungsphysiologie, Fakultät für Biologie, Ruhr-Universität Bochum, Germany

Summary. The sedimentation of *Loxodes striatus* was determined for *g*-values between 1*g* and 5*g* employing a new method of immobilization by $MnCl_2$, and using a low-speed centrifuge microscope to induce hypergravity. Cells immobilized by $MnCl_2$ can be used for at least 4 hours compared to 30-60 minutes after common immobilization in solutions of $NiCl_2$. The sedimentation rates of *Loxodes*, as determined from the medians of several hundred cells, agree with published values of $NiCl_2$-immobilized cells. The sedimentation velocities between 1*g* and 2*g* are fitted by a linear regression line resulting in an extrapolated rate of 42 µm/s at 1*g*. Deviations of the measured values from this linearity at higher accelerations are explained by a methodical experimental variable assuming that proportionality between sedimentation rate and acceleration is applicable according to Stokes´ law.

Key words: immobilization, *Loxodes striatus* (Protozoa, Ciliata), sedimentation velocity.

Abbreviations: EDTA - ethylene-diamine-tetra-acetic acid; *g* - terrestrial acceleration at sea level (9.81 m s^{-2}); NIZEMI -(Niedergeschwindigkeits-Zentrifugen-Mikroskop), low-speed centrifuge microscope.

INTRODUCTION

The cilia of *Loxodes* and other ciliates are always active. Their motion in terms of beat direction and beating rate is modified by external stimuli, such as light, ions, chemicals and gravity, and hence locomotion is an indicator of the cellular response to such stimuli (Machemer 1988, Machemer and Teunis 1996). The analysis of velocities of vertically swimming cells requires the determination of the sedimentation rate because the velocity of a free swimming cell, *V*, is the vector sum of three terms of speed: the active propulsion, *P*, the sedimentation, *S*, and a possible physiological response to gravity, Δ (Machemer et al. 1991). The term of *P* is independent of the swimming direction, *S* obviously depends on the gravity vector, and so does Δ which tends to compensate *S* (Bräucker et al. 1994). Measurements of the sedimentation rate require cells which do not move actively. This means that the cilia must be stopped from active beating.

Immobilization of ciliates is no trivial task. The osmotic properties of the cytoplasmic membrane must not be disturbed to prevent changes of shape and volume. Immobilization may be accomplished either by paralyzing the cilia or by removing them. $NiCl_2$ - used most commonly - immobilizes the cilia (von Gelei 1935, Kuźnicki 1963b, Machemer and Bräucker 1992, Naitoh 1966). Chloral hydrate (Kuźnicki 1963a, Nelson 1995) or low concentrations of ethanol (Nelson 1995, Ogura 1981)

Address for correspondence: Dorothea-Ch. Neugebauer Arbeitsgruppe Zelluläre Erregungsphysiologie, Fakultät für Biologie, Ruhr-Universität, D-44780 Bochum, Germany; Fax: ++49 234 7094 186; E-mail: machemer@neurobiologie.ruhr-uni-bochum.de

immobilize by inducing the cells to shed their cilia. The latter method may require some mechanical treatment of the cells in addition to the chemical agents employed.

Cells of *Loxodes* are very easily damaged mechanically. A method requiring chemical agents alone is therefore particularly desirable. The only method so far successfully employed for immobilizing *Loxodes* uses $NiCl_2$ (Bräucker et al. 1992, Machemer-Röhnisch et al. 1993). This method has some inherent problems, e.g., the range of Ni^{2+} concentrations from physiological immobilization to severe damage to the cells is very narrow. Oral and somatic cilia require slightly different concentrations of $NiCl_2$, and the time interval between complete immobilization and morphological changes preceding cell death does not exceed 30-60 min. Moreover, this time interval varies unpredictably. Apparently, it depends on so far uncontrolled properties of the cell cultures. Therefore, we developed an alternative method using a combination of $MnCl_2$, EDTA and $CaCl_2$. The quality of the immobilization was tested by measuring the sedimentation velocity of *Loxodes* at 1*g* and at increased *g*-values in the NIZEMI (Bräucker 1995, Kreuzberg et al. 1990). The sedimentation data are compared with published data obtained with cells immobilized by $NiCl_2$. Part of the results have been previously reported at a workshop in preliminary form (Neugebauer and Machemer 1996).

MATERIALS AND METHODS

Immobilization

Loxodes striatus (Penard 1917) was cultivated in soil extract at 18°C in the dark as described (Bobyleva 1981, Machemer-Röhnisch et al. 1993). Cells were fed twice a week with *Euglena gracilis*. Experiments were carried out at 20-24°C using cells 2 to 6 days after the last feeding. The cells were washed once in experimental solution (1 mM $CaCl_2$, 0.5 mM KCl, 0.1 mM $MgCl_2$, 0.41 mM Na_2HPO_4, 0.18 mM NaH_2PO_4, pH 7.0). Washing was done most gently by adding a few millilitres of cells in culture medium to 10-15 ml experimental solution in a conical test tube. As the experimental solution is air-saturated and thereby high in oxygen concentration compared to the culture medium, the *Loxodes* cells swim actively to the bottom (Fenchel and Finlay 1984) of the test tube within 10-15 min and stay there.

Concentrated cell suspension (200-250 µl) in experimental solution were added to 200 µl of 50 mM $MnCl_2$ (final conc. 20-25 mM) buffered with 10 mM Tris to pH 7.4. The solutions were mixed by slowly aspiring the whole volume into a Pasteur pipette. After 5-10 min at room temperature (20-24°C) 10 µl of 50 mM EDTA (final conc. 1-1.5 mM), pH adjusted to 7.0-7.2 with KOH, were added and mixed as before. After 5-10 min, the same volume (300-500µl) of experimental solution or, alternatively, 50 mM $CaCl_2$ to a final concentration of 0.5-1.0 mM Ca^{2+}, was added and mixed as before. The sample was then diluted to the desired volume with an appropriate solution.

Sedimentation

The immobilized cells were carefully and gently infused into the chamber for recording (34 x 34 mm, height 2 mm, volume 2.3 ml). The chamber was left in horizontal position for 15-30 min at 22°C and was then fixed in the NIZEMI with the plane of observation perpendicular to the direction of *g*-force. This position was kept during acceleration (1*g* per min) to prevent premature sedimentation of the cells. When the desired *g*-value was reached, the chamber was rotated into the measuring position within 30 s, that is, with the plane of observation parallel to the direction of the *g*-vector (Bräucker 1995). The field of 13.5 x 17.5 mm was then videotaped for 4 min using green dark-field illumination (light-emitting diodes, λ = 565 nm), as soon as the chamber had reached the vertical position. After deceleration, the chamber was rotated to its initial position, taken out, and put back after a rotation through 180°. Every 8 to 10 min a new measurement was started. All sedimentation experiments were carried out at 22°C. Sequential video frames were digitized and superimposed after colour-coding. The resulting tracks represent the direction and the speed of individual cells. The colour sequence depicts the direction, and the lengths of coloured sections show the speed. Cell tracks were measured using an interactive computer program (for details see Bräucker et al. 1992).

The time t at which evaluation of cell tracks could start depended on the *g*-value. At high acceleration (3 to 5*g*) the first 40 to 60 s of the video record were not evaluated because larger particles such as aggregates of cells caused a transient turbulence of the fluid.

RESULTS

Immobilization

Loxodes striatus reacted to the addition of manganese ions with a series of reversals. The frequency of these reversals decreased with time and subsided completely after 5-10 min. At this time EDTA was added. The vanishing of reversals is an indicator of the correct duration of incubation with manganese alone. The initial frequency and the duration of reversals depended on the feeding state of the cells. Upon addition of EDTA, the cells became instantaneously immotile. Only a few cells (≤1 in 500) remained active for many hours for unknown reasons.

Immobilized cells did not change their shape or morphology for at least 36 h as monitored at a magnification of 50x. At high magnification (250-400x) some morphological changes were visible. A slight shrinkage and the development of small blisters (diameter ≤ 10 µm) could be observed in most cells within the first 30 min after immobilization. The morphological state reached after one hour, however, was unchanged for at least 36 h at room temperature. The cells kept their cilia.

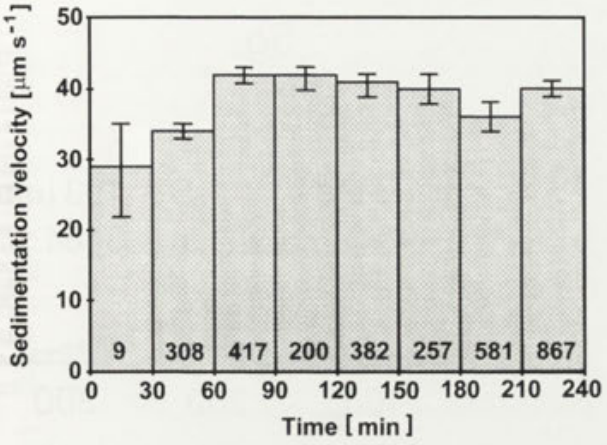

Fig. 1. Sedimentation velocities of *Loxodes* at 1*g* versus time after immobilization with $MnCl_2$. Each column represents data accumulated from at least 3 separate experiments. Data were grouped in classes 30 min wide. The median of the sedimentation velocity is given. Bars mark the 95% confidence interval. Numbers in the columns indicate the number of cell tracks measured within each time interval. Note the low number of cells measured within the first 30 min

The immobilization was reversible by the addition of Ca^{2+} to a final concentration of 2 mM $CaCl_2$ within 30-60 s after the addition of EDTA. Remobilized cells did not show morphological changes for at least 48 h in a medium containing 25 mM $MnCl_2$, 1 mM EDTA and 2 mM $CaCl_2$ at pH 6.8-7.4.

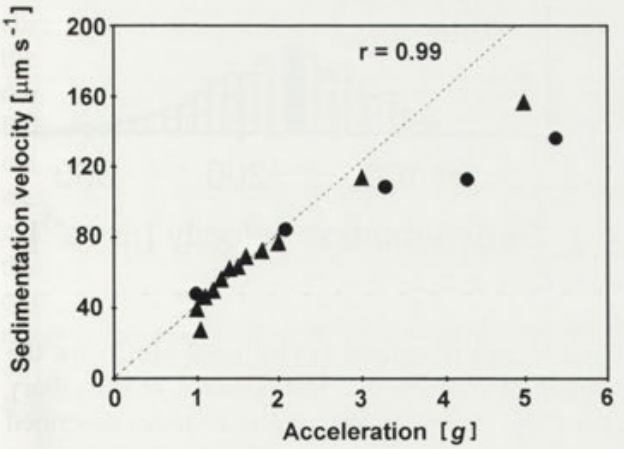

Fig. 2. Sedimentation of *Loxodes* plotted as a function of acceleration. Data from $MnCl_2$-immobilized cells (triangles; n = 1038 - 4110 per data point), and from cells immobilized using $NiCl_2$ (dots; n = 175 - 370 per data point; Machemer-Röhnisch et al. 1993). The dashed line shows the linear regression using $MnCl_2$-data between 1*g* and 2*g*

The important parameters for a successful immobilization of *Loxodes* are the concentration of Mn^{2+}, pH, and timing. At too high a concentration of Mn^{2+} (such as 50 mM) and reduced pH (6.6-7.0), the cells fold in the middle and become paralysed in that position. At raised pH (7.2-7.4) the cells are immotile within 15 min, develop vacuoles and burst within 30 min. At concentrations of Mn^{2+} below 20 mM, the cells do not immobilize before major *prae-mortem* changes have developed. The correct incubation time with $MnCl_2$ is determined for each sample by observing the behaviour of the cells at 50x magnification. The timing of the application of EDTA, as judged from the behaviour of the cells, allows reproducible results. Ca^{2+} must be added within 5 to 10 min after immobilization. If Ca^{2+} is added too late, or not at all, the cells vacuolate and burst within 30-60 min.

Sedimentation

Loxodes cells immobilized with $MnCl_2$ / EDTA adhered to the walls of the recording chamber for about 15 min. Measurements were started only after that period. The sedimentation velocity was determined throughout 4 h (Fig. 1). Up to 30 min very few cells were found sedimenting and their median velocity was lower than 39 µm/s. Between 30 and 60 min the number of sedimenting cells increased as well as the velocity of sedimentation. Only after 60 min had passed, the velocity of sedimentation did not increase further. A constant value of 39 µm/s was found at all time intervals up to four hours (Fig. 1).

Sedimentation velocity increases with increasing *g*-value (Fig. 2). A linear relationship between sedimentation velocity and *g*-value was found up to 2*g*. A sedimentation rate of 42 µm/s at 1*g* is extrapolated from the linear regression line using data of sedimentation between 1*g* and 2*g* (Fig. 2). Above 2*g*, the data points deviate from linearity towards lower values. The deviation rises with increasing acceleration.

DISCUSSION

Immobilization

Immobilized cells should be unaffected morphologically. Viability is no absolute requirement. However, *prae-mortem* changes such as vacuolization, deformation of the cell, and changes in specific density render them unsuitable for the determination of the sedimentation velocity. In addition, the immotile state should last for a reasonably long time (≥ 1 h) to carry out the experiments.

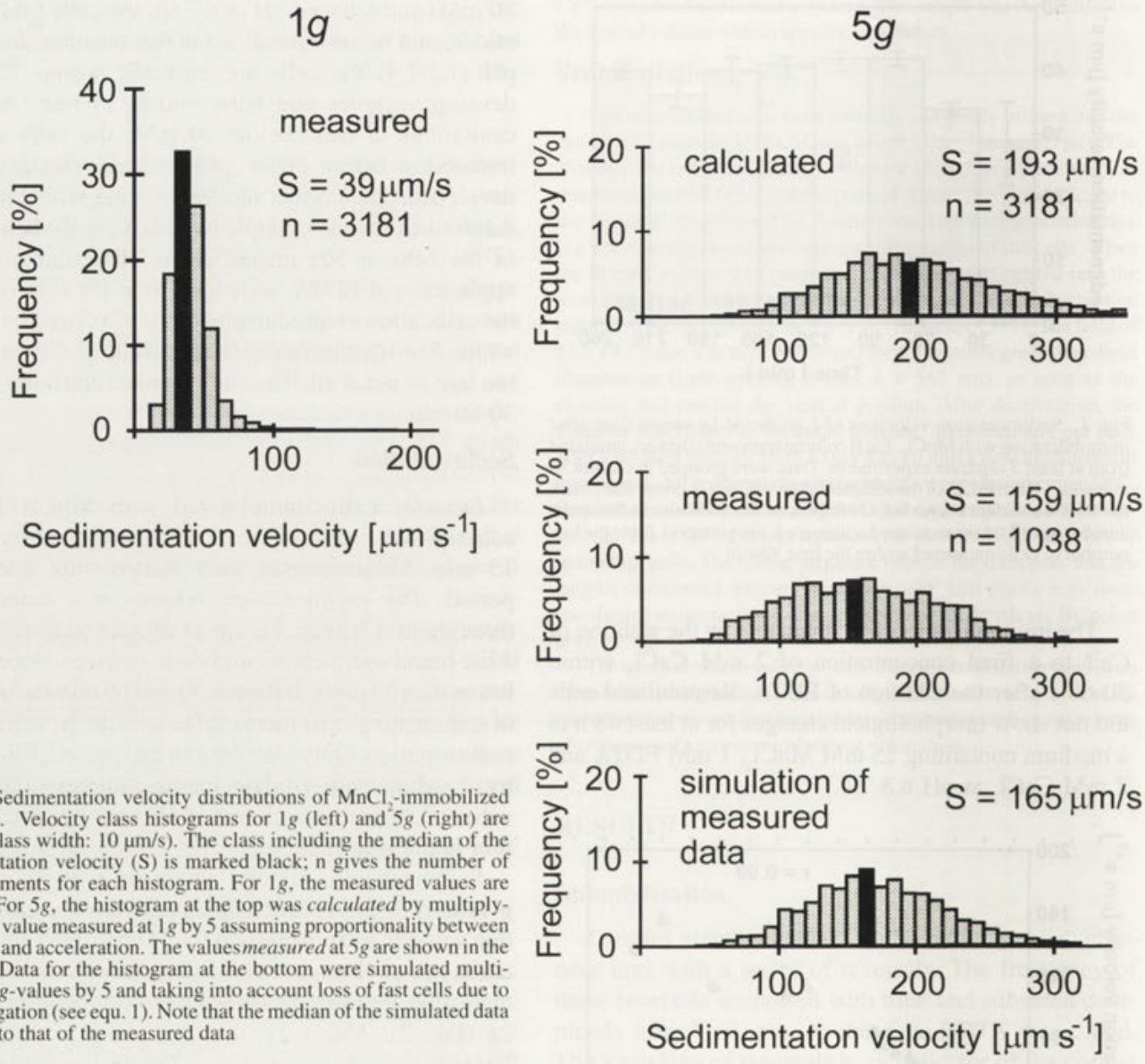

Fig. 3. Sedimentation velocity distributions of $MnCl_2$-immobilized *Loxodes*. Velocity class histograms for 1*g* (left) and 5*g* (right) are given (class width: 10 µm/s). The class including the median of the sedimentation velocity (S) is marked black; n gives the number of measurements for each histogram. For 1*g*, the measured values are shown. For 5*g*, the histogram at the top was *calculated* by multiplying each value measured at 1*g* by 5 assuming proportionality between velocity and acceleration. The values *measured* at 5*g* are shown in the middle. Data for the histogram at the bottom were simulated multiplying 1*g*-values by 5 and taking into account loss of fast cells due to centrifugation (see equ. 1). Note that the median of the simulated data is close to that of the measured data

The most widely used method of immobilization, application of $NiCl_2$ (Bräucker et al. 1992, von Gelei 1935, Kuźnicki 1963b, Naitoh 1966) is applicable to many species and requires only an adequate ratio of Ni^{2+} versus other divalent cations such as Ca^{2+} and Mg^{2+} (von Gelei 1935, Kuźnicki 1963b). However, the range of Ni-concentrations to induce ciliary arrest but no vacuolization of the cell is narrow. The period of time passing between ciliary arrest and vacuolization varies even within one species, and is much influenced by the state of the cell (e. g., feeding, cell cycle) preceding immobilization. The last point is especially important in the species of *Loxodes striatus*.

Fukushi and Hiwatashi (1970) used $MnCl_2$ for the deciliation of *Paramecium* and isolation of the ciliary fraction. The method to immobilize *Loxodes* described here was inspired by the recipe given by these authors.

A good test of the viability of cells is remobilization. In *Loxodes*, this occurs by addition of Ca^{2+} to a final concentration of 1 mM within 30 to 60 s after the addition of EDTA. Ni-immobilized *Paramecium* is reported to recover even after 60 min of immobile state (Kuźnicki 1963b). Although *Loxodes* is immobilized irreversibly by $MnCl_2$ / EDTA after the passage of 1 min, its morphology appears to be little affected and is stable for days; its sedimentation values were unchanged for at least 4 h (Fig.1).

Sequential application of $MnCl_2$, EDTA and $CaCl_2$ for immobilization is more convenient than using $NiCl_2$ for the following reasons: (1) the concentration of $MnCl_2$ is not very critical (20-25 mM); (2) a difference in sensitivity between oral and somatic cilia was not observed; (3) by using the behaviour of the cells for criterion, the incubation time with manganese can be adapted to the requirements of any batch of cells; (4) only minor morphological changes are detectable at high magnification; (5) Mn-immobilized cells are stable for many hours.

Sedimentation

The sedimentation velocity of perfectly immobilized cells should correspond to sedimentation of untreated cells and vary with the *g*-value only. Knowledge of the sedimentation rate is indispensable for quantitative treatment of swimming velocities as an indicator of the physiological reaction to gravity in ciliates (Machemer and Bräucker 1992). Since the sedimentation velocity is much influenced by the shape of the cell and its hydrodynamics, calculations from known cell dimensions, cytoplasmic density, and viscosity of the medium (Stokes´ law) can provide a crude approximation at best.

The sedimentation velocity of *Loxodes* immobilized with $MnCl_2$/ EDTA increased slightly with time during the first hour. This is presumably a consequence of the initial adherence of the cells to the walls of the recording chamber. This cell adherence is most likely responsible for the very low number of cells observed in sedimentation during the first 30 min following immobilization (Fig. 1). Reliable sedimentation velocities were therefore measured not before 1 h after immobilization. Constancy of the measured value of 39 µm/s for three more hours, and small confidence intervals from 1 hour onwards indicate that the preparation had stabilized indeed. The magnitude of the sedimentation velocity is in the lower range of published values (49 µm/s, Bräucker et al. 1992; 40 µm/s, Fenchel and Finlay 1984; 47 µm/s, Machemer-Röhnisch et al. 1993).

Between 1*g* and 2*g*, the measured values for $MnCl_2$-immobilized cells (this paper) and the published data for $NiCl_2$-immobilized *Loxodes* (Machemer-Röhnisch et al. 1993) fit almost perfectly the same linear regression line ($r = 0.99$; Fig. 2). This supports the view that both methods of immobilization are equally reliable. An extrapolated value of the sedimentation rate at 1*g* is 42 µm/s. We consider this figure to be more reliable than the median value obtained from measurements at 1*g*.

According to Stokes´ law, the sedimentation velocity should be directly proportional to the *g*-force at Reynolds numbers <1. At accelerations above 2*g*, the measured data show a depression towards values which are lower than expected from theory. A possible explanation is a methodical error in the determination of sedimentation. Cells which have passed the video field at the beginning of registration, are lost for measurement. At raised *g*-values, cells pass the measuring field within a shorter time than at 1*g*. Consequently, the proportion of fast cells is reduced. This effect is not negligible because the reservoir of cells above the video field may be depleted after a critical period of time.

An estimate of the time-dependent error (see Appendix) shows that this effect can explain the deviation of the $MnCl_2$-immobilized cells at 5*g* from the prediction of Stokes´ law. The even larger offset of the published results of $NiCl_2$-immobilized *Loxodes* may be due to the fact that those data were obtained with a previous version of the NIZEMI (Kreuzberg et al. 1990), in which the chamber was permanently in the recording position and cells had been exposed to rising acceleration for 5 min prior to the measurement (Bräucker et al. 1994, Machemer-Röhnisch et al. 1993).

Because the deviation from linearity (Stokes´ law) at higher accelerations can be explained by a methodical effect of the experimental procedure, it may be justified to use the linear regression line to extrapolate sedimentation velocities for *Loxodes* beyond accelerations of 1*g* (see Appendix). Sedimentation velocities for *g*-values below 1*g* might be obtained by downward extrapolation from this line.

APPENDIX

Estimation of an error in determination of sedimentation rates

At 1*g* cells of *Loxodes striatus* sedimented at velocities between 10 µm/s and 100 µm/s. The median velocity was 39 µm/s (Fig. 3). Assuming applicability of Stokes´ law, each cell is likely to sediment with the 5-fold 1*g*-velocity at 5*g* (195 µm/s median velocity). Distance and time are measured to determine the speed of the cell. The video field was 13.5 x 17.5 mm, and the free space above (or centripetally to) this field was approximately 10 mm. After the chamber had been oriented parallel to the vector of gravity, sedimentation rates of the fastest cells tended to "dilute" the previously even distribution of cells in the top region of the chamber. Evaluation of sedimenting cells was possible about 1 min after the start of sedimentation for technical reasons (see Methods).

During this time, cells sedimenting at a velocity of 195 µm/s have passed about 12 mm. "Influx" of these cells into and "efflux" from the central video field are no longer equal after 1 min, and the initial distribution of sedimentation velocities in the registered population of cells shifts in favour of ever lower velocities.

The velocity distribution of a cell population may be represented by a class histogram showing the relative frequencies (or proportions) of particular velocity classes within a given cell population (Fig. 3). The *measured* velocity distribution at, e. g., 5*g* is assumed to shift to the left of the velocity-axis with time progressing. A measured distribution at 5*g* can be *simulated* (f_s) from frequencies (f_c) which were *calculated* from 1*g*-distributions and multiplied by 5 under Stokes´ law assumptions:

$$f_S = f_C \frac{1 - v_i t}{d_{max}}, \qquad (1)$$

where v_i represents a velocity class, t is the time passed since the start of sedimentation, and d_{max} is the maximal sedimentation distance of observable cells (from upper limit of fluid space to lower limit of video field). It is seen that the expression, $v_i t / d_{max}$, is zero at time zero, and grows toward unity at the time (t_{max}), when the last cell of velocity v_i has passed d_{max}. Consequently, with the assumptions made, any simulated frequency of a velocity class equals the frequency of calculated Stokes´ velocity of that class at time zero, and is reduced to zero at time t_{max}. Accordingly, a simulated frequency is expected to approximate the measured frequency at a time t larger than zero time and less than t_{max}. Because this time t is given by the experimental procedure, a measured frequency distribution of velocities can be compared with the simulated frequency distribution based on extrapolation of 1*g*-distributions.

Proportions of cells within velocity classes were simulated using the data obtained under 1*g*-conditions, equ. 1, and assuming proportionality of v_i and *g*. These simulated class frequencies were then used to calculate the median velocity. The simulated median velocity of sedimenting cells at 5*g* is 165 µm/s. This value is close to the value of 159 µm/s as measured at 5*g* (Fig. 3). The procedure applying equ. 1 supports the view that median velocities at time zero were close to the calculated value of 193 µm/s, and Stokes´ law is therefore applicable to *g*-dependent sedimentation of *Loxodes striatus*.

Acknowledgments. This work was supported by the Deutsche Agentur für Raumfahrtangelegenheiten (DARA, grant 50WB93193) and the Minister für Wissenschaft und Forschung of the state of Nordrhein-Westfalen (grant IV A1-21600588). We are grateful to Wilhelm Neugebauer for discussions regarding the mathematical treatment of the data. We thank Martin Krause for technical assistance.

REFERENCES

Bobyleva N.N. (1981) Cultivation and cloning of the primitive ciliates of the genus *Loxodes* and some aspects of their biology. *Citologija* **23:** 1073-1077 (in Russian)

Bräucker R. (1995) Hypergravity research in ciliates: achievements and shortcomings of the latest NIZEMI version. In: Proc. C.E.B.A.S. Workshops, Annual Issue 1995, (Ed. R. Bräucker), Bochum, 49-55

Bräucker R., Machemer-Röhnisch S., Machemer H.,Murakami A. (1992) Gravity-controlled gliding velocity in *Loxodes*. *Europ. J. Protistol.* **28:** 238-245

Bräucker R., Machemer-Röhnisch S., Machemer H. (1994) Graviresponses in *Paramecium caudatum* and *Didinium nasutum* examined under varied hypergravity conditions. *J. exp. Biol.* **197:** 271-294

Fenchel T., Finlay B.J. (1984) Geotaxis in the ciliated protozoon *Loxodes*. *J. exp. Biol.* **110:** 17-33

Fukushi J., Hiwatashi K. (1970) Preparation of mating reaction cilia from *Paramecium caudatum* by $MnCl_2$. *J. Protozool.* **17:** Suppl. 21, 63

Gelei, J. von (1935) Ni-Infusorien im Dienste der Forschung und des Unterrichtes. *Biol. Zbl.* **55:** 57-74

Kreuzberg K., Behrle R., Joop O., Treichel R. (1990) The slow-rotating centrifuge microscope (NIZEMI): a new research tool for terrestrial and space-related gravitational biology. In: Proc. IV. Eur. Symposium "Life Sciences Research in Space" (Ed. V. David), Trieste 1990, ESA Publications, ESTEC, Noordwijk, 471-474

Kuźnicki L. (1963a) Recovery in *Paramecium caudatum* immobilized by chloral hydrate treatment. *Acta Protozool.* **1:** 177-185

Kuźnicki L. (1963b) Reversible immobilization of *Paramecium caudatum* evoked by nickel ions. *Acta Protozool.* **1:** 301-312

Machemer H. (1988) Motor control of cilia. In: *Paramecium*, (Ed. H.D. Görtz), Springer Verlag, Berlin, Heidelberg, New York, Tokyo, 216-235

Machemer H., Bräucker, R. (1992) Gravireception and graviresponses in ciliates. *Acta Protozool.* **31:** 185-214

Machemer H., Teunis P.F.M. (1996) Sensorimotor coupling and motor responses. In: Ciliates: Cells as Organisms, (Eds. K. Hausmann, P.C. Bradbury), Gustav Fischer, Stuttgart, New York, 379-402

Machemer H., Machemer-Röhnisch S., Bräucker R., Takahashi K. (1991) Gravikinesis in *Paramecium*: Theory and isolation of a physiological response to the natural gravity vector. *J. Comp. Physiol. A* **168:** 1-12

Machemer-Röhnisch S., Bräucker R., Machemer H. (1993) Neutral gravitaxis of gliding *Loxodes* exposed to normal and raised gravity. *J. comp. Physiol. A* **171:** 779-790

Naitoh Y. (1966) Reversal response elicited in nonbeating cilia of *Paramecium* by membrane depolarization. *Science* **154:** 660-662

Nelson D.L. (1995) Preparation of cilia and subciliary fractions from *Paramecium*. *Methods in Cell Biol.* **47:** 17-24

Neugebauer D.-Ch., Machemer H. (1996) G-dependent sedimentation of *Loxodes striatus* using a new method of immobilization. In: Proc. C.E.B.A.S. Workshops, Annual Issue 1996, (Ed. R. Bräucker), Bochum, 133-138

Ogura A. (1981) Deciliation and reciliation in *Paramecium* after treatment with ethanol. *Cell Structure and Function* **6:** 43-50

Penard E. (1917) Le genre *Loxodes*. *Rev. Suisse Zool.* **25:** 453-488

Received on 10th January, 1997; accepted on 20th March, 1997

Acta Protozoologica (1997) 36: 131 - 135

ACTA
PROTOZOOLOGICA

First Report of *Sarcocystis rangiferi* and a Second *Sarcocystis* Species with Parasite-induced Encapsulation in Cervids from Central Europe

Manuela STOLTE, Ingrid BOCKHARDT and Klaus ODENING

Institute for Zoo Biology and Wildlife Research, Berlin, Germany

Summary. The protozoan *Sarcocystis rangiferi* Gjerde, 1984 was found for the first time in the skeletal muscle of a reindeer (*Rangifer tarandus*), born in a German zoological garden. It is characterized by the ultrastructural cyst wall type 15 of Dubey et al. (1989). Another, not determinable *Sarcocystis* species with parasite-induced encapsulation was found in the oesophageal musculature of a free ranging roe deer (*Capreolus capreolus*) from Germany. Its cyst wall was similar to type 24 of Dubey et al. (1989).

Key words: *Capreolus capreolus,* encapsulation by host, Germany, *Rangifer tarandus, Sarcocystis rangiferi, Sarcocystis* sp.

Abbreviations: GS - ground substance, LM - light microscopy, PCW - primary cyst wall, TEM - transmission electron microscopy

INTRODUCTION

The reindeer in Norway are intermediate host of six *Sarcocystis* species (Sarcocystidae), according to Gjerde (1986) and Dubey et al. (1989). Four of them resemble more or less the four species which are known from roe deer (Sedlaczek and Wesemeier 1995) and, in part, from other cervids (Wesemeier and Sedlaczek 1995a, b) in Central Europe: *S. grueneri* Yakimoff and Sokoloff, 1934 is similar to or morphologically indistinguishable from *S. cervicanis* Hernández-Rodríguez et al., 1981 and *S. wapiti* Speer and Dubey, 1982, *S. tarandi* Gjerde, 1984 to *S.* cf. *hofmanni* Odening et al., 1994, *S. rangi* Gjerde, 1984 to *S. capreolicanis* Erber et al., 1978, and *S. tarandivulpes* Gjerde, 1984 bears a remote resemblance to *S. gracilis* Rátz, 1909. The present report suggests that at least one of the two other species (*S. rangiferi* Gjerde, 1984) of reindeer may occur also in Central Europe. Our findings emphasize that the knowledge of *Sarcocystis* in large, wild ruminants remains rudimentary.

Address for correspondence: Klaus Odening, IZW, PF 60 1103, D-10252 Berlin, Germany; Fax: (+49) 30-5126104; E-mail: odening@izw-berlin.de

MATERIALS AND METHODS

The domestic reindeer, *Rangifer tarandus* (L.), was born in the Tierpark Berlin-Friedrichsfelde on 3rd May 1980 and died there on 15th March 1993. The roe deer, *Capreolus capreolus* (L.), was shot on 26th November 1995 in the region of Neustrelitz (Land Mecklenburg-Vorpommern, Germany).

Samples of muscle tissue were investigated in the fresh state under a dissecting microscope. Sarcocysts were processed for fresh-state examination and/or histological and transmission electron microscopic investigations (TEM). For the latter the sarcocysts were fixed according to Karnowsky (1965), post-fixed in 1% osmiumtetroxide (Serva Feinbiochemica Heidelberg, Germany), dehydrated with ethanol and embedded in glycidether (Serva Feinbiochemica Heidelberg, Germany). Ultrathin sections were examined with a Zeiss EM 902 A.

RESULTS

Sarcocystis rangiferi Gjerde, 1984 (Figs. 1-4)

Host: *Rangifer tarandus* (Cervidae).

Site: skeletal musculature.

Description: this species formed sarcocysts within muscle fibres. The cyst wall (interior envelope: GS plus PCW) was 1.2-2.0 μm wide (TEM). It formed finger-shaped villar protrusions with microtubules in the core

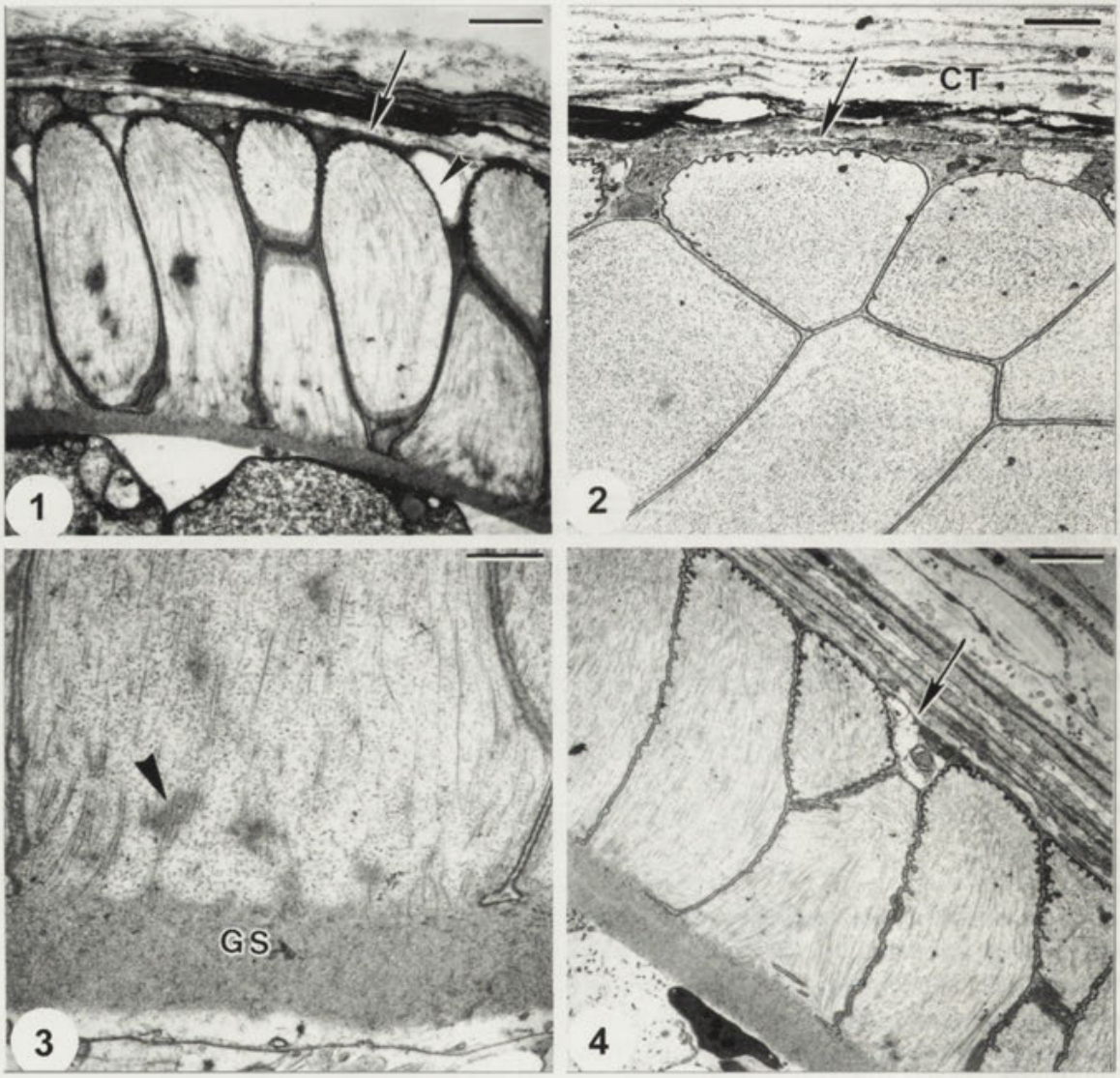

Figs. 1-4. *Sarcocystis rangiferi* from *Rangifer tarandus*. TEM micrographs of the cyst wall region. 1 - longitudinal cuts of villar protrusions (arrowhead) with rounded tip. Plasma membrane of the host muscle fibre (arrow), bar - 2.5 μm; 2 - cross-section of villar protrusions. Plasma membrane of the host muscle fibre (arrow). CT- connective tissue layer, bar - 1.8 μm; 3 - basis of a protrusion with small bundles of microtubules (arrowhead). GS - ground substance, bar - 0.77 μm; 4 - longitudinal cuts of villar protrusions with angular tip. Plasma membrane of the host muscle fibre (arrow), beneath which is a region with vacuolized detritus and above the connective tissue layer, bar-2.5μm

Figs. 5-11. *Sarcocystis* sp. from *Capreolus capreolus*. TEM micrographs of the cyst wall region. 5,6- the whole cyst wall with encapsulation. Thickened plasma membrane of the host muscle fibre (arrows), longitudinally cut villar protrusions (black arrowhead); 5 - bar -2.5 μm; 6 - a layer of vacuolised detritus and mitochondria between plasma membrane and main (dark) layer of the muscle fibre remnant, bar - 1.5 μm; 7,8- longitudinal cuts of villar protrusions (black arrowhead) with the median bundle of microtubules (white arrowheads); 7 - bar - 0.46 μm; 8 - bar - 0.77 μm; 9-11-cross-sections of villar protrusions at their base with the central bundle of microtubules; 9- a villar protrusion seems to arise from another one-bar - 0.77 μm; 10 -the central bundle of microtubules within the base of a villar protrusion and the continuation of such a bundle within the ground substance (white arrowheads),10,11 - bar - 0.46 μm. Inset: magnification of an elevation of the undulating surface of a villar protrusion. Note the "brush trimming", bar -0.15 μm

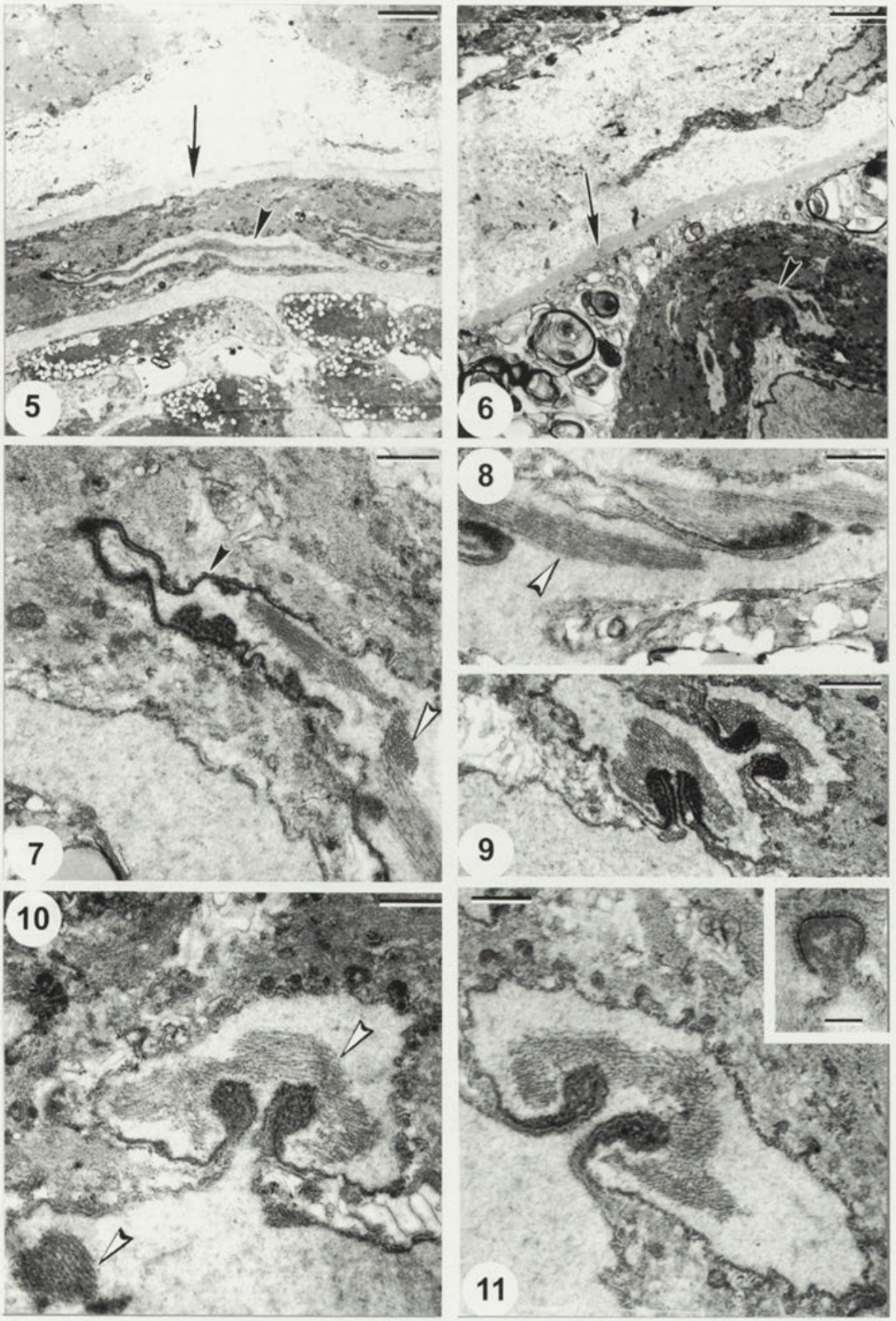

(Figs. 1-4), corresponding to type 10 (or 15) of the classification by Dubey et al. (1989). The villar protrusions were 10.3-11.3 µm long and 2.8-6.5 µm wide. The remnant of the host cell was surrounded by a layer of collagenous fibres (Figs. 1, 2, 4), followed peripherally by loose connective tissue (Figs. 1, 4).

***Sarcocystis* sp. (Figs. 5-11)**

Host: *Capreolus capreolus* (Cervidae).

Site: muscle of the oesophageal wall.

Description: there was only one relative small sarcocyst (1.5 mm x 96 µm), which contained mainly mature cystozoites. By LM the surface of the sarcocyst appeared smooth and the wall thin. The cyst wall (GS plus PCW) was 0.3-2.8 µm wide (TEM). Flat villar protrusions arose from the cyst wall at greater, unequal interspaces, mostly lying close to the cyst wall surface (Figs. 5, 7, 8). They were shaped like an irregular arrowhead. Their surface, mainly in cross-sections, was more undulated than in the PCW regions between the villar protrusions (Figs. 9-11). The surface of the undulations was provided with a kind of "brush trimming" (Fig. 11, inset). In the core of each villar protrusion a bundle of microtubules (Figs. 5, 7-11) was present. On longitudinal sections the villar protrusions tapered toward their tips; the bundle of microtubules reached from the region near the tip into the GS of the cyst wall (Figs. 5, 7, 8, 10). The villar protrusions were 5-8 µm long (LM) or (TEM) 6.0-11.8 µm long, 0.3-3.6 µm wide and 0.3-1.1 µm thick. On cross-sections their base showed a 0.5-1.2 µm long and 0.1-0.2 µm wide stalk surrounded by the upper wider part, so that the base of the protrusions appeared to be flanked by two narrow indentations (Figs. 9-11).

The host muscle fibre was altered. No intact myofibrils were left. In some regions a layer of vacuolized detritus was present within the host cell remnant. The bordering membrane of the muscle fibre was thickened homogeneously and had a width of 0.4-0.6 µm (Figs. 5, 6). Peripheral to this bordering layer was a layer of loose connective tissue with fibrocytes (Figs. 5, 6).

DISCUSSION

Only 13 of the about 180 *Sarcocystis* species known so far induce an encapsulation by the intermediate host, covering the infected muscle fibre or host cell (the encapsulation is also referred to as "secondary cyst wall", but this is inaccurate because it is not derived from the parasite, cf. Gjerde 1985a). These 13 species are *S. mucosa* (Blanchard, 1885), *S. gigantea* (Railliet, 1886), *S. moulei* Neveu-Lemaire, 1912, *S. mongolica* Machul'skii, 1947, *Sarcocystis* sp. type B of Rzepczyk and Scholtyseck (1976), *Sarcocystis* sp. type B of Colwell and Mahrt (1981), *S. hardangeri* Gjerde, 1984, *S. rangiferi* Gjerde, 1984, *Sarcocystis* sp. (1) of Fedoseenko (1986), *S. hoarensis* Matuschka et al., 1987, *S. neotomafelis* Galavíz-Silva et al., 1991, *S. jorrini* Hernández-Rodríguez et al., 1992, and *S. phoeniconaii* Göbel et al., 1996; cf. Odening et al. (1996a). Therefore, such an encapsulation, mostly present already in young sarcocysts, represents an important feature for the determination of corresponding *Sarcocystis* species.

The encapsulation takes place in different manner, according to the 11 cases so far described in detail:

(1) The plasma membrane of the host cell remains unaltered. It is about 0.1 µm wide as in uninfected cells. Peripherally a layer of reticular or collagenous fibres and fibroblasts/fibrocytes of different numbers follows (*S. rangiferi, S. jorrini, Sarcocystis* sp. type B of Rzepczyk and Scholtyseck (1976), *S. mucosa, S. hoarensis, S. phoeniconaii* - see Gjerde (1985a), Hernández-Rodríguez et al. (1992), Rzepczyk and Scholtyseck (1976), O'Donoghue et al. (1987), Matuschka et al. (1987), Göbel et al. (1996).

(2) The plasma membrane of the host cell is distinctly thickened and honeycombed with adherent collagenous fibrils. It has been described as being hyaline, but it has a distinct laminar structure (*S. gigantea, S. moulei*). A connective tissue envelope with fibroblasts/fibrocytes may follow peripherally. See Bergmann and Kinder (1975), Ghaffar et al. (1989).

(3) The plasma membrane of the host cell is distinctly thickened and appears to be homogeneous. It shows no distinct laminar structure (*S. hardangeri, Sarcocystis* sp. type B of Colwell and Mahrt (1981), *S. mongolica, Sarcocystis* sp. in this paper). A connective tissue layer follows peripherally, consisting of collagenous fibrils and fibroblasts/fibrocytes, enveloped by loose connective tissue. See Gjerde (1985b), Colwell and Mahrt (1981), Odening et al. (1996a).

The assignation of the sarcocysts found in reindeer born in a German zoological garden to *S. rangiferi* is unambiguous.

The *Sarcocystis* species found in roe deer, however, cannot be determined. The species *S. cornagliai* Odening et al., 1996b from chamois and *Sarcocystis* sp. of Novak et al. (1987) from cattle, with a similar ultrastructure of the cyst wall, are not considered because the host cells of their sarcocysts are not encapsulated. Among the species with

encapsulation only *S. hardangeri* from reindeer and *Sarcocystis* sp. type B of Colwell and Mahrt (1981) from moose bear a remote resemblance. However, the microtubules of the villar protrusions apparently do not reach into the ground substance of the cyst wall in these forms. This sarcocyst may represent a new species, but our data are insufficient to make that determination.

Acknowledgment. We are grateful to Dr. H.-H. Wesemeier for the TEM micrographs of *Sarcocystis rangiferi*. Furthermore, we would like to thank Mrs. Dagmar Viertel and Mrs. Marion Biering for their technical support in electron microscopy as well as Mrs. Gisela Jarzombinski for seeking for sarcocysts and technical assistance.

References

Bergmann V., Kinder E. (1975) Unterschiede in der Struktur der Zystenwand bei Sarkozysten des Schafes. *Mon.h. Vet.med.* **30:** 772-774

Colwell D. D., Mahrt J. L. (1981) Ultrastructure of the cyst wall and merozoites of *Sarcocystis* from moose (*Alces alces*) in Alberta, Canada. *Z. Parasitenkd.* **65:** 317-329

Dubey J. P., Speer C. A., Fayer, R. (1989) Sarcocystosis of animals and man. CRC Press, Inc., Boca Raton, Florida

Fedoseenko V. M. (1986) *Sarcocystis* sp. from the Altai pika *Ochotona alpina*. *Materialy X Konf. Ukrain. Obshch. Parazitol.* Part 2: 281 (in Russian)

Galavíz-Silva L., Mercado-Hernández R., Ramírez-Bon E., Arredondo-Cantú J. M., Lazcano-Villarreal D. (1991) *Sarcocystis neotomafelis* sp. n. (Protozoa; Apicomplexa) from the woodrat *Neotoma micropus* in Mexico. *Rev. Latinoam. Microbiol.* **33:** 313-322

Ghaffar F. A., Heydorn A. O., Mehlhorn H. (1989) The fine structure of cysts of *Sarcocystis moulei* from goats. *Parasitol. Res.* **75:** 416-418

Gjerde B. (1985a) Ultrastructure of the cysts of *Sarcocystis rangiferi* from skeletal muscle of reindeer (*Rangifer tarandus tarandus*). *Can. J. Zool.* **63:** 2669-2675

Gjerde B. (1985b) Ultrastructure of the cysts of *Sarcocystis hardangeri* from skeletal muscle of reindeer (*Rangifer tarandus tarandus*). *Can. J. Zool.* **63:** 2676-2683

Gjerde B. (1986) Scanning electron microscopy of the sarcocysts of six species of *Sarcocystis* from reindeer (*Rangifer tarandus tarandus*). *Acta Pathol.Microbiol. Immunol. Scand., Sect. B* **94:** 309-317

Göbel E., Erber M., Grimm F. (1996) *Sarcocystis phoeniconaii* n. sp. Murata, 1986 (Apicomplexa: Sarcocystidae) des Lesser Flamingo (*Phoeniconaias minor*: Ciconiiformes). *Berl. Münch. Tierärztl. Wochenschr.* **109:** 239-244

Hernández-Rodríguez S., Acosta I., Navarrete I. (1992) *Sarcocystis jorrini* sp. nov. from the fallow deer *Cervus dama*. *Parasitol. Res.* **78:** 557-562

Karnowsky M. J. (1965) A formaldehyde-glutaraldehyde fixative of high osmolarity for use in electron microscopy. *J. Cell Biol.* **27:** 137a

Matuschka F.-R., Mehlhorn H., Abd-Al-Aal Z. (1987) Replacement of *Besnoitia* Matuschka and Häfner 1984 by *Sarcocystis hoarensis*. *Parasitol. Res.* **74:** 94-96

Novak M. D., Fedoseenko V. M., Orazalinova V.A. (1987) The ultrastructure of the cyst of *Sarcocystis* sp. in cattle. *Izvestiya Akad. Nauk Kazakh. Sov. Sots. Respubl., Ser. Biol.* **2:** 46-49 (in Russian)

Odening K., Stolte M., Lux E., Bockhardt I. (1996a) The Mongolian gazelle (*Procapra gutturosa*, Bovidae) as an intermediate host of three *Sarcocystis* species in Mongolia. *Appl. Parasitol.* **37:** 54-65

Odening K., Stolte M., Bockhardt I. (1996b) On the diagnostics of *Sarcocystis* in chamois (*Rupicapra rupicapra*). *Appl. Parasitol.* **37:** 153-160

O'Donoghue P. J., Obendorf D. L., O'Callaghan M. G., Moore E., Dixon, B. R. (1987) *Sarcocystis mucosa* (Blanchard 1885) Labbé 1889 [sic] in unadorned rock wallabies (*Petrogale assimilis*) and Bennett's wallabies (*Macropus rufogriseus*). *Parasitol. Res.* **73:** 113-120

Rzepczyk C., Scholtyseck E. (1976) Light and electron microscope studies on the *Sarcocystis* of *Rattus fuscipes*, an Australian Rat. *Z. Parasitenkd.* **50:** 137-150

Sedlaczek J., Wesemeier H.-H. (1995) On the diagnostics and nomenclature of *Sarcocystis* species (Sporozoa) in roe deer (*Capreolus capreolus*). *Appl.Parasitol.* **36:** 73-82

Wesemeier H.-H., Sedlaczek J. (1995a) One known *Sarcocystis* species and two found for the first time in red deer and wapiti (*Cervus elaphus*) in Europe. *Appl. Parasitol.* **36:** 245-251

Wesemeier H.-H., Sedlaczek J. (1995b) One known *Sarcocystis* species and one found for the first time in fallow deer (*Dama dama*). *Appl. Parasitol.* **36:** 299-302

Received on 16th October, 1996; accepted on 26th February, 1997

Acta Protozoologica (1997) 36: 137 - 142

ACTA
PROTOZOOLOGICA

New Testate Amoebae Taxa from the Polar Regions

Louis BEYENS[1] and Didier CHARDEZ[2]

[1]Departement of Biologie, (R)UCA, Antwerpen; [2]Unité de Zoologie Générale et Faunistique, F.S.A., Communauté française de Belgique, Gembloux, Belgium

Summary. Four new species, and one variety are described. *Schoenbornia smithi* sp. n. from SW-Spitsbergen is an aquatic taxon living in small pools with an extensive moss vegetation. *Paraquadrula ogdeni* sp. n. and *Netzelia labeosa* sp. n. are terrestrial moss dwelling species. *Centropyxis gasparella* var. *corniculata* var n. occurs in alkaline waters. These three taxa were observed in Victoria Island (NWT, Canada). *Microcorycia husvikensis* sp. n. from the subantarctic island South Georgia was sampled in acid to slightly alkaline pools and lakes, vegetated with mosses. It can be stated that altogether only few new species are known from the Arctic.

Key words: polar regions, systematics, testate amoebae.

INTRODUCTION

Although the biodiversity in polar regions is lower than can be observed in the biomes of the moderate to warmer climatic regions, sustained fieldwork in these regions yielded nevertheless some new testate amoebae taxa, which we described in Beyens et al. (1986) and Chardez (1994), Chardez et al. (1987, 1988). In the present paper we continue this survey with the description of four new species and one new variety.

DESCRIPTION OF THE NEW SPECIES

Paraquadrula ogdeni sp. n. (Figs. 3; 7c-e)

Diagnosis and description

The shell is perfectly oval, in cross-section circular or slightly oval. The aperture is terminal, circular, without prominent lip or collar. It is entirely composed of calcareous, quadrangular shell-plates, arranged in transversal rows. Sometimes the arrangement is rather irregular, and some superposition may occur. The aperture has sometimes a angular border due to the bordering shell-plates. It makes an angle of approximate 40° till 45° to the longitudinal axis of the shell. A cyst has been observed, which is spherical, colourless, and smooth.

Comparison with related species: this species is distinguished from *P. madarica* Valkanov by the smaller dimensions and the circular aperture.

Dimensions (n = 12): length of shell 24-26 µm, diameter of shell 14-16,5 µm, aperture diameter 6-6,5 µm, scale 4 - 4 µm till 4-4.5 µm, cyst diameter 13-14 µm.

Type preparation: n° V4/22 at the Lab. de Zoologie Gen. Faunist., F.S.A., Gembloux.

Type location: Cambridge Bay area, Victoria Island, NWT (Canada). Site 227, July 1992.

Dedication: this species is named after, and dedicated to the late Dr Colin Ogden.

Ecology: half wet (FV according the moisture degree

Address for correspondence: Louis Beyens, Departement Biologie, (R)UCA, Groenenborgerlaan, 171, B-2020 Antwerpen, Belgium

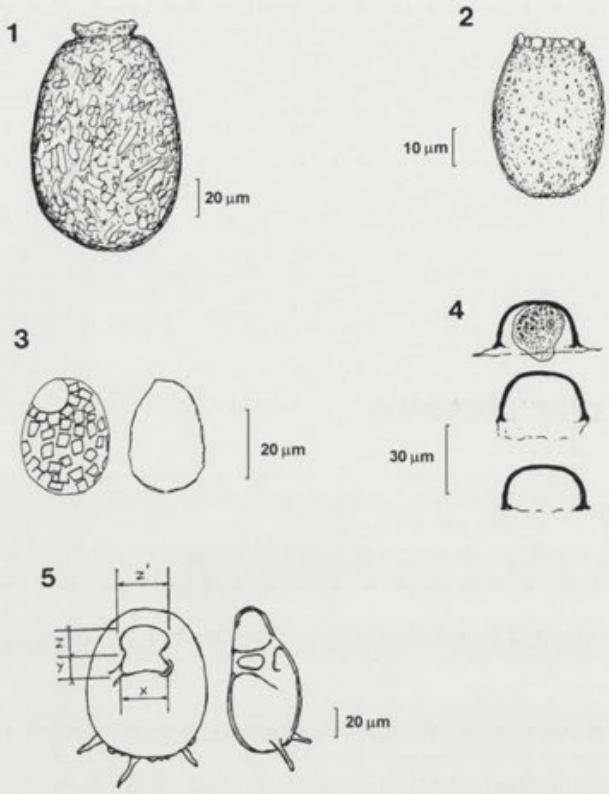

Fig. 1. *Netzelia labiosa* sp. n.
Fig. 2. *Schoenbornia smithi* sp. n.
Fig. 3. *Paraquadrula ogdeni* sp. n.
Fig. 4. *Microcorycia husvikensis* sp. n.
Fig. 5. *Centropyxis gasparella* var. *corniculata* var. n.

classification of Jung 1936) terrestrial mosses in a *Cassiope tetragona* vegetation (sample M310).

Netzelia labeosa sp. n. (Figs. 1; 7a, b)

Diagnosis and Description

The shell is ovoid, in cross-section circular. The circular aperture is formed by a refolding of the shell-wall, featuring thus a lip-like short collar. The shell wall is coated with irregular platelets, vermicular elements, and reworked diatom valves, all embedded in a dense organic layer, which is transparent with a yellowish to brownish tint. This new species is characterised by the remarkable structure of the region near the aperture.

Comparison with related species. *Netzelia oviformis* (Cash) Ogden has a lobate aperture.

Dimensions (n = 14): length of shell 118-125 µm, shell diameter 82-90 µm, aperture diameter 26-29 µm, height of collar 5-7 µm.

Type preparation: n° V4/23 at the Lab. de Zoologie Gen. Faunist., F.S.A., Gembloux.

Type location: Cambridge Bay area, Victoria Island, NWT (Canada). Site 213 and 215, July 1992.

Derivatio nominis: from the Latin word „labeosus", an adjective of labea, provided with a lip.

Ecology: wet mosses.

Site 213: moist *Carex* - moss vegetation, samples M297 (F III) and M298(F IV).

Site 215: sample M 300 (F III).

Type: n° V4/23 at the Lab. de Zoologie Gen. Faunist., F.S.A., Gembloux.

Schoenbornia smithi sp. n. (Fig. 2)

Diagnosis and Description

The shell is oval, circular in cross-section. The short circular collar is bordered by irregular formed mineral particles. The shell wall is composed of a thick organic layer, encrusting some thin polymorphic inorganic particles. The shell is transparent or yellow. A thick-walled spherical cyst with diameter of 26 µm has been observed.

Comparison with related species: it is distinguished from the other two species from this genus (*Sch. viscidula* Schönborn and *Sch. humicola* Decloitre) by the presence of the collar with mineral particles, and the structure of the shell. It is clearly bigger then *Sch. humicola*. The habitat is also different, the two other species living in a terrestrial environment.

Dimensions (n = 10): length of shell 37-40 µm, diameter of shell 26-30 µm, diameter of aperture 15-18 µm.

Type preparation: V4/9 at the Lab. de Zoologie Gen. Faunist., F.S.A., Gembloux.

Type location: Sørkappland, SW-Spitsbergen. Site SH6, August 1991.

Dedication: this species is named after Dr Humphrey G. Smith (Coventry University, U.K.), the main contributor to our knowledge of testate amoebae in the Antarctic.

Ecology: aquatic taxon found in a small pool in an extensive moss vegetation, bordering a brook. Parameters of water from the brook: temp. 7°C, pH 8.6, conductivity 55µS. Sample W293.

Microcorycia husvikensis sp. n. (Figs. 4; 6a, b, c)

Diagnosis and Description

In side view the shell looks basin-shaped, with a flattened or slightly bulged (swelled) top, forming thus a short conical cylinder, open at the base. The shell wall is composed of a yellowish organic layer. At great magnifications fine alveoli are visible. The shell membrane consists of two agglutinated layers, which are separated near the base. One of these layers forms a thin and hyaline

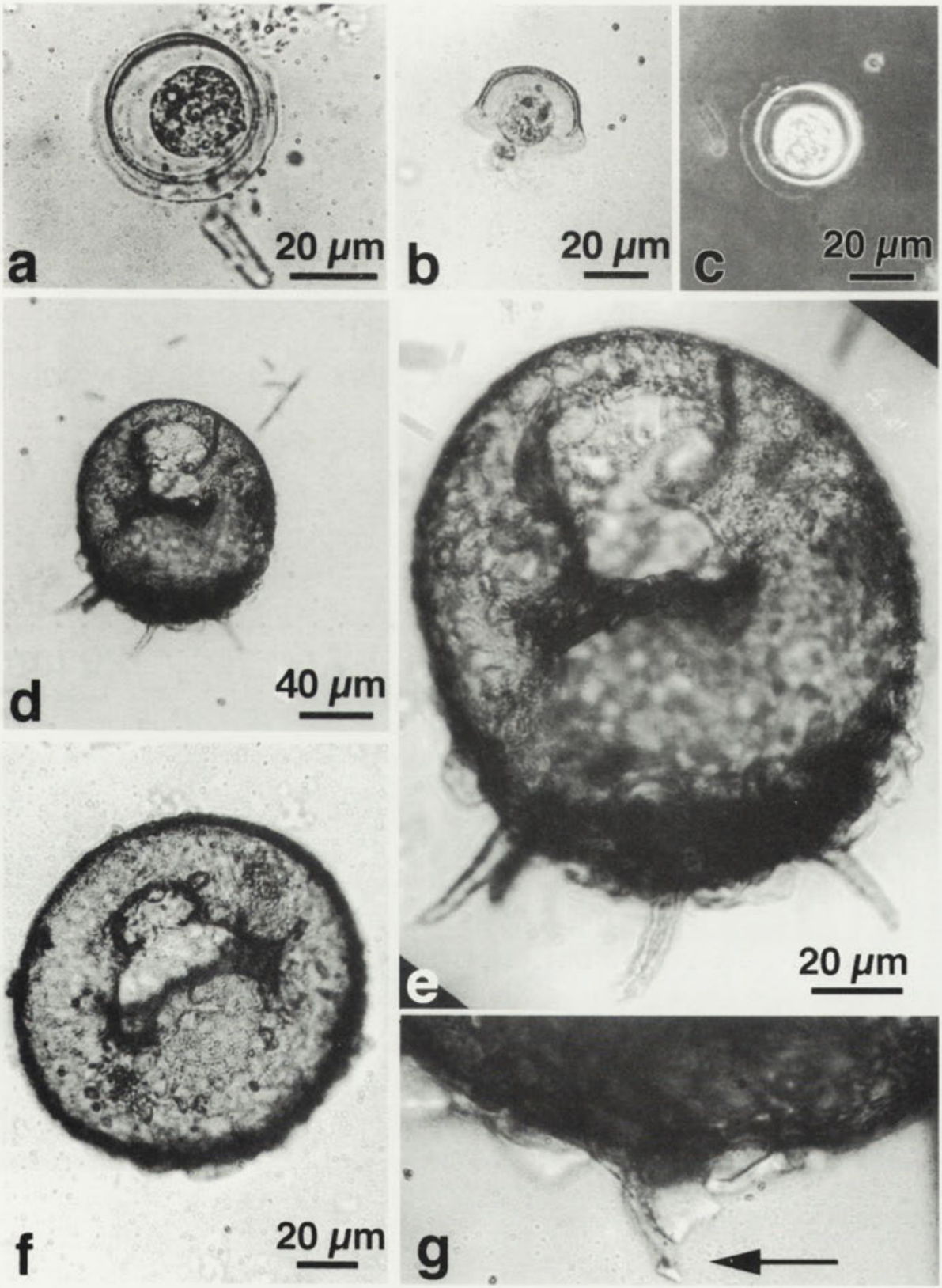

Fig. 6. a-c - *Microcorycia husvikensis* sp. n.; d,e,g - *Centropyxis gasparella* var. *corniculata* var. n.; f - *Centropyxis gasparella* Chardez et Beyens; g - *Centropyxis gasparella* var. *corniculata* var. n., spine

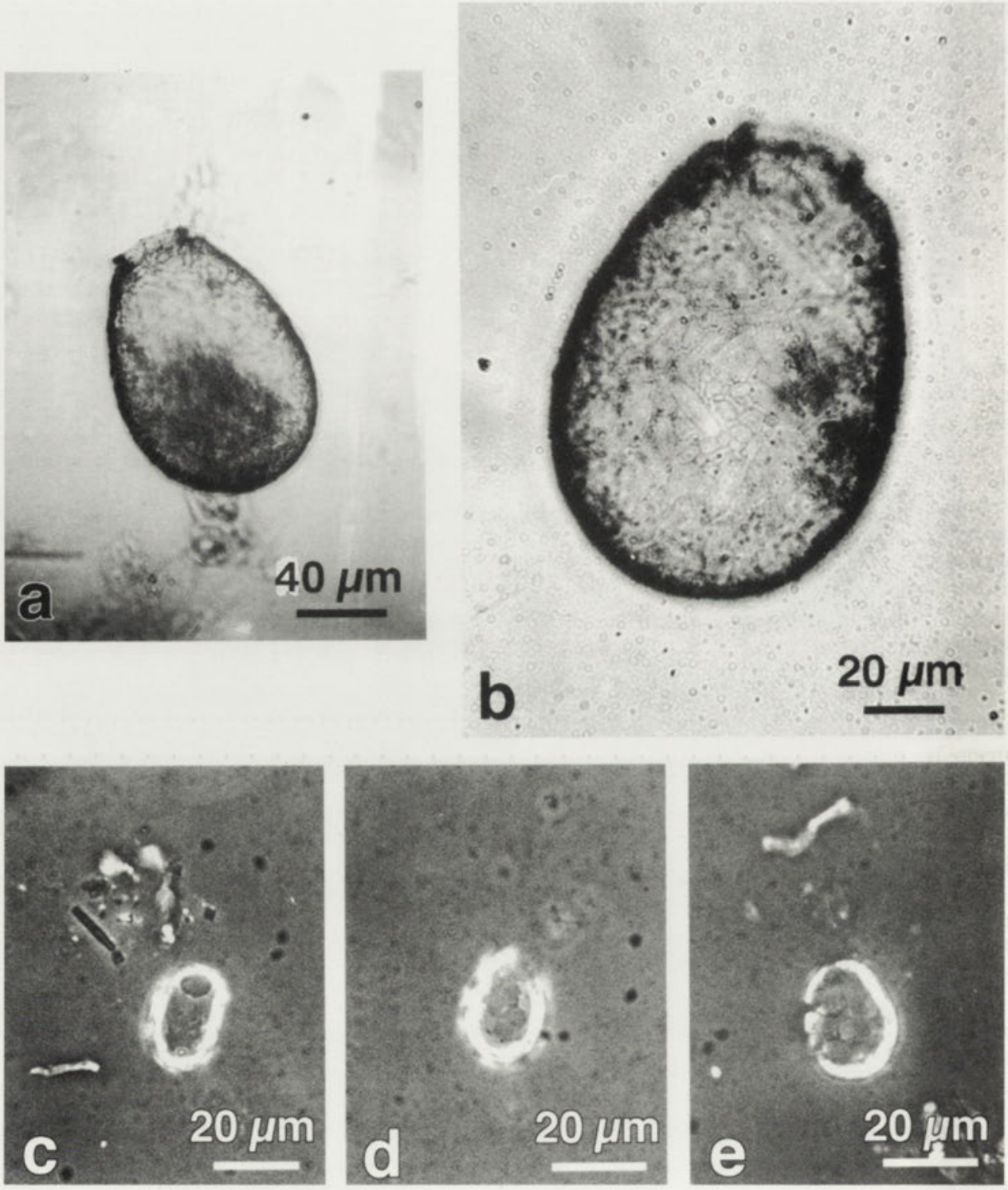

Fig. 7. a-b - *Netzelia labeosa* sp. n.; c-e - *Paraquadrula ogdeni* sp. n.

extensible membrane, which is in a circular way displayed around the shell. It can also be transformed like a sail, or be folded to reduce the opening at the base.

In our samples, the amoeba fixed with formalin looks like a globular mass attached to the interior wall opposite the opening. The cytoplasm is finely granulated, grey, with

an easily observed spherical nucleus containing a central nucleolus.

Dimensions (n=20): diameter of shell 32-34 µm, diameter of the nucleus 2-2.4 µm, diameter of the contracted cytoplasm 18µm, diameter of the extended membrane 38-40 µm, height of the shell 16-18 µm,.

Type preparation: n° V5/4 at the Lab. de Zoologie Gen. Faunist., F.S.A., Gembloux.

Type location: Husvik area, South Georgia (Sub-Antarctica).

Sites 262, 265, 268, 279. Austral summer 1992-1993.

Derivatio nominis: after the locality Husvik, a former whaling station, now the site of a British Antarctic Survey scientific station.

Ecology: in acid to slightly alkaline pools and lakes, vegetated with mosses.

Site 262: lake. Temp. 8.8°C, pH 5.7, cond. 22µS. Sample W 388 (mosses).

Site 265: pool. Temp. 16.6°C, pH 5.6, cond. 40µS. Sample W 393 (mosses).

Site 268: lake. Temp. 11.9°C, pH 7.5, cond. 52µS. Samples W 397 (mosses) and 398 (sediment).

Site 279: lake. Temp. 9.6°C, pH 6.2, cond. 26µS. Sample W 412 (mosses). It belongs to the *Trinema lineare* and *Nebela collaris* assemblages (Beyens et al. 1995).

***Centropyxis gasparella var. corniculata* var. n. (Figs. 5; 6d, e, g)**

Diagnosis and Description

The overall morphology, dimensions and the internal structure of the region near the aperture are the same as in *Centropyxis gasparella* Chardez et Beyens (Fig. 6 f). This new variety has long, thin spines, closed at the apex. They are positioned rather high on the posterior side of the shell. Their number varies from 1 to 5.

Dimensions (n=10): length of shell 100-125µm, diameter of shell 99-106µm, depth of shell 40-45µm, length of spines 24-35µm, diameter of aperture (Fig. 5) X : 28-32µm, Y : 14-19µm, Z : 4-16µm, Z' : 15-26µm.

Type preparations: n° V4/19 and V4/20 at the Lab. de Zoologie Gen. Faunist., F.S.A., Gembloux.

Type location: Cambridge Bay area, Victoria Island, NWT (Canada). Site 245, 212, 230, 231, 238. July 1992.

Derivatio nominis: from the Latin 'corniculatus', provided with a small horn.

Ecology: an aquatic taxon, found in alkaline water habitats, ranging from small pools to lakes.

Site 245: shallow part of a lake, with submerged mosses, temperature of the water 9.8°C, pH 8.5, cond. 187 µS. Sample W331 was taken from the sediment.

Site 212: small lake. temp. 7.1°C, pH 8.6, cond. 107 µS. Sample W327: sediment.

Site 230: shallow, small pool, bottom covered with mosses. Temp. 20°C, pH 7.4 cond. 424 µS. Sample W 351: submerged mosses.

Site 231: shallow pool. Temp. 19.5°C, pH 9.2, cond. 214 µS. Sample W 352: organic sediment.

Site 238: outlet of a brook in a lake. Temp. 14.2°C, pH 8.3, cond. 171µS. Sample W 361: organic sediment.

DISCUSSION

New testate amoebae taxa are seldom reported from the arctic regions. Although we made an extensive survey by sampling and analysing no less than 1142 samples from different parts of the Arctic (Beyens and Chardez 1995), only 11 new taxa were discovered. As already mentioned, the polar regions show a lower biodiversity, which is nicely reflected in net total number of taxa we encountered in these 1142 samples, i.e. 223. Most communities are dominated by cosmopolitic and ubiquistic species (Beyens and Chardez 1994). Nevertheless, some of the new described taxa were found in different places in the Arctic, which is an interesting observation in view of the biogeographical problem of dispersal. A further question thus raised concerns the age of speciation, which must probably be considered in relation with the glacial refuge hypothesis and the post-glacial geographic history of the Arctic. With the help of our database, we hope to elucidate such questions in the near future.

Acknowledgements. The work at Husvik, South Georgia was made possible by the British Antarctic Survey (Cambridge, U.K.), with the help of Dr D. Walton and the staff of the Terrestrial and Freshwater Science Division. The fieldwork in Cambridge Bay was authorised by the Science Institute of the Northwest Territories (Canada) under licence number #12073D. Processing of the photographic plates was done by Mr. A. De Munck and Mr. A. Schallenberg (Emat, UCA). The two anonymous referees are acknowledged for their positive criticism. Last but not at all least, funding for all the field work was provided by the National Science Foundation (NFWO).

REFERENCES

Beyens L., Chardez D. (1994) On the habitat specificity of the testate amoebae assemblages from Devon Island (NWT, Canadian Arctic), with the description of a new species : *Difflugia ovalisina*. *Arch. Protistenkd.* **144:** 137-142

Beyens L. ,Chardez D. (1995) An annotated list of testate amoebae observed in the Arctic between the longitudes 27° E and 168°W. *Arch. Protistenkd.* **146:** 219-233

Beyens L., Chardez D., De Bock P. (1986) Some new rare testate amoebae from the Arctic. *Acta Protozool.* **25:** 81-91

Beyens L., Chardez D., De Baere D., Verbruggen C. (1995) The aquatic testate amoebae fauna of the Stromness Bay area South Georgia. *Antarctic Science* **7** 3-8

Beyens L., Chardez D., De Baere D., Verbruggen C. (1995) The aquatic testate amoebae fauna of the Stromness Bay area, South Georgia. *Antarctic Science* **7:** 3-8

Chardez D., Beyens L., De Bock P. (1988) *Centropyxis gasparella* sp. nov. and *Parmulina louisi* sp. nov., new testate amoebae from the Canadian High Arctic (Devon Island, N.W.T.). *Arch. Protistenkd.* **136:** 337-344

Jung W. (1936) Thecamöben ursprünglicher lebender deutscher Hochmoore. *Abh Landesmuseum Westf* **7:** 1-87

Received on 3rd April, 1996; accepted on 11th October, 1996

Acta Protozoologica (1997) 36: 143 - 145

ACTA
PROTOZOOLOGICA

Isospora lacertae: A New Coccidian Parasite (Apicomplexa: Eimeriidae) from the Oriental Garden Lizard, *Calotes versicolor* (Squamata: Agamidae) from Singapore

Leilani P. SAUM[1], C. H. DIONG[2] and Thomas E. McQUISTION[1]

[1]Department of Biology, Millikin University, Decatur, Illinois, USA, and [2]Nanyang Technological University, National Institute of Education, Singapore, Republic of Singapore

Summary. A new species of *Isospora* (Apicomplexa: Eimeriidae) is described from the feces of the oriental garden lizard, *Calotes versicolor* from Singapore. Oocysts of a previously undescribed isosporan species were found in 3/40 lizards. Sporulated oocysts are ovoidal, 28.1 x 26.5 (23-31 x 23-28) µm with a smooth, colorless, bilayered wall with the inner wall thinner and darker than the outer, striated wall; shape index (length/width) 1.06. Micropyle, oocyst residuum, and polar granules are absent. Sporocysts are ovoidal, 14.6 x 10.3 (13-15 x 7-11) µm with a smooth, single layered wall; average shape index is 1.42. Stieda body is broad, dome-like with a larger, prominent, substieda body located directly beneath. Each sporocyst contains a residuum of coarse granules in a subspherical cluster, four vermiform sporozoites marked anteriorly with incomplete, concentric lines and centrally located nuclei but lacking visible refractile bodies.

Key words: Agamidae, Apicomplexa, *Calotes versicolor*, Coccidia, Eimeriidae, *Isospora lacertae* sp. n., Squamata.

INTRODUCTION

The oriental garden lizard, *Calotes versicolor* Daudin, 1802 is semi-arboreal and spends much of its time in trees or on large rocks in semi-arid regions (Diong et al. 1994) of Iran, Afghanistan, the Indian subcontinent, Sri Lankia, China, peninsular Malaysia, and Sumatra. *C. versicolor* is primarily an insectivore with its principle diet consisting of butterflies, ants, insect larvae, and beetles (Asana 1931) but often supplementing its diet with bird eggs, crabs, and earthworms (McCann 1937). There are several reports of helminth parasites in *C. versicolor*, but only one incomplete description of a coccidian parasite has been reported in *C. versicolor* (Bhatia 1938). This study describes a new isosporan species in the oriental garden lizard, *Calotes versicolor*.

MATERIALS AND METHODS

During lizard collecting trips in Singapore from July 1994 to August 1995, fecal samples were obtained from 40 oriental garden lizards and sent to the third author's laboratory for examination. Procedures for preserving fecal material and for measuring and photographing oocysts were as described by McQuistion and Wilson (1989). All measurements are given in micrometers (µm) with size ranges in parentheses following the means. Oocysts were approximately one month old when examined, measured, and photographed.

Address for correspondence: Thomas E. McQuistion, Department of Biology, Millikin University, 1184 West Main Street, Decatur, Illinois 62522, USA; Fax: (217) 424-3993; E-mail: tmcquistion@post.millikin.edu

RESULTS

Three of the 40 adult lizards, all from Ang Mo Kio Park in Singapore were passing hundreds of coccidian oocysts which appeared similar in morphological characteristics. Upon sporulation, these oocysts were found to represent a previously unreported species, which is described below.

Isospora lacertae sp. n. (Figs. 1,2)

Description of oocysts: subspherical to ovoidal, colorless, 28.1 x 26.5 (23.0-31.0 x 23.0-28.0) (N=38) with a smooth, bilayered wall *ca* 2.0 thick; the inner wall is darker, and there are light perpendicular striations in the outer, thicker wall; shape index (length/width) 1.06 (1.0-1.15). Micropyle, oocyst residuum, and polar granules absent. Sporocysts ovoidal, 14.6 x 10.3 (13.0-15.0 x 7.0-11.0) (N = 18) with smooth, thin wall *ca*. 0.5 thick; shape index 1.42 (1.27-1.67). The Stieda body is broad, dome-like with a conspicuous, large substieda body located directly below the Stieda body. Sporocyst residuum present, consisting of coarse granules in a subspherical cluster. Sporozoites are vermiform (*ca* 12.0 x 2.0-3.0), with an ovoid, centrally located nucleus with the anterior end marked with incomplete concentric lines and lacking refractile bodies. They are arranged randomly around the residuum in the sporocyst.

Type-host: *Calotes versicolor* Daudin, 1802 "Oriental Garden Lizard" (Squamata: Agamidae).

Type specimens: phototypes and buffered formalin preserved syntypes of *Isospora lacertae* sp. n. have been deposited in the U. S. National Parasite Collection in Beltsville, Maryland as USNPC No. 86669 (phototypes) and USNPC No. 86670 (syntypes).

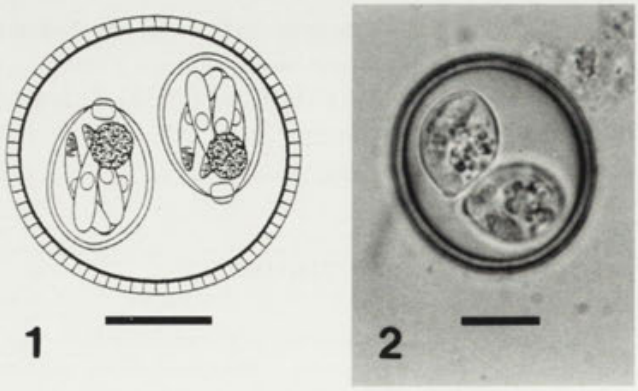

Fig. 1. Composite line drawing of sporulated oocyst of *Isospora lacertae* sp. n. from *Calotes versicolor.* Bar - 10 µm
Fig. 2. Bright field photomicrograph of sporulated oocyst of *Isospora lacertae* sp. n. Note the large sporocyst residuum composed of coarse granules and the prominent substieda body directly beneath the dome-shaped Stieda body. Bar - 10 µm

Type location: Singapore, Ang Mo Kio Park.

Prevalence: 3/12 were infected from Ang Mo Kio Park, Singapore; 0/28 were infected from Marina South Park, Singapore.

Sporulation time: unknown; oocysts were partially sporulated when received at the laboratory and became fully sporulated after exposed to air for several days prior to examination.

Site of infection: unknown, oocysts found in feces.

Etymology: the specific epithet, *lacertae,* is the Latin word for lizard.

DISCUSSION

Only one coccidian species has been reported in *Calotes versicolor.* Unfortunately, only the endogenous stages of *Isospora calotes* were described from the intestinal epithelium of *C. versicolor* (Setna 1933, Bhatia 1938): no description of the sporulated oocyst has been documented. *Isospora choochotei,* described from *Calotes mystaceus* from Thailand (Finkelman and Paperna 1994), has a similar oocyst length/width ratio (1-1.1) and some overlap in oocyst size (28-32.5 x 24-32) with *I. lacertae,* but there are substantial differences in oocyst wall, sporocyst, and sporozoite structure. *Isospora lacertae* has a double layered oocyst wall with a thicker, outer, striated layer compared to the single layered, nonstriated oocyst wall of *I. choochotei.* The sporocysts of *I. lacertae* are smaller than *I. choochotei* (13-15 x 7-11 for *I. lacertae vs* 15.5-18 x 11 for *I. choochotei)* and possess a prominent substieda body while *I. choochotei* sporocysts do not have a substieda body. Additionally, the sporozoites of *I. choochotei* have two refractile bodies while those of *I. lacertae* do not possess any visible refractile bodies.

Another agamid lizard sympatric with *C. versicolor* on the Malaysian peninsula is *Gonyocephalus grandis* which is host to *Isospora caryophila* (Rogier and Colley 1976). The sporulated oocysts of *I. lacertae,* however, differ from the oocysts of *I. caryophila* in several characteristics. *I. lacertae* oocysts are larger than those of *I. caryophila* (28.1 x 26.5 *vs* 23.5 x 21.9 for *I. caryophila),* have a bilayered wall with the outer wall striated, and lack a polar granule. The sporocysts of *I. caryophila* appear to lack a substieda body, have a smaller and more spherical Stieda body than *I. lacertae,* and the sporocyst residuum of *I. caryophila* is scattered with irregularally shaped granules compared to the compacted residuum composed of uniform granules of *I. lacertae.*

Acknowledgements. The authors thank colleagues of Dr. C. H. Diong at the Nanyang Technological University for collecting f ecal samples in Singapore. Our appreciation also goes to Kirk Gustafson for the line drawing and to Ms. Mary Ellen Martin for assistance with the Latin names.

REFERENCES

Asana J. J. (1931) The natural history of *Calotes versicolor. J. Bombay Nat. Hist. Soc.* **34:** 1041-1047

Bhatia B. L. (1938) The Fauna of British India. Taylor and Francis, Ltd. London

Diong C. H., Chou L. M., Lim K. K. P. (1994) *Calotes versicolor:* A changeable lizard. *Nature Malaysiana* **19:** 46-54

Finkelman S., Paperna I. (1994) The endogenous development of three new intranuclear species of *Isospora* (Apicomplexa: Eimeriidae) from agamid lizards. *Syst. Parasitol.* **27:** 213-226

McCann C. (1937) Notes on *Calotes versicolor. J. Bombay Nat. Hist. Soc.* **39:** 843-48

McQuistion T. E., Wilson M. (1989) *Isospora geospizae,* a new coccidian parasite (Apicomplexa: Eimeriidae) from the small ground finch (*Geospiza fuliginosa)* and the medium ground finch (*Geospiza fortis)* from the Galapagos Islands. *Syst. Parasitol.* **14:** 141-144

Rogier E., Colley F. (1976) Description d'isospora caryophila n. sp. parasite d'un agamidé de Malaisie Péninsulaire. *Protistologica* **12:** 369-373

Setna S. B. (1933) Fish coccidia. Reptilian coccidia. *Curr. Sci.* **2:** 97

Received on 1st July, 1996; accepted on 10th January, 1997

Acta Protozoologica (1997) 36: 147- 151

ACTA
PROTOZOOLOGICA

Gregarina sitophili sp. n., a Septate Gregarine (Apicomplexa: Eugregarinoida) from the Larvae of *Sitophilus oryzae* (Insecta: Coleoptera: Curculionidae)

Karnica SAHA[1], Srikanta GHOSH[2] and Durga Prasad HALDAR[1]

[1]Protozoology Laboratory, Department of Zoology, University of Kalyani, Kalyani, West Bengal; [2]Division of Parasitology, Indian Veterinary Research Institute, Izatnagar, India

Summary. A new cephaline gregarine belonging to the genus *Gregarina, G. sitophili* sp.n. from the larvae of *Sitophilus oryzae* is described. The trophozoite is elongated, cylindrical with a spherical epimerite measuring (35.4-124.8 µm, $\bar{X}$ - 95.0 µm). Solitary as well as biassociative sporadins with cone-shaped protomerite and cylindrical deutomerite. Sporadin measures 20.8-118.6 µm, $\bar{X}$ - 74.7 µm. Caudo-frontal association. Gametocysts spherical having a diameter of 83.2 µm. Barrel shaped thick double-walled spores; liberated in chains. The spore measures 7.2 x 5.04 µm . The ratio of LP : TL and WP : WD is 1:14.2 and 1:3.1, respectively.

Key words: cephaline gregarine, *Gregarina sitophili* sp.n., larvae of *Sitophilus oryzae*.

Abbreviations: Cv - coefficient of variations, SE - standard error.

INTRODUCTION

Dufour 1828 created the genus *Gregarina* to include a species *G. ovata* from dermopteran insect, *Forficula auricularia* Linn. Siebold (1839) later reported a similar gregarine in the intestine of *Blatta orientalis* Linn. which he originally identified as an insect egg or as helminth egg. Actually gregarines were not aligned with other protozoans until 1848, when Kölliker (1848) recognised them as true protozoans. Hammerschmidt (1838) erected a new genus *Clepsidrina* in order to accommodate a single species of gregarine, *C. polymorpha*. The generic characters proposed by Hammerschmidt (1838) for the genus *Clepsidrina* were as follows: sporonts solitary and obese; protomerite large, cylindrical-shaped, terminates anteriorly in an obtuse-angled cone; deutomerite short, ovoidal in shape; and epimerite a retractile, digitiform processes, flattened or button like in shape.

Hammerschmidt (1838) also renamed *G. ovata* Dufour as *C. conoidea*. All these had created confusion with regard to the validity of the genera *Gregarina* Dufour and *Clepsidrina* Hammerschmidt. Both Diesing (1851) and Schneider (1875) later confirmed that the two genera were synonymous. The synonym of the two genera was accepted by Ellis (1913) and later by Watson (1916). Ultimately the genus *Gregarina* Dufour was established as the senior synonym according to the law of priority and the genus *Clepsidrina* Hammerschmidt was eliminated.

Based on the observations of many species in the genus *Gregarina*, Watson (1916) proposed the following revised diagnosis of the genus: sporonts biassociative; epimerite a simple globular or cylindrical papilla; cysts with

Address for correspondence: Srikanta Ghosh, Division of Parasitology, Indian Veterinary Research Institute, Izatnagar 243 122, Bareilly U.P., India, Fax: 0091-581-50284

sporoducts; and spores barrel shaped or dolioform, liberated in chains.

In our studies on the cephaline gregarine of insects we have obtained some parasites which are characterised by having associative sporadins, spherical epimerites, gametocysts dehiscing by three sporoducts, and barrel-shaped spores liberated in chains. These parasites therefore were identified as belonging to the genus *Gregarina*. Based on several distinctive characters the gregarine is described here in as a new species.

MATERIALS AND METHODS

The host insect *Sitophilus oryzae* (Insecta: Coleoptera: Curculionidae) was collected from Chinsurah, Hooghly, West Bengal, India on January 15, 1991 by K. Saha.

Insects were reared in glass jars covered by fine mesh nylon nets. Jars were kept in an insect rearing incubator. The temperature of 30±1°C and humidity of 70±2% r.h. were maintained.

Larvae were decapitated, their midguts carefully removed and teased apart with fine needles to locate the gregarines. In order to study fresh specimens thin smears were prepared and covered with a cover glass, the edges of which were sealed with paraffin wax. To prepare permanent slides, smears were partially dried, fixed in Schaudinn's fluid and subsequently stained with Heidenhain's hematoxylin. Gametocysts were collected from 32 heavily infected larvae and cultured in moist chamber for sporulation (Sprague 1941). The structure of spores was studied by preparing spore suspension. This was placed on a glass slide containing a drop of Lugol's iodine. A coverslip was placed on it and the edges were sealed with paraffin. Observations were done under oil immersion lens.

Measurements of both fresh and stained materials were made. Thirty specimens each of trophozoites, sporadins, syzygies, thirty five gametocysts and one hundred and fifty individual spores were measured. All measurements are given in µm.

RESULTS

Gregarina sitophili sp. n. (Figs. 1-11; Tables 1, 2)

Trophozoites (Figs. 1-4): trophozoites elongated, cylindrical. Epimerite spherical in shape, minute stalk attached to sphere rarely observed (Fig. 1); in stained preparations epimerite appears as solid jet black sphere. Protomerite small, stalk-like cylindrical; width equal at both ends, approximately as wide as long. Septum between protomerite and deutomerite thick and convex. Deutomerite slender, elongated, rounded at both ends. Pellicle thin; epicyteal striations not evident. Nucleus spherical, sometimes ovoidal, variously located in the deutomerite.

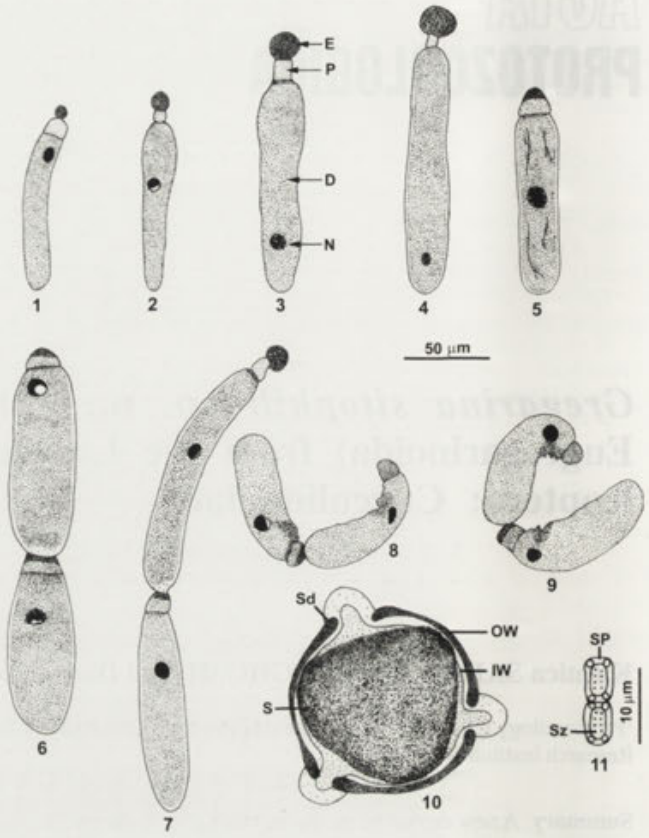

Figs. 1-11. *Gregarina sitophili* sp. n. stages in the life cycle. 1-4 - trophozoites of different sizes; 5 - sporadin; 6 - syzygy; 7-9 - syzygies showing bending patterns;10 - gametocyst, advanced stage with three sporoducts; 11 - two adherent spores each with eight sporozoites. D-deutomerite, E-epimerite, IW-inner wall, N-nucleus, OW-outer wall, P-protomerite, S-sporoblast, Sd-sporoduct, Sp-spore, Sz-sporozoites

Sporadins (Fig. 5): sporadins cylindrical with cone-shaped protomerite and cylindrical deutomerite; septum prominent and straight. Small cytoplasmic granules scattered uniformly and thickly in protomerite and deutomerite. Nucleus rounded and situated differently. Spherical granules of chromatin scattered within nucleus.

Associations (Figs. 6-9): caudo-frontal associations. Primite retains epimerite in about 14% of associations. Primite typically larger than satellite. Nuclei generally located anteriorly in both primite and satellite.

Gametocysts (Fig. 10): gametocysts spherical in shape with two distinct walls; measurements of 35 gametocysts; diameter, 80.3-84.9 ($\bar{x}$ - 83.2, SE± 3.27, Cv - 23.23%). Creamy white in colour when live. Outer wall thick, separated from inner wall by hollow space of 4.1 µm. Sporoplasm spherical, diameter 70.7 µm bounded by inner membrane. At 48 h of development three sporoducts each with a width of 16 .6 µm are formed. Thick outer wall at the base of the sporoducts which are equidistant and 62.4 µm apart from each other.

Table 1. *Gregarina sitophili* sp. n.-measurement of 30 fresh and 30 preserved (fixed and stained) trophozoites, sporadins and syzygy. All measurements in µm

Stages and	Fresh				Preserved			
Measurements	Range	$\bar{X}$	±SE	Cv%	Range	$\bar{X}$	±SE	Cv%
Trophoozoites								
total length	35.8-125.4	95.2	3.8	23.6	35.4-124.8	95.0	5.1	31.7
epimerite length	2.4-12.9	8.1	0.5	36.5	2.1-12.5	7.9	0.4	29.9
epimerite width	2.5-12.7	8.3	0.5	33.5	2.1-12.5	8.1	0.4	29.2
protomerie length	4.6-10.9	7.3	0.2	19.4	4.2-10.4	7.0	0.2	16.9
protomerie width	4.7-12.8	7.8	0.4	30.3	4.2-12.5	7.5	0.4	23.6
deutomerite length	21.2-106.4	80.0	3.6	26.6	20.8-106.1	79.8	3.6	27.0
deutomerite width	8.5-25.2	14.9	0.7	27.8	8.3-24.9	14.8	0.4	16.0
					LP:TL=1:4.3-28.7 ($\bar{X}$ =14.2); WP:WD=1:1.0-3.9 ($\bar{X}$ =3.1)			
Sporadins								
total length	21.1-118.9	75.1	4.4	36.6	20.8-118.6	74.7	4.3	34.0
protomerite length	4.7-12.8	8.4	0.3	23.9	4.2-12.5	8.2	0.3	21.6
protomerite width	4.4-14.9	10.3	0.5	26.4	4.2-14.6	10.2	0.4	23.2
deutomerite length	15.0-108.7	64.5	4.4	40.3	14.6-108.4	63.5	4.1	38.2
deutomerite width	6.4-25.4	15.6	0.8	30.3	6.2-25.0	15.5	0.4	15.3
nucleus diameter					2.1-6.2	4.1	0.2	28.8
					LP:TL=1:3.3-14.7($\bar{X}$ =9.0); WP:WD=1:1.0-2.5($\bar{X}$ =1.5)			
Syzygy								
total length	116.5-263.5	200.4	5.2	15.2	116.5-263.1	200.2	5.1	15.0
primite length	79.2-175.9	108.2	2.8	15.5	79.0-175.7	108.2	2.8	15.3
protomerite of primite length	4.6-12.7	8.0	0.4	25.8	4.7-12.4	7.9	0.3	22.4
protomerite of primite width	4.4-12.6	9.3	0.4	23.5	4.2-12.4	9.2	0.3	19.3
deutomerite of primite length	73.0-167.8	99.3	2.8	16.5	72.8-167.4	99.1	2.7	16.1
deutomerite of primite width	10.8-21.0	16.6	0.6	21.4	10.4-20.8	16.5	0.5	17.9
satellite length	62.7-125.1	91.8	3.5	22.3	62.4-124.8	91.2	3.2	20.7
protomerite of satellite length	4.4-12.7	8.5	0.3	20.9	4.2-12.4	8.4	0.3	21.1
protomerite of satellite width	8.8-16.9	11.1	0.4	21.3	83.3-16.6	10.9	0.4	21.7
deutomerite of satellite length	54.4-112.9	85.6	2.4	16.3	54.0-112.3	85.2	2.3	16.0
deutomerite of satellite width	8.6-25.2	16.9	0.8	28.0	8.3-25.0	16.7	0.7	24.8

Spores (Fig. 11): spores barrel-shaped, thick double-walled; liberated in chains. Measurements of 150 spores: lengths 6.9-7.4 ($\bar{X}$ - 7.2, SE±0.01, Cv - 2.34%); widths, 4.9-5.2 ($\bar{X}$ - 5.04, SE±0.03, Cv - 2.18%). Four angles each with knob-like structure; knobs facilitate attachment to adjacent spore. Each spore contains 8 dot-like sporozoites arranged in two rows.

Symbiotype: larvae of *Sitophilus oryzae* L. (Insecta: Coleoptera: Curculionidae)

Type locality: Chinsurah, Hooghly, West Bengal, India.

Location in host: mid gut.

Prevalence: 32.32%.

Syntypes: trophozoites, sporadins and syzygies on slide Nos. SLR/6,7,8; prepared from smears of the larvae of *Sitophilus oryzae* L. deposited in the National Zoological Collection, Zoological Survey of India, Alipore, Calcutta, West Bengal, India.

SYSTEMATIC POSITION

The gregarine obtained from larvae of the beetle *Sitophilus oryzae* L. belongs to the family Gregarinidae Labbé, 1899 and the genus *Gregarina* Dufour, 1828. It

Table 2. Comparative characters of related species in the genus *Gregarina*. All measurements in µm

Characters	*G. alcidesii*	*G. cavalierina*	*G. crescentica*	*G. oviceps*	*G. spraguei*	*G. statirae*	*G. sitophili* sp.n.
Total length	52-350	500-1000	72-380	to 500	112-280	300-350	35.4-124.8
Epimerites:							
shape	knob-like	not described	knob-like	not described	hyaline knob	short papilla	spherical
size	5.0	do	7.5-10	do	10-15	-	7.9
Protomerite shape:							
trophozoites	hemispherical	flattened	subspherical	hemisperical	hemispherical	hemispherical	cylindrical
sporadins	subspherical	ellipsoidal	-do-	-do	dome-shaped	-do-	cone-shaped
Spordains		-do-					
(primite size)	smaller	?	smaller	?	smaller	?	larger
Gametocysts:							
shape	ovoidal	spherical	oval	spherical	oval	?	spherical
size	220x150-230x170 (excluding ecocyst)	400	340x210	250	270x200-310x200	?	83.2
Sporoduct number	3	?	6	2-5	4	?	3
Spores: shape	oval	ellipsoidal	dolioform	barrel-shaped	ovoidal	?	barrel-shaped
size	6x5	8x6	7x6	4.5x2.25	8x6	?	7.2x5.04
Ratios: LP:TL	1:5.5	1:15	1:3.7	1:3	1:3.5	1:5	1:14.2
WP:WD	1:1.2	?	1:1.2	1:1.1	1:1.2	1:3.5	1:3.1
Insect host:	*Alcides* sp.	*Dendarus tristis*	*Amblyrrhinus* sp.	*Gryllus abbreviatus*	unidentified beetle	*Statira unicolor*	*Sitophilus oryzae* (larvae)
Locality	India	France	India	USA	India	Argentina	India
Author and date	Haldar and Chakraborty 1978	Blanchard 1905	Haldar and Chakraborty 1978	Diesing 1859	Haldar and Chakraborty 1978	Frenzel 1892	Present study

has biassociative sporadins, a simple epimerite and gametocysts with sporoducts. By careful comparison with previously described species in the genus *Gregarina* it can be concluded that the gregarine in *Sitophilus oryzae* is a new species. *Gregarina sitophili* sp. n. is compared to the related species *G. crescentica, G. alcidesii, G. spraguei, G. cavalierina, G. statirae* and *G. oviceps* as summarised in Table 2.

In India three species of *Gregarina* have been described from curculionid beetles other than *S. oryzae*, namely: *G. crescentica* Haldar and Chakraborty, 1978; *G. spraguei* Haldar and Chakraborty, 1978 and *G. alcidesii* Haldar and Chakraborty, 1978. There is not much similarities to be shared by the present form with any of these three species. The size of the epimerite and the shape and size of the spores of *G. sitophili* are similar to those of *G. crescentica* but it differs in the smaller lengths of the trophozoites, the number of sporoducts, the shape and size of the gametocysts, and the ratios of LP:TL and WP: WD are also distinctly different. There is only one similarity with *G. alcidesii* in that both produce three sporoducts. All characters are different in comparison with *G. spraguei*.

Among *Gregarina* species from hosts other than curculionid beetles *G. sitophili* show some similarities with *G. cavalierina* Blanchard 1905 in the ratio of LP:TL and in the spherical shape of the gametocysts, however, it differs in the much smaller in length of the trophozoites and other structural and morphological details as indicated in Table 2. *Gregarina statirae* Frenzel, 1892 is similar to *G. sitophili* in the ratio of WP:WD value and in the shape of the protomerite but no further similarity could be detected. The shape of the gametocysts and spores, and the number of sporoducts of *G. sitophili* and *G. oviceps* Diesing, 1859 are similar, but considerable differences are observed in the size of sporonts, LP:TL and WP:WD ratios, and sizes of gametocysts and spores.

Acknowledgements. Authors are grateful to University Grants Commission, New Delhi for financial assistance and Director, Indian Veterinary Research Institute, for providing facilities.

REFERENCES

Blanchard L.E. (1905) Deux Grégarines nouvelles parasites de Ténébrionides des maures. C.R. Assoc. France AV. Sc. **33:** 923-928

Diesing K.M. (1851) Systema helminthicum, **2:** 587-591

Diesing K.M. (1859) Revision der Rhyngodeen. Sitzb. Kais., *Akad. Wiss.*, Wien (Math. Natw Kl), 719-782

Dufour L. (1828) Note sur la grégarine nouveau genre de ver quivit en tropeau dans les intestin de divers insectes. *Ann. Sci. Nat.* **13:** 366-368

Ellis M.M. (1913) New gregarines from the United States. *Zool. Anz.* **41:** 462-465

Frenzel J. (1892) Uber einige argentinische Gregarinen. *Jen. Zeitschi. f. Naturns* **27:** 233-336

Haldar D.P., Chakraborty N. (1978) Observations on three new species of cephaline gregarines (Protozoa: Sporozoa) from insects. *Acta Protozool.* **17:** 233-244

Hammerschmidt K.E. (1838) Helminthologische Beyträge. *Isis* (Oken) **5:** 351-358

Kölliker A. (1848) Beiträge Zur Kenntniss niederer Thiere. *Z. Wise. Zool.* **1:** 1-37

Schneider A. (1875) Contributions à l'historie des grégarines des invertébrates de Paris et de Roscoff. *Archs. Zool. exp. gén.* **4:** 493-604

Siebold C.E.(1839) Beitrage zur Naturgeschichte der wirbellosen Thiere.IV Neuest. Schrift. d. Naturf. Gessek. Danzig **3:** 56-71

Sprague V. (1941) Studies on *Gregarina blattarum* with particular reference to the chromosome cycle. *Ill. Biol. Monogr.* **18:** 5-57

Watson M.E. (1916) Studies on gregarines. *Ill. Biol. Monogr.* **2:** 211-468

Received on 27th December, 1995; accepted on 13th January, 1997

Acta Protozoologica (1997) 36: 153 - 155

ACTA
PROTOZOOLOGICA

Short communication

X-ray Analysis and Cytochemical Staining of Some Tintinnid Loricae

Anna WASIK, Ewa MIKOŁAJCZYK, Małgorzata GOŁĘBIOWSKA and Jerzy SIKORA

Department of Cell Biology, Nencki Institute of Experimental Biology, Warszawa, Poland

Summary. Cytochemical staining and X-ray microanalysis were used to study the loricae of several tintinnid species. The results suggest that the loricae are mainly proteinaceous, and without mineralization. The loricae of partially agglutinated species contain acidic mucopolysaccharides.

Key words: *Codonellopsis gaussi, Cymatocylis affinis/convallaria,* cytochemical staining, *Helicostomella subulata, Laackmanniella naviculaefera, Parafavella denticulata, Tintinnopsis lobiancoi*, X-ray microanalysis.

INTRODUCTION

Protoplasts of ciliates from the suborder Tintinnina are protected by a lorica, which can be hyaline or agglutinated with foreign particles. These particles can cover the entire lorica or only its bowl (Kofoid and Campbell 1929; Hada 1970; Laval-Peuto and Brownlee 1986; Wasik et al. 1996, 1997). Studies of loricae have not been restricted to the shape (Kofoid and Campbell 1929, Laval-Peuto and Brownlee 1986, Wasik et al. 1997) but have also aimed to establish their chemical composition. Fauré-Fremiet (1908) and later Gold and Morales (1975) considered them to be organic. Schweyer (1910) suggested that the lorica's building material is possibly cellulosic, while Kofoid and Campbell (1929) have found them to be mainly chitinous, with some proteins. Dogiel et al. (1962) also found loricae to be comprised of proteins and carbohydrates and named the substance tektin.

Particle adhesion arises through the sticky properties of the lorica, so it would be reasonable to presume that the agglutinated parts differ from the hyaline in chemical composition. We selected loricae of several species representing three morphologically different types, hyaline, and entirely and partially agglutinated by foreign particles, which were then analyzed by X-ray and chemical stainings.

MATERIALS AND METHODS

Loricae of the following Tintinnina species were considered; *Helicostomella subulata, Cymatocylis affinis/convallaria, Parafavella denticulata, Laackmanniella naviculaefera, Codonellopsis gaussi*, and *Tintinnopsis lobiancoi*. Samples were collected from the Baltic and White Seas, and from Antarctic waters.

Address for correspondence: Anna Wasik, Department of Cell Biology, Nencki Institute of Experimental Biology, ul. Pasteura 3, 02-093 Warszawa, Poland; Fax: (4822) 22-53-42

Loricae were selected and prepared as previously described (Wasik et al. 1996).

For energy-dispersive X-ray spectroscopy, loricae were carefully washed with distilled water, placed directly on the metal "stub", air-dried, coated with carbon and examined in a JEOL 1200 EX fitted with a LINK AN 10000 energy dispersive X-ray micro-analysis system (LINK Analytical Ltd., High Wycombe, Bucks, England). Three sites on a single lorica, and not less than 10 loricae of each species were analyzed.

For cytochemical staining loricae were rinsed with distilled water and treated with mercuric bromphenol blue or alcian blue. The mercuric bromphenol blue reaction for the presence of proteins, was carried out according to Mazia et al. (1953). Alcian blue was made by dissolving the dye in 3% acetic acid (Dunlap et al. 1983). Staining for acidic glycosaminoglycans by 1% alcian blue was carried out at pH 2.5 and loricae stained for 15 min prior to examination under a light microscope (JENALUMAR, Carl Zeiss, Jena).

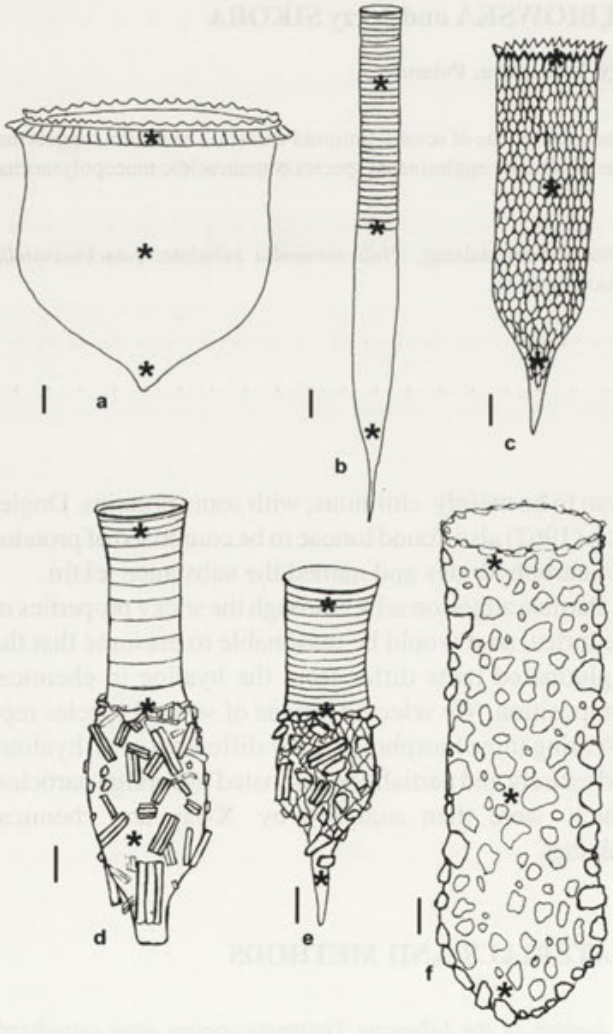

Fig. 1. Areas (asterisks) of tintinnid loricae undergo X-ray analysis. a - *Cymatocylis affinis/convallaria*, b - *Helicostomella subulata*, c - *Parafavella denticulata*, d - *Laackmanniella naviculaefera*, e - *Codonellopsis gaussi*, f - *Tintinnopsis lobiancoi*. Bar - 10 μm

RESULTS AND DISCUSSION

Although some information about the chemical nature of tintinnid loricae are available (Fauré-Fremiet 1908, Dogiel et al. 1962, Ogden and Coûteaux 1989), elemental analysis by X-ray spectroscopy has only been carried out by Gold and Morales (1975); they found the lorica of *Parafavella gigantea* to be non-mineralized.

As mentioned earlier, adhesion of particles is possible through the sticky properties of the material making up the loricae, so it is reasonable that the chemical nature of agglutinated and hyaline loricae might differ. Loricae of the species we considered, *Helicostomella subulata, Cymatocylis affinis/convallaria*, and *Parafavella denticulata* were hyaline, *Laackmanniella naviculaefera* and *Codonellopsis gaussi* were partially, while those of *Tintinnopsis lobiancoi* were entirely agglutinated by foreign particles. To compare these morphologically different loricae and various regions of a single lorica, we examined the collar, the bowl and a border zone between them by X-ray (Fig. 1). The loricae of all the tintinnids we considered, regardless of the tested area, showed no mineralization (Fig. 2). These results agree with those described by Gold and Morales (1975).

After staining *P. gigantea* loricae with mercuric bromphenol blue, Gold and Morales (1975) found them to be proteinaceous. The coloration of the loricae we examined by MBB staining also indicated their proteinaceous nature. In the case of agglutinated bowls (*L. naviculaefera*, *Cd. gaussi*) and entirely agglutinated loricae (*T. lobiancoi*) the coloration could be visualized only in particle-free areas.

Studying the external and internal architecture of loricae of different morphological types (Wasik et al. 1997), we found variations in their surface structure, revealed as bristles, granules and threads. Alcian blue, dye for acidic mucopolysaccharides caused various degrees of coloration reflecting the configuration of the lorica surface. Greatest intensity was found on *Cd. gaussi* loricae whose collar surface is covered by distinct bristles, while the bowl is circled by threads. Lighter coloration was observed in loricae of *P. denticulata* and *L. naviculaefera*; the whole external surface of the former is covered by short bristles and small granules, while the surface of the later is only lumpy. Neither the slightly granulated surface of the entirely hyaline loricae of *H. subulata* and the smooth *C. affinis/convallaria*, nor the smooth, particle-free surface of *T. lobiancoi*, show coloration.

In light of this study, the loricae of tintinnids we have described seem to be of an organic and non-mineralized nature, confirming previous reports (Fauré- Fremiet 1908,

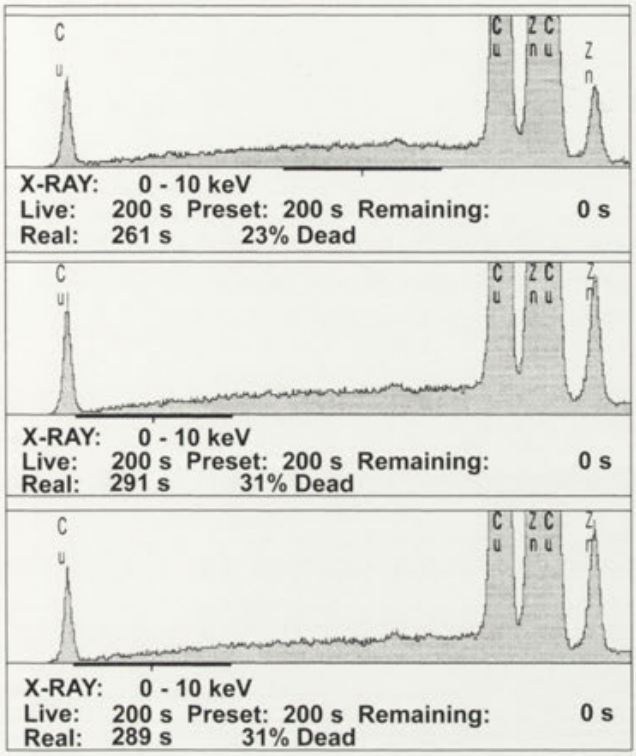

Fig. 2. X-ray elemental microanalysis of *Laackmanniella naviculaefera* lorica. a - control spectrum, b - spectrum of collar, c - spectrum of bowl

Dogiel et al. 1962, Gold and Morales 1975, Ogden and Coûteaux 1989). Our results also support those of authors who suggested that the lorica has a proteinaceous character (Kofoid and Campbell 1929, Dogiel et al 1962). In addition, we found that the partially agglutinated loricae of *Laackmanniella* and *Codonellopsis* contain acidic mucopolysaccharides.

Acknowledgements. This work was supported by a statutory grant to the Nencki Institute of Experimental Biology from the State Committee for Scientific Research. The authors would like to thank the Department of Antarctic Biology in Warsaw and the Center of Marine Biology in Gdynia for making samples available. The X-ray microanalysis were carried out in the Electron Microscopy Laboratory at the Nencki Institute.

REFERENCES

Dogiel W. A., Poljansky J. I., Cheissin E. M. (1962) General Protozoology. Russian Acad. Sci. Press, Moscow, Leningrad, 1-592 (in Russian)

Dunlap J. R., Walne P. L., Bentley J. (1983) Microarchitecture and elemental spatial segregation of envelopes of *Trachelomonas lefevrei* (Euglenophyceae). *Protoplasma* **117:** 97-106

Fauré-Fremiet E. (1908) Le *Tintinnidium inquilinum*. *Arch. Protistenk.* **11:** 225-251

Gold K., Morales E. A. (1975) Tintinnida of the New York Bight: loricae of *Parafavella gigantea*, *P. parumdentata*, and *Ptychocylis obtusa*. *Trans. Amer. Micros. Soc.* **94:** 142-145

Hada Y. (1970) The protozoan plankton of the Antarctic and Subantarctic seas. *Jap. Antarct. Res. Exp., Scient. Rep. Ser. E* **31:** 1-51

Kofoid C. A., Campbell A.S. (1929) A conspectus of the marine and fresh water Ciliata belonging to the suborder Tintinninea with descriptions of new species principally from the Agassiz expedition to the eastern tropical Pacific, 1904-1905. *Univ. Calif. Publ. Zool.* **34:** 1-403

Laval-Peuto M., Brownlee D. C. (1986) Identification and systematics of the Tintinnina (Ciliophora): evaluation and suggestions for improvement. *Ann. Inst. Oceanogr. Paris* **62:** 69-84

Mazia D., Brewer P. A., Alferti M. (1953) The cytochemical staining and measurement of protein with mercuric bromphenol blue. *Biol. Bull.* **104:** 57-67

Ogden C. G., Coûteaux M.-M. (1989) Interstitial marine rhizopods (Protozoa) from littoral sands on the east coast of England. *Europ. J. Protistol.* **24:** 281-290

Schweyer A. W. (1910) Zur Kenntnis des Tintinnodeen-weichkörpers, nebst einleitenden Worten über die Hülsenstruktur und die Hülsenbildung. *Arch. Protistenk.* **18:** 134-189

Wasik A., Mikołajczyk E., Ligowski R. (1996) Agglutinated loricae of some Baltic and Antarctic Tintinnina species (Ciliophora). *J. Plank. Res.* **18:** 1931-1940

Wasik A., Mikołajczyk E. Gołębiowska M. 1997 Morphology and microarchitecture of the loricae of some Tintinnina species. *Acta Protozool.* **36:**31-38

Received on 4th February, 1997; accepted on 10th February,1997

Erratum to: Vol. 36 No. 1, February 1997 issue of Acta Protozoologica

G. Gothe, K. J. Böhm and E. Unger (1997) Different stages of the plasmodial rhizopod *Reticulomyxa filosa*. *Acta Protozool.* **36:** 23-29

As the result of error during preparation of manuscript, on page 25, right column, line 11 appeared incorrect line - „....elastic inner layer and thicker (20-30 mm) outer one ...." the correct line - „....elastic inner layer and thicker (20-30 μm) outer one ...."

INSTRUCTIONS FOR AUTHORS

ACTA PROTOZOOLOGICA publishes original papers embodying the results of experimental or theoretical research in all fields of protistology with the exception of faunistic notices of local character and purely clinical reports. Short (rapid) communications are acceptable but also long review articles. The papers should be as concise as possible, be written in English. Submission of a manuscript to ACTA PROTOZOOLOGICA implies that it has not been submitted for publication elsewhere and that it contains unpublished, new information. There are no page charges except colour illustration. Names and addresses of suggested reviewers will be appreciated. In case of any question please do not hesitate to contact Editor. Authors should submit papers to:

Miss Małgorzata Woronowicz
Managing Editor of ACTA PROTOZOOLOGICA
Nencki Institute of Experimental Biology,
ul. Pasteura 3
02-093 Warszawa, Poland
Fax:48- 22 225342

Organization of Manuscripts

Submissions

Please enclose three copies of the text, one set of original of line drawings (without lettering!) and three sets of copies with lettering, four sets of photographs (one without lettering). In case of photographs arranged in the form of plate, please submit one set of original photographs unmounted and without lettering, and three sets of plates with lettering.

The ACTA PROTOZOOLOGICA prefers to use the author's word-processor disks (3.5"and 5.25" format IBM or IBM compatible, and MacIntosh 6 or 7 system on 3.5" 1.44 MB disk only) of the manuscripts instead of rekeying articles. If available, please send a copy of the disk with your manuscript. Preferable programs are Word or Wordperfect for Windows and DOS Wordperfect 5.1. Disks will be returned with galley proof of accepted article at the same time. Please observe the following instructions:

1. Label the disk with your name: the word processor/computer used, e.g. IBM; the printer used, e.g. Laserwriter; the name of the program, e.g. Word for Windows or Wordperfect 5.1.
2. Send the manuscript as a single file; do not split it into smaller files.
3. Give the file a name which is no longer than 8 characters.
4. If necessary, use only italic, bold, underline, subscript and superscript. Multiple font, style or ruler changes, or graphics inserted the text, reduce the usefulness of the disc.
5. Do not right-justify and use of hyphen at the end of line.
6. Avoid the use of footnotes.
7. Distinguish the numerals 0 and 1 from the letters O and l.

Text (three copies)

The text must be typewritten, doublespaced, with numbered pages. The manuscript should be organized into Summary, Key words, Abbreviations used, Introduction, Materials and Methods, Results, Discussion, Acknowledgments, References, Tables and Figure Legends. The Title Page should include the full title of the article, first name(s) in full and surname(s) of author(s), the address(es) where the work was carried out, page heading of up to 40 characters. The present address for correspondence, Fax, and E-mail should also be given.

Each table must be on a separate page. Figure legends must be in a single series at the end of the manuscript. References must be listed alphabetically, abbreviated according to the World List of Scientific Periodicals, 4th ed. (1963). Nomenclature of genera and species names must agree with the International Code of Zoological Nomenclature, third edition, London (1985) or International Code of Botanical Nomenclature, adopted by XIV International Botanical Congress, Berlin, 1987. SI units are preferred.

Examples for bibliographic arrangement of references:

Journals:

Häder D-P., Reinecke E. (1991) Phototactic and polarotactic responses of the photosynthetic flagellate, *Euglena gracilis*. *Acta Protozool*. **30:** 13-18

Books:

Wichterman R. (1986) The Biology of Paramecium. 2 ed. Plenum Press, New York

Article's from books:

Allen R. D. (1988) Cytology. In: Paramecium, (Ed. H.-D. Görtz). Springer-Verlag, Berlin, Heidelberg, 4-40

Zeuthen E., Rasmussen L. (1972) Synchronized cell division in protozoa. In: Research in Protozoology, (Ed. T. T. Chen). Pergamon Press, Oxford, **4:** 9-145

Illustrations

All line drawings and photographs should be labeled, with the first author's name written on the back. The figures should be numbered in the text as arabic numerals (e.g. Fig. 1). Illustrations must fit within either one column (86 x 231 mm) or the full width and length of the page (177 x 231 mm). Figures and legends should fit on the same page. Lettering will be inserted by the printers and should be indicated on a tracing-paper overlay or a duplicate copy.

Line drawings (three copies + one copy without lettering)

Line drawings should preferably be drawn about twice in size, suitable for reproduction in the form of well-defined line drawings and should have a white background. Avoid fine stippling or shading. Computer printouts of laser printer quality may be accepted, however *.TIF, *.PCX, *.BMP graphic formats on disk are preferred.

Photographs (three copies + one copy without lettering)

Photographs at final size should be sharp, with a glossy finish, bromide prints. Photographs grouped as plates (in size not exceeding 177 x 231 mm **including legend**) must be trimmed at right angles accurately mounted and with edges touching and mounted on firm board. The engraver will then cut a fine line of separation between figures. Magnification should be indicated. Colour illustration on transparent positive media (slides 60 x 45mm, 60 x 60mm or transparency) are preferred.

Proof sheets and offprints

Authors will receive one set of page proofs for correction and are asked to return these to the Editor within 48-hours. Fifty reprints will be furnished free of charge. Orders for additional reprints have to be submitted with the proofs.

Indexed in Chemical Abstracts Service, Current Contents (Agriculture, Biology and Environmental Sciences), LIBREX-AGEN, Protozoological Abstracts. POLISH SCIENTIFIC JOURNALS CONTENTS - AGRIC.& BIOL. SCI. data base is available in INTERNET under URL (UNIFORM RESOURCE LOCATOR) address: http://saturn.ci.uw.edu.pl /psjc/ or http://ciuw.warman.org.pl /alf/psjc/ any WWW browser; in graphical operating systems: MS Windows, Mac OS, X Windows - mosaic and Netscape programs and OS/2 - Web Explorer program; in text operating systems: DOS, UNIX, VM - Lynx and www programs.

ACTA
PROTOZOOLOGICA

REVIEW ARTICLE

ORIGINAL ARTICLES

SHORT COMMUNICATION

1997 MAY
VOLUME 36 NUMBER 2